UNIVERSIDAD DE MÁLAGA

IHSM La Mayora
Instituto de Hortofruticultura Subtropical y Mediterránea

CSIC
Consejo Superior de Investigaciones Científicas

Tesis doctoral

Unravelling the molecular mechanism of TTL proteins in cellulose biosynthesis

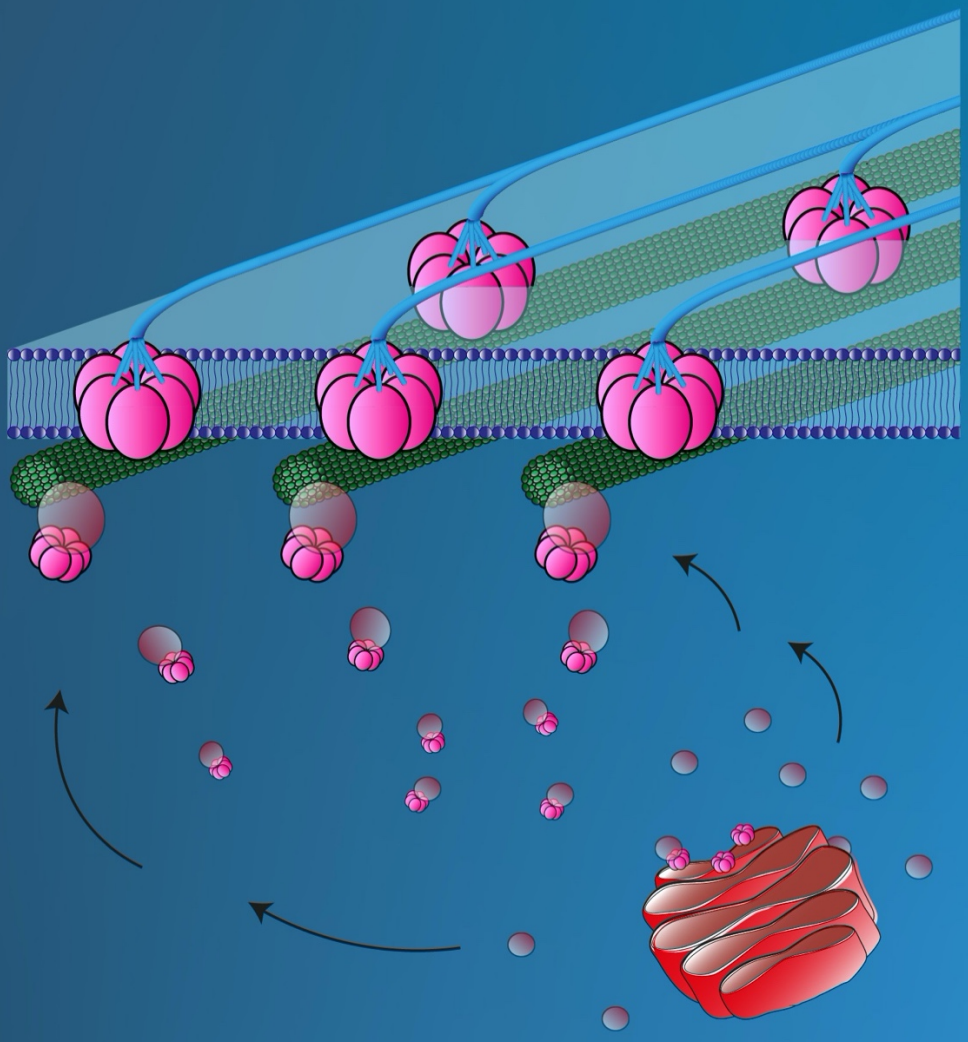

Álvaro García Moreno

Directores: Miguel Ángel Botella Mesa y Vítor Sérgio Amorim e Silva

Programa de doctorado en Biotecnología Avanzada. Facultad de Ciencias. Universidad de Málaga, 2020

AUTOR: Álvaro García Moreno

http://orcid.org/0000-0001-7007-998X

EDITA: Publicaciones y Divulgación Científica. Universidad de Málaga

Nunca consideres el estudio como una obligación, sino como una oportunidad para penetrar en el maravilloso mundo del saber

Albert Einstein

UNIVERSIDAD DE MÁLAGA

Instituto de Hortofruticultura Subtropical y Mediterránea

CONSEJO SUPERIOR DE INVESTIGACIONES CIENTÍFICAS

Facultad de Ciencias

Departamento de Biología Molecular y Bioquímica

Como directores, el Dr. **MIGUEL ÁNGEL BOTELLA MESA**, Catedrático de Bioquímica y Biología Molecular de la Universidad de Málaga, y Dr. **VÍTOR SÉRGIO AMORIM E SILVA**, Investigador Postdoctoral en el Departamento de Biología Molecular y Bioquímica de la Universidad de Málaga

INFORMAN:

Que D. **ÁLVARO GARCÍA MORENO** ha realizado bajo nuestra dirección y supervisión el trabajo de investigación correspondiente a su Tesis Doctoral titulada "Unravelling the molecular mechanism of TTL proteins in cellulose biosynthesis" con la cual aspira a la obtención del grado de Doctor en Biología.

Y para que así conste, y tenga los efectos oportunos, en cumplimiento de la legislación vigente, se extiende el presente informe en Málaga, a 3 de Julio de 2020.

Dr. Miguel Ángel Botella Mesa

Dr. Vítor Sérgio Amorim e Silva

DECLARACIÓN DE AUTORÍA Y ORIGINALIDAD DE LA TESIS PRESENTADA PARA OBTENER EL TÍTULO DE DOCTOR

D./Dña ÁLVARO GARCÍA MORENO
Estudiante del programa de doctorado BIOTECNOLOGÍA AVANZADA de la Universidad de Málaga, autor/a de la tesis, presentada para la obtención del título de doctor por la Universidad de Málaga, titulada: UNRAVELLING THE MOLECULAR MECHANISM OF TTL PROTEINS IN CELLULOSE BIOSYNTHESIS

Realizada bajo la tutorización de MIGUEL ÁNGEL BOTELLA MESA y dirección de MIGUEL ÁNGEL BOTELLA MESA Y VÍTOR SÉRGIO AMORIM E SILVA (si tuviera varios directores deberá hacer constar el nombre de todos)

DECLARO QUE:

La tesis presentada es una obra original que no infringe los derechos de propiedad intelectual ni los derechos de propiedad industrial u otros, conforme al ordenamiento jurídico vigente (Real Decreto Legislativo 1/1996, de 12 de abril, por el que se aprueba el texto refundido de la Ley de Propiedad Intelectual, regularizando, aclarando y armonizando las disposiciones legales vigentes sobre la materia), modificado por la Ley 2/2019, de 1 de marzo.

Igualmente asumo, ante a la Universidad de Málaga y ante cualquier otra instancia, la responsabilidad que pudiera derivarse en caso de plagio de contenidos en la tesis presentada, conforme al ordenamiento jurídico vigente.

En Málaga, a 3 de JULIO de 2020

Fdo.: ÁLVARO GARCÍA MORENO

Edificio Pabellón de Gobierno. Campus El Ejido. 29071
Tel.: 952 13 10 28 / 952 13 14 61 / 952 13 71 10
E-mail: doctorado@uma.es

Esta tesis ha sido realizada en el Departamento de Biología Molecular y Bioquímica, Universidad de Málaga y en el Instituto de Hortofruticultura Subtropical y Mediterránea "La Mayora" CSIC. Ha sido financiada con: (1) Ayudas para contratos predoctorales para la formación de doctores 2015 (BES-2015-071256) del Ministerio de Economía y Competitividad, dentro del proyecto "Incremento de la tolerancia a sequía en plantas por la manipulación de las características de la raíz usando aproximaciones biotecnológicas" (BIO2014-55380-R) concedido al Dr. Miguel Ángel Botella Mesa; (2) Short-Term Fellowship Number 7632 de La Organización Europea de Biología Molecular (EMBO).

Agradecimientos

A continuación, me gustaría agradecer a todas aquellas personas que han permitido la realización de esta tesis doctoral. Probablemente se me queden personas en el tintero, no lo desarrollaré tanto como debería, pero los que me conocéis sabéis que la escritura no es lo mío y el ser cariñoso menos, pero voy a intentarlo.

En primer lugar, agradezco la presente tesis a mis directores. A Miguel Ángel, mi padre científico, el que me ha dado la oportunidad de ejercer mi profesión, el que creyó en mí desde el minuto uno a pesar de ponérselo difícil y el que me ha hecho una persona más segura de sí misma y con unas aptitudes profesionales que me hacen ser lo que soy hoy. Por supuesto a Vítor, por enseñarme casi todo lo de laboratorio que sé, por decirme siempre lo que quiero escuchar cuando dudo, el que siempre me apoyaba y me daba una positividad envidiable en cada uno de mis agobios, tu familia tiene una gran suerte de tenerte y por supuesto, tú a ellos.

También agradecer a Vito, Eduardo, Araceli, Sonia, Iri, Carmen y Javi, por todas vuestras aportaciones en los lab meetings que me han hecho crecer en cada presentación y quitarme el miedo de hacer exposiciones.

A mi hermano Mario, empezamos juntos, terminamos juntos. Tú eres el que me ha derribado mis esquemas de la competitividad en el laboratorio. Eso queda atrás contigo, en su lugar nos hemos reído hasta mearnos (y otras cosas) a veces, los momentos que hemos compartido no los puedo contar, somos uña y carne a pesar de que no podía con tu repipipería al principio. A Bego, Blanca y aunque la veo menos a Alba, porque para llegar a donde estoy, ha sido pasando la mejor etapa de mi vida y ha sido gracias en parte a vosotras y no sabéis lo que me alegro

de haber pasado esta última etapa con vosotras, las risas, los agobios y la procrastinación que he pasado con vosotras no lo cambio por nada. A José, Selene, Fran y Carlos por amenizarnos a Mario y a mí esta última parte del doctorado y hacer del laboratorio una verdadera familia.

Por supuesto, a mis compañeros de laboratorio: Lidia, Delphine, Ali, Noemí, Jessi, Mariem, Vicky, Karen, David, Carmen, María, Eva, Sara, Fran P., Caro, Gemma. A la gente de genética de la Torre: Pepe, Miguel, Tábata, Ana, Bea, Angelito, Laura. A todos vosotros, gracias por hacerme con vuestra compañía una estancia maravillosa y perdón si se me olvida alguien, no sabéis el ejercicio mental que es el acordarse de todos y hace mucho calor.

Agredecer también a los que me ayudaron durante mis estancias como fue en Lyon, muchas gracias a Yvon y Laia por su atención y hacerlo todo más fácil. Por supuesto, a los que me trataron como uno más y me hicieron ser uno más de la familia en Zúrich como son Álex, Chris, Fran, Clara, Polo, Gloria, Yao, Sascha y Suzanne, sois un grupo profesional y humano excepcional.

Un lugar especial para mi familia. A mi madre María José que me ha proporcionado la vida que siempre he querido tener, gracias a su esfuerzo cada día que poco podemos hacer o al menos yo, aguantar niños pequeños tantas horas al día. A mis hermanos Dani y Jorge, las personas más fuertes que jamás haya conocido. A mi abuela Filo, porque sigue ahí al pie del cañón, cuidando de nosotros como hacía desde pequeños. A mis tíos y primos, que sois tantos que ocuparíais la mitad de mi tesis, muchas gracias por vuestro apoyo desde siempre.

A Laura, sin ella no hubiera sido posible nada de esto, es mi pozo de calma, mi segunda mitad, llegó sin querer a mi vida y se ha quedado. Otra gran parte de este trabajo, te lo dedico a ti.

Y por ultimo, pero no menos importante, a los que ya no están con nosotros, pero nos vigilan desde arriba. La parte que más me cuesta escribir y que no volveré a revisar de toda la tesis, pero han tenido gran parte de culpa de ser lo que soy hoy. A mis yayos Fernando e Isabel, por haber sido parte de generar una familia numerosa de verdad, en los que todos se apoyan los unos a los otros, tenéis que estar muy orgullosos de los hijos y nietos que tenéis, muchas gracias. Al yayo Sebas, es que no sé qué escribirte, eres un referente para mí, tienes una bondad que todos envidian, gracias por cuidarnos, por llevarnos al parque de los patos, de las palomas de pequeños, por cuidar tan bien de nosotros, estoy orgulloso de ti yayo y esto va también para ti. A mi padre Antonio, tampoco sé qué decirte, gracias por inculcarme tus valores, gracias por habernos dado junto a mama todo lo que tenemos, por haberme apoyado siempre, nunca se me olvidará lo que me dijiste: "Alvaro, continua en esto porque un doctorado es un doctorado…", parece una tontería pero en un momento malo, esa frase me ayudó muchísimo, no sabes lo que me fastidia que no estés aquí, pero sé de sobra que desde arriba me ves cada día que pasa, te he admirado y te admiraré siempre. Esto, sobre todo, va para ti.

INDEX

General Introduction

Table of contents

1. Abiotic Stress in Plants

1.1 Abiotic Stress in Crops: Drought and Salt Stress

Limitation in freshwater resources, arable land, progressive increasing of the population and climate change has a direct effect in ability of agriculture to cope with the current high demand for food, fibres and fuel (Fedoroff et al., 2010; Nguyen et al., 2020). Plants are normally exposed to a variety of different conditions/stresses that affect their growth, development and productivity, and that can either be biotic, when imposed by living organisms, or abiotic, when they are the result of a deficit or an excess in the physical or chemical environment (Buchanan, 2015). Indeed, it is normally believed that abiotic stresses are the main factors that reduces global yields of major crop (Boyer, 1982; Powell, 2006; Munns and Tester, 2008; Reynolds and Tuberosa, 2008). The estimated potential yield losses due to abiotic stresses are: 17% due to drought, 20% due to salinity, 40% due to high temperature, 15% due to low temperature and 8% by other factors (Athar and Ashraf, 2009). Therefore, drought and salinity and high temperatures are the major abiotic stresses that have profound implications in agricultural productivity (Athar and Ashraf, 2009).

Similar to limitations in freshwater availability due to drought stress, high concentration of soluble salts in soil is another major abiotic threat for agriculture productivity. Like drought, soil salinization quickly limits water uptake and causes osmotic stress, with the later ion accumulation leading to ionic stress (Munns and Tester, 2008). Furthermore, high temperature is generally known to enhance the water deficit and saline conditions. Thus, the negative effect of both drought stress and salt stress is exacerbated due to the current global temperature increase, which contributes to increase the desertification and

salinization world-wide. It is estimated that more that 10% of arable land are affected by drought and salinity and it is predicted that more than 50% of all arable lands by the year 2050 (Athar and Ashraf, 2009; Wang et al., 2003; Zafar et al., 2017; Kerry et al., 2018).

Several agronomic and management-based strategies to improve food production have been developed. However, it is still crucial to improve crops tolerance to water limitation and salinity (Tester et al., 2010).

1.2 Plant Signalling Response to Drought and Salt Stress

In plants, abiotic stresses are perceived by sensory mechanisms that respond to the physical and chemical environment, such as water availability and salt stress, and traduce it into physiological responses (Lamers et al., 2020). For drought and salt stress, it is important to distinguish between primary stress signals and secondary signals/effects of water deficit or high salt. The primary signal caused by drought is hyperosmotic stress, commonly referred as osmotic stress because hypo-osmotic condition usually is not a problem for plant agriculture. On the other hand, salt stress has both osmotic and ionic or ion-toxicity effects on cells. Moreover, the secondary effects of drought and salinity include oxidative stress; damage to cellular components such as membrane lipids, proteins, and nucleic acids; and metabolic dysfunction. Although some cellular responses derive from primary stress signals, others arise primarily from secondary signals. Thus, drought and salt have overlapping signals that trigger plant responses (Zhu, 2016).

Drought stress can occur at any growth stage and can affect crops productivity to variable degrees depending on the onset time, duration, and intensity (Hu and Xiong, 2014). Plant response to drought stress requires the

coordination of multiple processes which include stress signal perception, transduction and amplification, leading to the adaptation at the morphological, physiological, and molecular levels. The purpose of these processes to deal with drought results causing growth delay, shorter life cycle with accelerated flowering, osmotic adjustment, transpiration reduction (by closing stomata and increasing the thickness of the leaf cuticle) and improving water uptake (by developing a deep and thick root system) among others (Hu and Xiong, 2014). These pathways are coordinated by hundreds of genes that have been identified by genetic, genomic and transgenic approaches with the role of some of them resulting in increased drought resistance of various crops (Hu and Xiong, 2014). A putative sensor for hyperosmotic stress is the *Arabidopsis reduced hyperosmolality-induced calcium increase 1* (*OSCA1*), that encodes a hyperosmolality-gated calcium channel located at the plasma membrane (Yuan et al., 2014). High extracellular osmotic potential by water deficit cause the opening of the pore and allows Ca^{2+} influx very rapidly after stress conditions (Liu et al., 2018).

In addition to drought stress, soil salinity affects a considerable percentage of cultivated land and is an important factor restricting agricultural productivity, as mentioned above. High Na^{+} levels (due to saline conditions) cause ion toxicity, hyperosmotic stress, and secondary stresses such as oxidative damage (Zhu, 2016). Salt stress also produce osmotic changes that could be sensed through similar mechanisms as described for water deficit. However, is necessary an additional mechanism for sensing the ionic component.

Saline stress could be generally sensed via Ca^{2+} signalling for the exclusion of Na^{+} by the *SALT OVERLY-SENSITIVE* (*SOS*) pathway. In the SOS pathway, SOS3 and SCaBP8 act as Ca^{2+} sensors, whereas other kinase components such as the SOS2 and SOS-LIKE PROTEIN KINASE5 (PKB5) protein kinases regulate

downstream elements, including the SOS1 Na^+/H^+ antiporter (Fig. 1) (Lamers et al, 2020). Dysfunction in any of the SOS genes, significantly increases the sensitivity of the mutant plants to salt stress (Qiu et al., 2002).

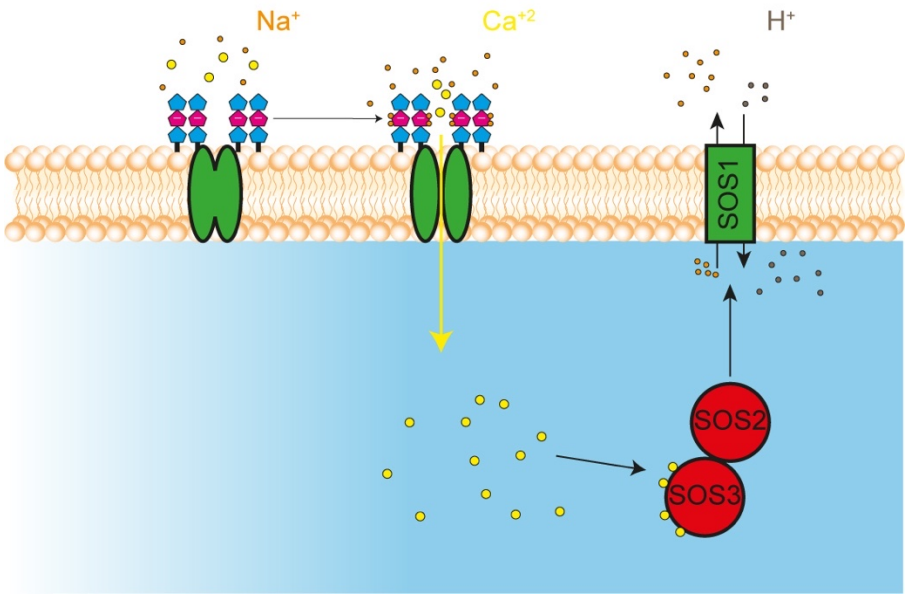

Figure 1. Plant response during salt stress. Upon salt stress, Na^+ ions are sensed by GIPCs (glycosyl inositol phosphorylceramide) that binds to the negatively charged glucuronic acid (purple pentagon) in GIPC. Subsequently, this binding produces an opening of an unidentified calcium channel facilitating the influx of Ca^{2+} in the presence of high extracellular Na+ levels. The intracellular Ca^{2+} binds SOS3 which forms a complex with SOS2 to activate the Na+/H+ antiporter SOS1. Blue pentagon represents IPC (inositol phosphorylceramide). Adapted from Lamers et al., 2020.

In the SOS pathway, the EF-hand calcium-binding protein SOS3 senses the cytosolic calcium signal elicited by salt stress. Then, SOS3 interacts and activates SOS2 protein kinase. The Ca^{2+} sensor SOS3 is preferentially expressed in the root, whereas the SOS3 paralog, SCaBP8/CBL10 mainly expressed in the shoot, performing an equivalent role to that of SOS3 (Quan et al., 2007). The activated SOS2 phosphorylates and activates SOS1, a Na^+/H^+ antiporter at the plasma membrane (Qiu et al., 2002). The SOS1 Na^+/H^+ antiporter regulation mainly depends on SOS3 and SOS2 activity. Furthermore, SOS1 is expressed in root

epidermal cells and xylem parenchyma cells, thereby activated SOS1 extrude Na^+ from the xylem parenchyma cells into the apoplastic space of mesophyll cells. (Zhu, 2016).

1.3 Abiotic Stress and Plant Cell Walls

Cell-wall perturbations have a direct effect in plant stress tolerance. Indeed, defects in the plant cell wall caused by the loss-of-function mutation in the putative pectin biosynthesis enzyme AtCSLD5 (CELLULOSE SYNTHASE-LIKE D5) in the *Arabidopsis sos6* (salt overly sensitive 6), mutant results in oxidative stress and greatly increased sensitivity to osmotic treatments and salt and drought stress (Zhu et al., 2010).

The primary cell wall in plants consists of cellulose microfibrils inter-connected by hemicellulose polymers, such as xyloglucan and arabinoxylan, and embedded in a pectin gel (Tenhaken, 2015). Salt, drought, and other osmotic stresses lead to Reactive Oxygen Species (ROS) accumulation that results in cell-wall thickening via phenolics and cell-wall glycoproteins such as extensins, which are known to be upregulated by stress (Tenhaken, 2015). In addition, salt stress can also cause the wall to lose Ca^{2+}, thus negatively affecting to the cross-linking between homogalacturonic acid polymers, structural backbone of the cell wall pectins (Demarty et al., 1984; Tenhaken, 2015; Zhu, 2016). Although the identities of plant cell-wall stress sensors are unclear, recent advances put emphasis on the role of plasma membrane receptor-like kinases (RLKs) (with more than 600 members in *Arabidopsis*) with an extracellular domain, a transmembrane domain, and a cytoplasmic kinase domain, in the transmission of signals from the outside to the inside of the cell. For example, loss-of-function mutations in *THESEUS* (*THE1*), which encodes a member of the *Catharanthus roseus* protein kinase-1-like (CrRLK1L) family, suppress growth defects and gene

expression changes in cell wall mutants (Hématy et al., 2007). FERONIA (FER), ANXUR1, and ANXUR2 (ANX1, 2), THE1 and ERULUS (ERU) are others CrRLK1L members that are also involved in cell wall sensing and signalling (Wolf, 2017). The FEI1 and FEI2 receptors, and the MALE DISCOVERER1-INTERACTING RECEPTOR LIKE KINASE 2 (MIK2), are members of Leucine-rich repeat receptor-like kinases (LRR-RLKs), that have also been shown to participate in the cell wall stress response (Xu et al., 2008; Harpaz-Saad et al., 2011; Van der Does et al., 2017). In addition, the atypical LRR-RLK STRUBBELIG (SUB) that control organ development in *Arabidopsis*, also promotes the cell response to reduced amounts of cellulose (Chaudhary et al., 2020). Hence, there are several plasma membrane receptors known to be involved in cell-wall perturbations sensing, although the molecular mechanism in not fully described (Wolf, 2017).

2. Plant Cell Walls

2.1 Biotechnological applications of Plant Cell Walls

Plants are the primary producers on our planet of essential supplies. In the form of wood, cotton, and other plant fibres, plant cell wall materials have been vital throughout human life as energy sources, building materials, and clothing (Klemm et al., 2005). Therefore, the biotechnological study of plant cell walls becomes essential. In addition, manipulation of plant cell wall synthesis and remodelling has the potential to improve agricultural yield and sustain biofuel production (Pauly and Keegstra, 2010). In fact, several approaches were used to remodel the composition and structure of the plant cell wall. However, these approaches have had a limited success due to plant cell wall plasticity, that

neutralize introduced modifications with compensatory mechanisms (Bacete and Hamann, 2020).

2.2 Plant Cell Wall Structure: Primary and Secondary Cell Walls

The plant cell wall is a polysaccharide-based extracellular matrix that is characterized by its complexity, dynamic structure and strength. From allowing individual protoplasts to adhere together to build multicellular organisms, the plant cell wall provides a structural skeleton to support plant growth and acts as the first line of defence against pathogens. Due to the dynamic structure of the plant cell wall can be rapidly remodelled in response to developmental, biotic and environmental changes (Kieber and Polko, 2019).

There are two types of plant cell walls, the primary and the secondary. The primary cell wall is generally a thin, flexible and extensible layer formed while the cell is growing, while the secondary cell wall is a thicker layer formed inside the primary cell wall after cell growth is accomplished, which strengthens and waterproofs the wall. Secondary cell walls are not found in all cell types, only are present in vascular tissue, such as xylem cell walls, and in wood cells of trees (Meents et al., 2018). In some species are synthetized gelatinous layer walls, mainly composed of polysaccharides and capable of generating contractile forces, where cellulose contributes with the 85% of the composition and is deposited between the plasma membrane and the secondary cell wall (Gorshkova et al., 2018; Anderson and Kieber, 2020).

2.2.1 Primary Cell Walls

Chemically, primary cell walls (PCWs) are composed primarily of cellulose, hemicellulose (aprox 20-30%), pectins and glycoproteins (McNeil et al. 1984; Meents et al., 2018). Cellulose is a paracrystalline structure of linear chains of β-(1–4) glucans, which aggregate to form cellulose microfibrils that are crystallized together by many intra- and intermolecular hydrogen bonds and Van der Waals forces (Fig. 2). Cellulose is synthesized at the plasma membrane, and new glucan chains are generated for crystallization of cellulose microfibrils, which are the main load bearing elements of cell walls. Pectins and hemicelluloses form a matrix of soluble polysaccharides together with cellulose microfibrils. Indeed, the hydrophobic surfaces of cellulose microfibrils are bound to xyloglucan, the principal type of hemicellulose, whereas pectins bind to their hydrophilic surfaces and both, pectins and hemicellulose fill the gaps between microfibrils and can cross-link cellulose microfibrils (Xiao et al., 2016; Kieber and Polko, 2019). Pectins are a class of polysaccharides that contain a base of associated galacturonic acid (Atmodjo et al., 2013) that interact with cellulose via hydrogen bonds (McFarlane et al., 2014). Hemicelluloses are typically characterized as β-(1→3,1→4) glucans linked to xylose, glucose, or mannose and influence cellulose crystallinity providing the strength to the interconnected cellulose microfibrils (McFarlane et al., 2014).

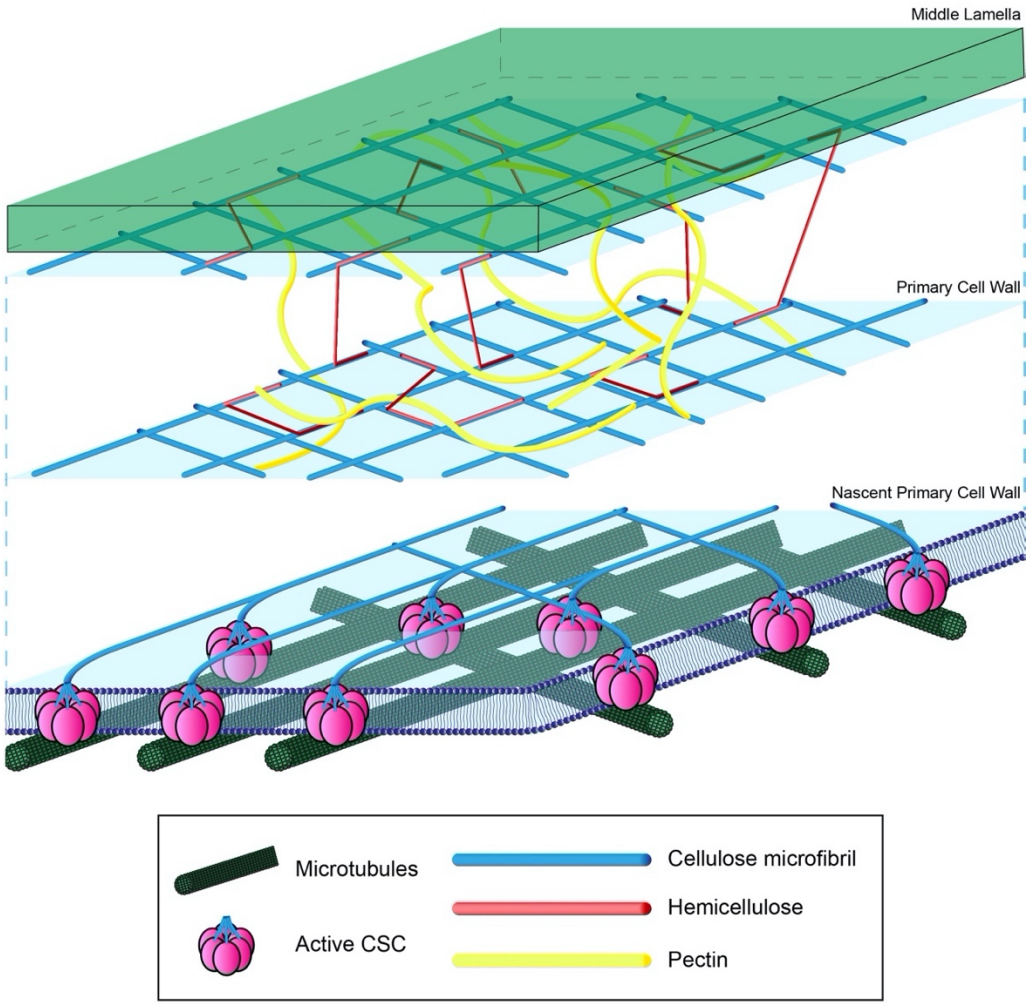

Figure 2. Typical structure of a primary cell wall. The primary plant cell wall, comprises cellulose, hemicellulose and pectin as major carbohydrates. Cellulose microfibrils are linked via hemicellulosic chains (commonly xyloglucan), forming the cellulose-hemicellulose network, which is embedded in the pectin matrix.

2.2.2 Secondary Cell Walls

A secondary cell wall (SCWs) is sometimes deposited between the PCW and the protoplasm and is responsible for generating woody tissue (McFarlane et al., 2014). The SCWs structure includes a dissimilar composition compared with PCWs. In the SCWs of terrestrial plants, cellulose comprises up to 60% of the SCW, compared with 20–30 % in PCWs (McNeil et al. 1984). When cellulose microfibrils are produced, they interact with hemicelluloses to form a stable

network in SCWs. Hemicellulose, which make up 10–40 % of the SCW, are essential for normal growth and development. Interestingly, SCWs are characterized by the absence of pectin, compared with PCWs, that is substituted by lignin at the end of SCW maturation. Lignin comprises about 30 % of woody cell wall biomass (Campbell and Sederoff, 1996), thus representing an important SCW component. Lignin synthesis (or lignification) is the last step of SCW biosynthesis, establishing the final, functionally mature wall that supports the plant and persists after vascular cells, undergoing programmed cell death.

3. Cellulose: The Main Component of Plant Cell Walls

3.1 Chemical Structure of a Cellulose Polymer

Cellulose is a linear polymer of glucose molecules in which individual glucose units are connected via glycosidic bonds between the C1 and C4 positions (Fig. 3). The anomeric C1 carbon is in the β-configuration, and every glucose unit is rotated by ~180◦ with respect to each adjacent unit, thereby forming a cellobiose disaccharide repeating unit. The unmodified C1- and C4-hydroxyl groups of cellulose form the polymer's reducing and nonreducing ends, respectively. The nascent polymer is elongated at its nonreducing end via transferring a glucose unit from UDP-glucose to the C4-hydroxyl group. This particular structure, first described by (Gardner and Blackwell, 1974), represents a twofold screw symmetry that is typical for β-1,4-glucans, in contrast to the water-soluble helical structures that α-1,4-glucans can adopt (Tester et al., 2004; McNamara et al., 2015).

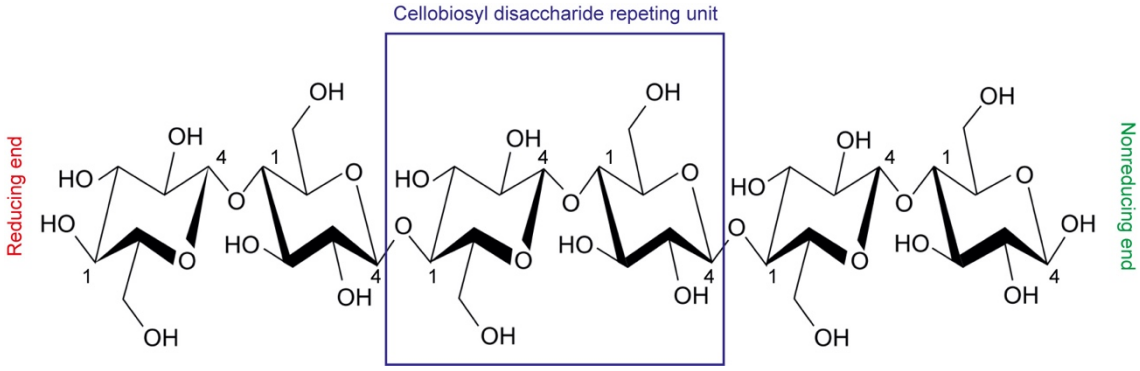

Figure 3. Chemical structure of a typical cellulose polymer. Individual glucose units are connected via glycosidic bonds between the C1 and C4 positions, where new glucose units that form the polymer are added through its nonreducing end. Adapted from George and Sabapathi, 2015.

3.2 Cellulose Is Synthesized by Cellulose Synthase Complexes

3.2.1 Characterization of Cellulose Synthase Complexes

The complex synthesis of cellulose depends on the appropriate activity of large motile PM-localized cellulose synthase complexes (CSCs). The CSC was first described in freeze fracture analyses (between the plasma membrane and the cell wall) of *Zea mays*. This allowed the observation of PM-associated globular complexes at the ends of some cellulose microfibrils, which the authors interpreted as being CSCs (Mueller et al., 1976). Indeed, a rosette structure with a six-fold symmetry was observed in association with plasma membrane impressions that may have been made by cellulose microfibrils (Mueller et al., 1976). Brown in 1985 described CSCs as granules structures that were associated with the cell wall microfibrils. Thereby, authors proposed a model in which the CSCs were the key catalytic structures of cellulose synthesis (Mueller and Brown, 1980; Brown, 1985). However, the characterization of the structure of CSCs remained unknown at that time, the comparison between bacterial genes and cotton cDNA sequences involved in cellulose biosynthesis identified the plant

cellulose synthase (*CESA*) genes (Pear et al., 1996). Once *CESA* genes were identified and cloned, antibodies were produced against cotton CESA to label these rosettes in freeze-fractured bean hypocotyls (Kimura et al., 1999). CESAs are enzymes with glycosyltransferase activity (GT-2 family), which is defined by: a N-terminal region involved in dimerization/oligomerization of CESA subunits (Kurek et al. 2002), eight transmembrane domains, a large internal cytoplasmatic loop and an intracellular C-terminal domain (Pear et al., 1996). The cytoplasmatic loop is positioned in the loop between transmembrane domains 2 and 3 and function as substrate binding and catalytic residues and consist of a D-D-D-QXXRW motif (Pear et al., 1996). Indeed, the crystallization of the bacterial cellulose synthase (BcS) allowed to further investigate the role of this intracellular loop in substrate binding and catalysis (Morgan et al., 2013). The first two aspartic acids coordinate UDP, the third provides the catalytic base for the glucan extension, and the QXXRW residues act as a binding site for the terminal glucan residues of the chain (McFarlane et al., 2014). Interestingly, deletion of the first aspartic acid in this region inhibits CESA UDP-glucose binding in cotton and point mutations in these residues in *Arabidopsis* leads to defective growth due to defects in cellulose biosynthesis (McFarlane et al., 2014). Hence, the characterization of the large cytoplasmic loop in cotton and its similarity with the BcS catalytic loop, suggest a common mechanism between bacterial and plant cellulose biosynthesis (Fig. 4A-B) (Morgan et al., 2013).

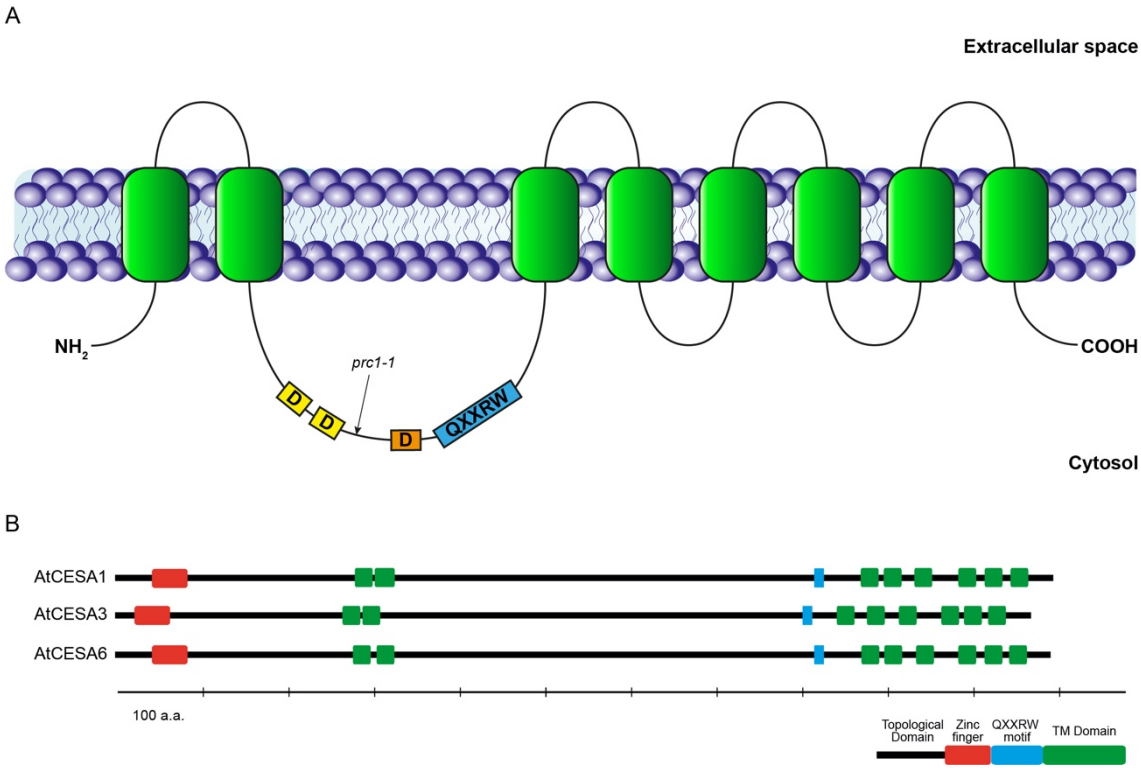

Figure 4. CESA proteins: structure and heterogeneity. (A) CESAs are predicted to have eight transmembrane domains and the N- and C-terminal regions facing the cytoplasm. The N terminus contains a zinc-binding region involved in dimerization/oligomerization of CESA subunits. The large cytosolic loop is positioned in the loop between transmembrane domains 2 and 3 and facilitates the glucan chain polymerization through the D-D-D-QXXRW motif, based on the crystal structure from a bacterial cellulose synthase. Mutations in the catalytic loop impairs cellulose biosynthesis. The position of the *prc1-1* mutation in CESA6 is indicated. Adapted from McFarlane et al., 2014. **(B)** Schematic representation of the predicted regions of the main primary cell wall CESAs.

3.2.2 Diversity of *CESA* Genes in *Arabidopsis*

In plants, the number of *CESA* genes is highly variable. Indeed, *Arabidopsis* has 10 *CESA* genes; *CESA1*, *CESA3*, and *CESA6*-like genes (*CESA2*, *CESA5*, *CESA6* and *CESA9*) are involved in PCW cellulose synthesis (Fig. 4B), whereas CESA4, *CESA7*, and *CESA8* participate in SCW cellulose synthesis (Kieber and Polko, 2019). Knockout mutations in either *CESA1* or *CESA3* are gamete lethal, which indicates the essential role of these two genes in the formation of a

functional CSC. Milder defects in any of these two genes resulted in a drastic reduction in cellulose synthesis and a wide array of cellulose-deficient phenotypes (McFarlane et al., 2014). For example, the *eli1* mutant (*CESA3* mutant allele) shows a decrease in cellulose content and enhanced ectopic lignification production in *Arabidopsis*, typically associated with phenotypes related with cellulose deficiency (Caño-Delgado et al. 2003). On the other hand, single-knockout mutations in the other primary cell wall genes *CESA2, CESA6* and *CESA9* resulted in milder phenotypes. However, *cesa2cesa5cesa6* and *cesa2cesa6cesa9* triple mutants are seedling and gamete lethal, respectively (Desprez et al., 2007; Persson et al., 2007) indicating partial redundancy among these *CESA* genes. Thus, PCWs require CESA1 and CESA3 as structural backbone and one additional member from the CESA6-like group. However, experiments using a *CESA6* promoter fused to *CESA2* or *CESA5* genes, only partially complemented *cesa6* mutant phenotypes (McFarlane et al., 2014). SCWs requires CESA4, CESA7 and CESA8 enzymes and these genes are non-redundant.

3.2.3 Structure of the CSC

CSC rosettes (Fig. 5) originally were structurally identified as a hexamer of CESA hexamers (Somerville, 2006), hence containing 36 individual CESA subunits. However, several studies support a microfibril diameter of approximately 2.5 nm, consistent with of 18-24 cellulose chains (Kieber and Polko, 2019). Furthermore, recent modelling the of cellulose microfibril organization within an 18-chain microfibrils demonstrated that cellulose chains are stacked in the microfibril in a 34443 arrangement resulting in a structure of three chains, followed by four chains, and so on (Kubicki et al., 2018). Analyses of PCW and SCW CESA stoichiometry using co-immunoprecipitation, mass spectrometry and quantitative immunoblotting support that each isoform occurs

in equimolar amounts (Kieber and Polko, 2019). This 1:1:1 stoichiometry, together with the trimeric nature of CESA proteins and analyses of microfibril width, suggests a model in which CSC rosettes contain 18 CESA subunits that synthesize 18 glucan chains. This is further supported by transmission electron microscopy (TEM) images of CSCs from the moss *Physcomitrella patens* combined with computational models suggesting that CSCs are composed of 18 CESA subunits (Nixon et al., 2016).

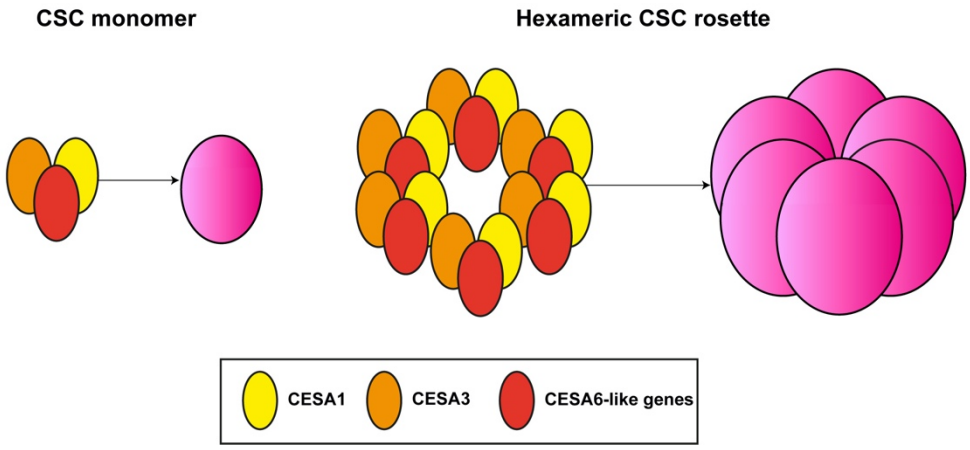

Figure 5. CESA organization into cellulose synthase complexes (CSCs). CESA1, CESA3, and CESA6-like proteins participate in the primary wall CSC, which oligomerization compose a CSC monomer. The CESA6-like position presumably may be filled with any of the CESA6-like proteins (CESA2, CESA5, CESA6 and CESA9). The oligomerization of CSC monomers becomes the typical hexameric structure of CSCs. Adapted from Polko et al., 2018.

3.2.4 Two Types of CSC may Co-Exist in the Plant Cell Wall Together

In certain tissues a SCW is deposited between the plasma membrane and the PCW. The generation of the SCWs implies a transition of primary to secondary CESAs in the plasma membrane. In early stages of this transition, the SCW CESAs are delivered in the plasma membrane, coexisting together with PCW CESAs. In this state, the catalytic speed of SCW CESAs is higher than primary CESA enzymes, which correlates with the increase in the cellulose

content required for SCWs. During mid-stages of this transition, where SCW is produced, PCW CESAs are continuously depleted from the plasma membrane, leading to their degradation via lytic vacuole. At the same time, a lignification of the SCW occurs while SCW is being generated. Finally, in the late stages, SCW is completely synthetized. During SCW maturation the lignification process ends, secondary CESAs disappear from plasma membrane and cell death occurs. (Haigler, 2018; Meents et al., 2018; Watanabe et al., 2018).

4. Plant Cell Growth: Anisotropic expansion

Plant development is the result of three essential processes: cell expansion growth, cell division and cellular differentiation (Geitmann and Ortega, 2009). Most plant growth is achieved by cell expansion (Powell and Lenhard, 2012), which can be either isotropic or anisotropic. When an area of cell wall expands at the same rate in all directions, expansion rate is isotropic (e.g. fruit parenchyma), whereas when the rate in one direction differs from the rate in another, expansion rate is anisotropic (e.g. root/shoots epidermal cells) (Fig. 6). Therefore, to accomplish directional growth, plant cells undergo anisotropic expansion and this process gives the organ its shape. Hence, understanding the mechanisms that allows anisotropic expansion of the cell is fundamental for understanding plant development, with the cell wall having a fundamental role (Baskin, 2005).

The cell wall that surround a cell is a continuous sheet and therefore cell stretching requires large forces to accomplish anisotropic growth. However, the forces acting on the plant cell wall are originated from hydrostatic pressure, which are mainly isotropic. In fact, in a single cylindrical cell, most of the forces caused by the hydrostatic pressure acting circumferentially (isotropic), is twice that acting longitudinally (anisotropic) (Probine and Preston, 1961). However,

cylindrical cells expand faster longitudinally than circumferentially, therefore the resistance of the cell wall to stress must be anisotropic (Fig. 6) (Baskin, 2005).

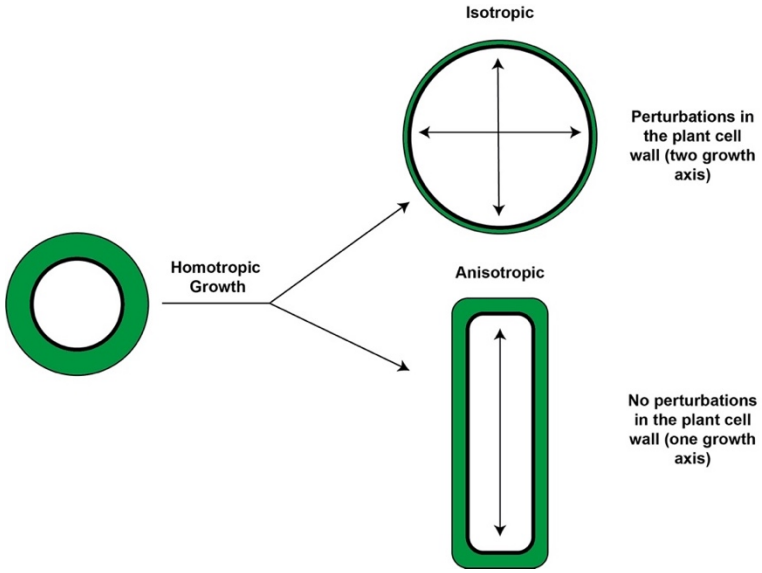

Figure 6. Overview of homotropic growth during cell wall expansion. Plant cell growth is accomplished by cell expansion rather than cell division. Plant cells undergo anisotropic expansion to achieve directional growth, and cellulose microfibrils are deposited perpendicular to the axis of growth. Perturbations in the plant cell wall leads to a decrease in the degree of anisotropy, resulting in an isotropic growth where cells adopt a circle-shaped morphology (cells achieve longitudinal and perpendicular growth at the same time). Adapted from Geitmann and Ortega, 2009.

In multicellular organs, the mechanical resistance of the cell wall is well described. Cell walls are reinforced anisotropically by cellulose microfibrils (Brett, 2000), that associate laterally to form a crystalline network (Doblin et al., 2002). Neighbouring microfibrils tend to be roughly parallel and its alignment is sometimes equated to resistance. However, resistance is defined as the interaction between microfibrils and with other wall components; giving the resistance of the wall to stress. Furthermore, this organization provides a high tensile strength (~100 GPa), comparable to that of steel (Höfte and Voxeur 2017) and its alignment commonly does reflect the direction of strain rate anisotropy. However, the magnitude of the resistances and hence the degree of anisotropy depend on the interactions between microfibrils (Baskin, 2005).

5. Microtubules play an essential role in plant growth

5.1 Microtubule Structure: α/β-tubulin dimers

It is widely known that cell expansion, critical determinant of plant organ size and shape, is regulated by a dynamic cortical microtubule array at the cell cortex, guiding cellulose microfibrils deposition in the extracellular space (Gutierrez et al., 2009).

Microtubules are highly dynamic filamentous protein polymers consisting of α-tubulin and β-tubulin heterodimer subunits that undergo cycles of rapid growth and disassembly (Desai and Mitchison, 1997). These α/β-tubulin dimers polymerize end-to-end into linear protofilaments that associate laterally to form a single microtubule. Furthermore, these ends are labelled as (-) and (+) ends, where only the α-subunits are exposed in the (-) end, while the (+) ends shows only β-subunits exposed. Furthermore, the microtubule (+) ends exhibit dynamic instability, characterized by episodes of subunit addition and loss (Ehrhardt and Shaw, 2006).

The GTP bound to α-tubulin is stable and it seems to play a structural function in the bound state with the β-tubulin as this GTP is not hydrolysed. However, the GTP bound to β-tubulin could be hydrolysed to GDP after assembly, while β-tubulin remains in the polymer. These GDP-tubulin dimers tend to fall at the (+) end of the microtubule, therefore a protection of GTP-bound tubulin is required to exist at the (+) end of the microtubule, safeguarding it from disassembly (Fig. 7). However, when hydrolysis occurs at the tip of the microtubule, it begins a rapid depolymerization and shrinkage (Mitchison and Kirschner, 1984). Upon depolymerization, the released tubulin subunits can

interchange GDP for GTP and undergo another round of polymerization (Desai and Mitchison, 1997).

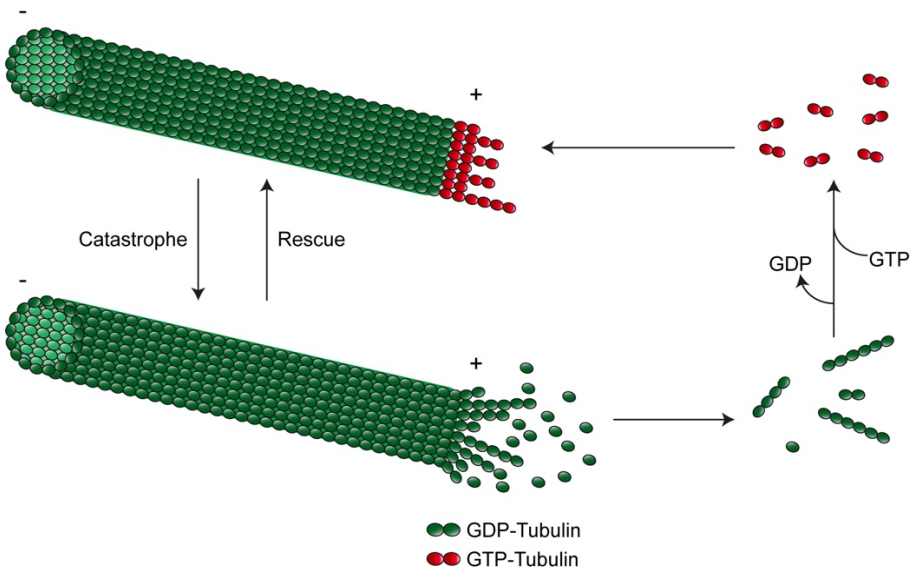

Figure 7. Dynamic instability is characterized by the coexistence of polymerizing and depolymerizing microtubules. GTP-tubulin is integrated at the polymerizing microtubule (+) end, the bound GTP is hydrolysed during or after polymerization, and Pi is subsequently released. A GTP cap at the (+) end is essential for safeguard microtubule stability as showed in the figure. Depolymerization phase (catastrophe) is characterized by the very rapid loss of GDP-tubulin subunits and oligomers from the microtubule (+) end. Furthermore, depolymerizing microtubules can also transit back to the polymerization phase (rescue) via formation of GTP-tubulin dimers that are subsequently added to the polymerizing microtubules. Adapted from Desai and Mitchinson, 1997.

5.2 Cross-talk Between Microtubules and CESAs

The relationship between microtubules and cellulose deposition has been extensively reviewed (Wasteneys 2004; Gutierrez et al. 2009; Li et al. 2015). It is well known that cortical microtubules and cellulose microfibrils generally co-align and that this alignment is perpendicular to the growth axis during anisotropic expansion (McFarlane et al., 2014). However, the guidance of cellulose microfibrils along cortical Microtubules is not observed in some cell

types, like the tip of root hairs or pollen tubes. Thus, microtubules do guide cellulose microfibrils in the primary walls of cells undergoing anisotropic growth and in the secondary walls of xylem cells (Baskin, 2001; Gardiner et al., 2003).

Cortical microtubules also play a role in defining the plasma membrane delivery sites for CESAs. Fluorescent tagged CESAs present in microtubule-associated cellulose synthase compartments (MASCs) and microtubule-associated vesicles that contained CESAs in small CESA compartments (SmaCCs), co-align with fluorescently tagged microtubules (Crowell et al., 2009; Gutierrez et al., 2009). However, in plant cells sometimes exists some autonomous CSCs that do not colocalize with microtubules and follow trails left by previous complexes independently to microtubules (Chan et al., 2020). Furthermore, when microtubules were completely depolymerized, CSCs realigned into ordered arrays (Paredez et al., 2006). This led authors to hypothesize that nascent cellulose microfibrils, or other factors in the extracellular matrix, could guide cellulose deposition (Paredez et al., 2006). However, it is clear that microtubules disorganization induced by drugs such as oryzalin, which binds to the α-tubulin monomer or microtubule realignment caused for example by blue-light results in realignment of CSC trajectories and cellulose microfibrils (McFarlane et al., 2014). Interestingly, cortical microtubule alignment was impaired in *cesa2* and *cesa6* mutants (Fisher and Cyr, 1998; Chu et al., 2007; Paredez et al., 2008), suggesting that feedback may exist between CSCs and the cortical microtubule array.

5.2.1 Key Partners that Safeguard Microtubule-CESAs association

The strong association between CSCs and microtubules is well described and several proteins responsible for microtubule-CESAs association are known. The CELLULOSE SYNTHASE INTERACTING1 (CSI1)/POM2 (hereafter CSI1)

was identified *in vitro* as a microtubule-interacting protein and is required for proper microtubule-CSC trajectory alignment, wild-type CSC velocity and proper cell elongation (McFarlane et al., 2014). In addition to this, Y2H assays revealed that CSI1 interact with CESA1, CESA3, and CESA6 cytosolic domains and visualization of fluorescent tagged CSI1 proteins revealed that these proteins tracked with CSC particles at the plasma membrane (Gu et al., 2010). Altogether, CSI1 seems to play an essential role as a mediator of the CSC-microtubule alignment. Additionally, other important components have been identified to be required to direct cellulose synthase movement through preserving the cortical microtubule array. Thus, the CESA MICROTUBULE UNCOUPLING (CMU) proteins are required for develop an appropriate microtubule arrangement and therefore maintaining an appropriate cellulose biosynthesis (Liu et al., 2016). Indeed, *cmu1cmu2* double mutant display lateral instability of microtubules and uncoupling of CESAs from the microtubules (Kieber and Polko, 2019). Hence, authors proposed that forces generated by CSC movement in microtubules are compensated by CMU proteins function (Liu et al., 2016).

6. Agents that influence cellulose biosynthesis

6.1 Salt stress

6.1.1 Cortical Microtubules are Dissociated During Salt Stress

As mentioned above, salt stress has serious consequences for plant growth and crop production. An important finding is that cellulose defective mutants are especially sensitive to saline conditions. Microtubules are disassembled rapidly after exposure to salt and other osmotic stresses (Komis et al., 2002) and the subsequent repolymerization is required for plant cells adaptation to stress

episodes (Wang et al., 2007). In *Arabidopsis*, mutations in genes involved in microtubule functions are associated with altered organization of cortical microtubule arrays (Shoji et al., 2006). Interestingly, mutation in *SPIRAL1* gene induce a right-handed helical growth phenotype in rapidly elongating epidermal cells and this abnormal phenotype could be genetically suppressed by mutation in the SOS1 Na^+/H^+ antiporter. Additionally, SPIRAL1 degradation via 26S proteasome is important for salt-stress tolerance (Wang et al., 2011). During depolymerization, promoted by high salt-stress conditions, the accumulation of phosphorylated α-tubulin through the atypical microtubule-associated protein kinase PROPYZAMIDE-HYPERSENSITIVE 1 (PHS1) blocks microtubule polymerization (Fujita et al. 2013a).

Cortical microtubules guide the appropriate cellulose alignment in plant cells. Therefore, perturbations in the cortical microtubule array can negatively influence in cellulose alignment, thus producing an increased isotropic growth. However, how microtubules influence in the structure of crystallized cellulose microfibrils remains unknown. Wasteneys (2004) proposes that microtubules safeguard the synthesis and integrity of long microfibrils by forming parallel arrays with cellulose-microfibril deposition. According to this model, under normal conditions microtubules are oriented in the direction of microfibril synthesis. This causes the generation of long microfibrils that are correctly separated. However, upon stress conditions, changes in the microtubule cortical array (e.g. depolymerization, changes in orientation…) generates fragilities in microfibrils, which are prone to breakage, allowing separation of microfibrils in the lateral as well as longitudinal direction (Wasteneys, 2004). Alternatively, microtubule instability affects the longevity or activity of cellulose synthase complexes, resulting in relatively short microfibrils. Thus, in this model, cells can undergo radial expansion while microfibril orientation remains transverse (Wasteneys, 2004).

6.1.2 Several Cellulose Related Components Are Crucial in Salt Stress Tolerance

Plant responses to salt stress also depend on the appropriate activity of the cellulose synthase complex. Mutation in *CESA6* gene conduct to abnormal root growth in *Arabidopsis* seedlings under salt stress (Zhang et al., 2016). In addition, mutation in *CSI1* gene also led to enhanced sensitivity to salt stress in *Arabidopsis* seedling roots (Zhang et al., 2016). The COMPANION OF CELULLOSE SYNTHASE 1 and 2 (named as CC1 and CC2, respectively) are other components of the CSCs that are important to salt stress tolerance. CC1 and CC2 proteins interact with microtubules and co-localize with CESAs (Endler et al., 2015) and mutation in both genes leads to hypersensitivity to salt. Indeed, the N-terminal parts of the CCs, which were essential for salt tolerance, interact with microtubules and promote microtubule dynamics during stress episodes. Time-lapse analysis of microtubule arrangement and CESA dynamics in hypocotyl epidermal cells revealed that the cortical microtubule array and plasma membrane-localized CESAs eventually recovered under salt conditions in wild-type cells. In contrast, in *cc1cc2* double mutant microtubules were not able to repolymerize and impaired CESAs alignment after salt stress (Endler et al., 2015). Altogether, authors show some insights on how plant cells respond to salt stress to safeguard cellulose biosynthesis through microtubule maintenance.

In silico analysis also revealed that genes involved in PCW homeostasis and genes involved in cellulose biosynthesis are transcriptionally co-regulated (Persson et al., 2005). For example, *SOS5* encodes a fasciclin-like arabinogalactan protein, predicted to be linked to the plasma membrane by a glycosylphosphatidylinositol lipid anchor (Shi et al., 2003). Mutation in *SOS5* gene leads to hypersensitivity to salt, but not to osmotic stress (Shi et al., 2003). SOS5, together with the receptor-like kinase FEI2, were implicated in seed coat

mucilage production, and defects in either of these genes could be phenocopied by *cesa5* mutants (Harpaz-Saad et al., 2012). Interestingly, SOS5 also promote cellulose biosynthesis together with *FEI1* and *FEI2* genes acting in the same pathway (Xu et al., 2008). However, how SOS5-FEI1-FEI2 pathway promote cellulose biosynthesis remains unknown.

6.2 Sucrose

6.2.1 Sucrose Metabolism in Plants

Sucrose, the primary product of photosynthetic tissues, is the main sugar transported from the source tissues through the phloem to non-photosynthetic tissues (Ruan, 2014). Glucose 6-phosphate (G6P) is used to form UDP-glucose (UDP-G), which combined with fructose 6-phosphate form sucrose 6-phosphate (sucrose-P) by action of the sucrose phosphate synthase (SPS). Sucrose-P is then dephosphorylated by sucrose phosphate phosphatase (SPP) to finally generate sucrose (Stein and Granot, 2019).

In sink non-photosynthetic tissues, sucrose can enter inside the cells through several different pathways (Ma et al. 2019). Sucrose can be unloaded from the phloem to the apoplast by sucrose transporters, where a cell-wall invertase transform sucrose into glucose (Glc) and fructose (Fru), which can enter the cells by hexose transporters (Ruan, 2014). Alternatively, sucrose could be internalized into the sink cells via plasmodesmata. In plant cells, sucrose is the main sugar used to form UDP-glucose, that is the substrate for cellulose biosynthesis. Indeed, sucrose is transformed in UDP-glucose through two independent processes: (1) a sucrose synthase (SuSy) catalyses the reversible cleavage of sucrose using UDP, obtaining fructose and UDP-glucose; (2) a

cytosolic invertase (cINV) catalyses the irreversible hydrolysis of sucrose into glucose and fructose, then glucose is transformed in glucose 1-phosphate (via hexose-phosphate enzyme). Finally, a UDP-Glc pyrophosphorylase (UGP-ase) use glucose 1-phosphate and UTP to generate UDP-glucose (McFarlane et al., 2014). It is postulated that the importance of the cINV could be higher compared with SuSy as main source of UDP-glucose. Consistent with this possibility, a double mutant defective in two of the nine *Arabidopsis* invertases (Barratt et al., 2009) show phenotypes associated with decreased cellulose synthesis, whereas a quadruple mutant defective in four of the six *Arabidopsis* SuSys did not (Barratt et al., 2009; McFarlane et al., 2014).

6.2.2 The Impact of High Sucrose on Cellulose Biosynthesis

Interestingly, high sucrose concentrations in the plant growth medium exacerbates many cell wall-related phenotypes of several mutants such as *cesa6*, *sos5*, and *fei1 fei2* (Fagard, 2000; Xu et al., 2008), however the molecular reasons for this remains unclear. Some insights provided by Yeats et al. suggests a mechanism that might explain this phenomenon. The *shaven3 shaven3-like1* (*shv3svl1*) double mutant displays reduced hypocotyl elongation than WT in darkness in presence of high levels of exogenous sucrose. This is associated with a reduction of cellulose content and increased starch content. Similarly, *fer* mutants have increased starch in presence of high levels of sucrose (Yang et al., 2015). These cellulose-related phenotypes were suppressed in the *shv3svl1* by a mutation in *SUC1* (PM-localized sucrose/H+ symporter). This suggests that sucrose accumulation could trigger cell expansion defects. Consistent with this hypothesis, both *shv3svl1* and *fer* display hyperpolarization of the plasma membrane and overaccumulation of intracellular sucrose that may results in increased partitioning of carbon to starch rather than cellulose. Furthermore, *SHV3* and *SVL1* genes may be involved in coordination of the proton pump

activity with cellulose biosynthesis (Yeats et al., 2016). Interestingly, high levels of sucrose result in a decrease of CESA density at the PM (Polko et al., 2018), providing evidences in the considerable role of exogenous high levels of sucrose in cellulose biosynthesis impairment.

6.3 Inhibition of Cellulose Synthesis by Isoxaben

Isoxaben, N-[3(1-ethyl-1-methylpropyl)-5-isoxazolyl] is a leaf herbicide used primarily on small grains, turf, and ornamentals (Desprez et al., 2002). This is because while is phytotoxic to dicotyledonous plants, most monocotyledonous species are tolerant. It is known that isoxaben specifically inhibits glucose incorporation into the acid insoluble cellulosic cell wall fraction (Heim et al., 1990). *IXR1* and *IXR2* have been characterized as isoxaben-resistant loci in *Arabidopsis* (Heim et al., 1990). Thus, *IXR1* was shown to encode a cellulose synthase catalytic subunit CESA3. Interestingly, a threonine-to-isoleucine mutation within the cytosolic domain in *AtCESA3* confers resistance to the herbicide isoxaben (Scheible et al., 2001), which suggest that isoxaben target is the catalityc domain of the CESA enzymes. Similarly, *IRX2* was further identified as *CESA6* and missense mutations, lead to increase tolerance to isoxaben (Desprez et al., 2002). Although it is unknown the inhibitory mechanism of isoxaben, the increased resistance toward the herbicide in these mutants accentuate the functional importance of this CESA cytosolic motif.

Isoxaben treatment results in a rapid depletion of the CESA complexes from the plasma membrane, producing isotropic growth (Xu et al., 2008). Due to the role played by cortical microtubules on the CSC array (Paredez et al., 2006; Gutierrez et al., 2009), isoxaben could influence cortical microtubules indirectly. Of note, isoxaben also alters the orientation of cortical microtubules while exogenous cellulose degradation did not (Paredez et al., 2008). Interestingly,

microtubules only became oriented after a nascent cell had established its anisotropic axis of growth, and that isoxaben treatment only disorganized microtubules after isotropic cell swelling started (Fisher and Cyr, 1998).

6.4 Brassinosteroid Signalling and Cellulose Biosynthesis

Brassinosteroids (BRs) are phytohormones that regulate morphogenesis, cell division and differentiation (Clouse, 2002; Nolan et al., 2020). Some studies on BR signalling indicate an implication in plant cell wall (Wolf et al., 2012). BR signalling is part of a compensatory response, protecting plants against the loss of cell wall integrity caused by the disproportion in pectin modification (Wolf et al., 2012). Thus, signalling from the cell wall is integrated by the BR signalling components to ensure homeostasis of cell wall biosynthesis and remodelling (Wolf et al., 2012). The integrity of plant cell walls of growing cells involves a balance between processes that promote cell wall relaxation and stiffening (e.g., removal and generation of new Ca^{2+}/pectate crosslinks) (Rojas et al., 2011; Proseus and Boyer, 2012). Inhibition of the pectin methylesterase enzyme (PME) (e.g. through epigallocatechin-3-gallate treatment) lead to a reduction of pectate in the cell wall, which would cause the activation of the BRASSINOSTEREOID INSENSITIVE 1 (BRI1) receptor through an unknown feedback mechanism and the compensatory upregulation of wall remodelling agents (Wolf et al., 2012). Thus, loss of integrity in the plant cell wall implies an activation of the BR perception response, in order to activate PME and cell wall loosening genes transcripts via BRASSINAZOLE-RESISTANT 1 (BZR1) and BRI1-ETHYL METHANESULFONATE SUPPRESSOR1 (BES1/BZR2) transcription factors (Fig. 8).

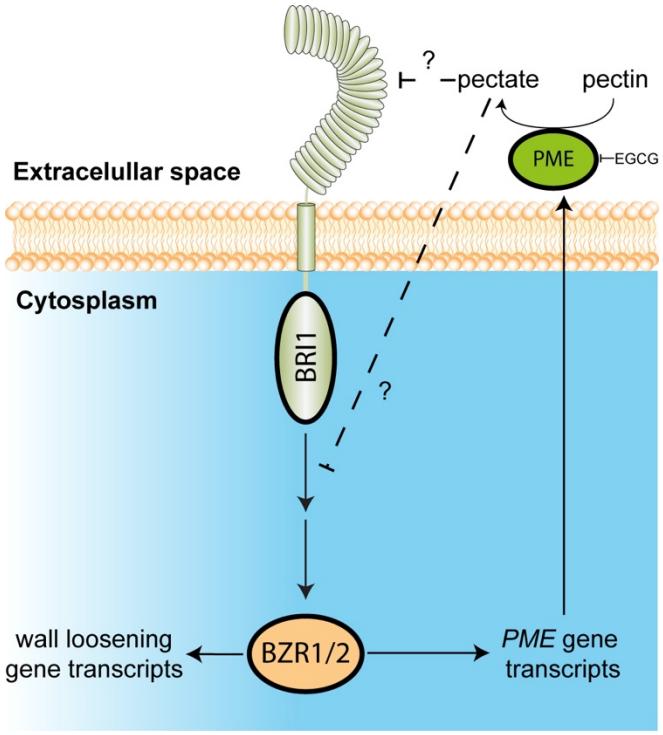

Figure 8. Plant cell wall homeostasis is mediated by BR signalling. Pectin is deposited in a highly methylesterified and demethylesterified form by pectin methylesterases (PME). Inhibition of PME activity by the chemical inhibitor EGCG causes the activation of the BRI1 receptor and/or a downstream BR signalling component through a so far unknown mechanism. This, in turn leads to the enhanced transcription in growing cells of cell wall-modifying genes including at least two PME genes through BZRs transcription factors. Adapted from Wolf et al., 2012.

Interestingly, the BR-regulated BZR1/BES1 transcriptional factors directly bind the promoters of CESA genes, involved in cellulose biosynthesis of the primary and secondary cell walls (Xie et al., 2011). Therefore, the implication of the core components of BR signalling in the integrity of the plant cell wall seems to be essential. Another of these components is the BRASSINOSTEROID INSENSITIVE2 (BIN2) protein kinase that negatively regulates the activity of the CSC in plant cells (Sánchez-Rodríguez et al., 2017). Mutations in *DET2* (*det2-1*, a key enzyme in BR synthesis) or a hypermorphic mutation in *BIN2* (*bin2-1*) results in overaccumulation of BIN2 protein, leading to reduced levels of crystalline cellulose. *In vitro* kinase assays revealed that BIN2 phosphorylate the Thr157 residue of CESA1. Phosphorylation of Thr157 is functionally relevant since a

phosphonull mutation at this position in CESA1 abolished BIN2-dependent regulation of cellulose synthase activity. However, in this study was observed that CESA1 is also phosphorylated at S162 by an unknown protein kinase and that this priming phosphorylation is necessary for efficient CESA1^{T157} phosphorylation by BIN2 (Sánchez-Rodríguez et al., 2017). This suggests that this phosphorylation of CESA1 by BIN2, together with a second kinase, regulates the effects of BR on cellulose biosynthesis, contributing to the role of BR perception in regulating cell growth.

7. TTL Proteins are Essential for Plant Stress Tolerance

7.1 TTL Proteins Function in BR Signaling

In *Arabidopsis*, the *TETRATRICOPEPTIDE THIOREDOXIN-LIKE (TTL)* gene family is composed of four members (*TTL1* to *TTL4*). Mutations in *TTL1*, *TTL3*, and *TTL4* cause marked defects in BR responses (Amorim-Silva et al., 2019). Phenotypic, molecular, and genetic analyses show that TTL proteins are positive regulators of BR signalling in *Arabidopsis* (Amorim-Silva et al., 2019). BRs are perceived at the plasma membrane by ligand-induced hetero-dimers of the receptor kinases BRASSINOSTEROID INSENSITIVE1 (BRI1) and SOMATIC EMBBRYOGENESIS RECEPTOR KINASE (SERK) protein family members, which activates an interconnected signal transduction cascade, leading to the transcriptional regulation of BR-responsive genes BZR1 and BES1 (Fig. 9) (Belkhadir and Jaillais, 2015). The product *TTL3*, the most expressed *TTL* gene, directly interact with several BR signalling component including BRI1, BRI1-SUPPRESSOR1 (BSU1), and BZR1. Furthermore, co-immunoprecipitation and split yellow fluorescent proteins (YFP) experiments show that TTL3 is present in

a complex that also contains BIN2 and BR-SIGNALING KINASE1 (BSK1), which are two additional core-BR signalling components (Amorim-Silva et al., 2019). Cellular studies of *Arabidopsis* plants transformed with a functional TTL3-GFP protein indicate that while TTL3-GFP is mainly localized at the cytosol, treatment with exogenous BR caused an increased localization of this protein at the plasma membrane. On the other hand, reducing the amount of endogenous BR caused dissociation of TTL3-GFP from the plasma membrane. Furthermore, expression of TTL3 strongly increased the plasma membrane association of the BSK1 and BZR1, a plasma membrane and a cytoplasmic BR signalling component respectively (Fig. 9) (Amorim-Silva et al., 2019).

To sum up, in this report (Amorim-Silva et al., 2019) in which I am second author, we propose three, non-mutually exclusive, molecular mechanisms to explain how TTL proteins may optimize BR signalling (Fig. 9):

a) by acting as a BR-dependent cell surface localized scaffold to bridge plasma membrane and cytosolic BR signalling components, namely inducing the interaction between BSK1 and BZR1 at the plasma membrane,
b) by promoting BIN2 degradation/destabilization, although the related mechanism is still unknown,
c) by promoting BZR1 nuclear accumulation, likely via degradation/destabilization and consequent inactivation of the BZR1 negative regulator BIN2.

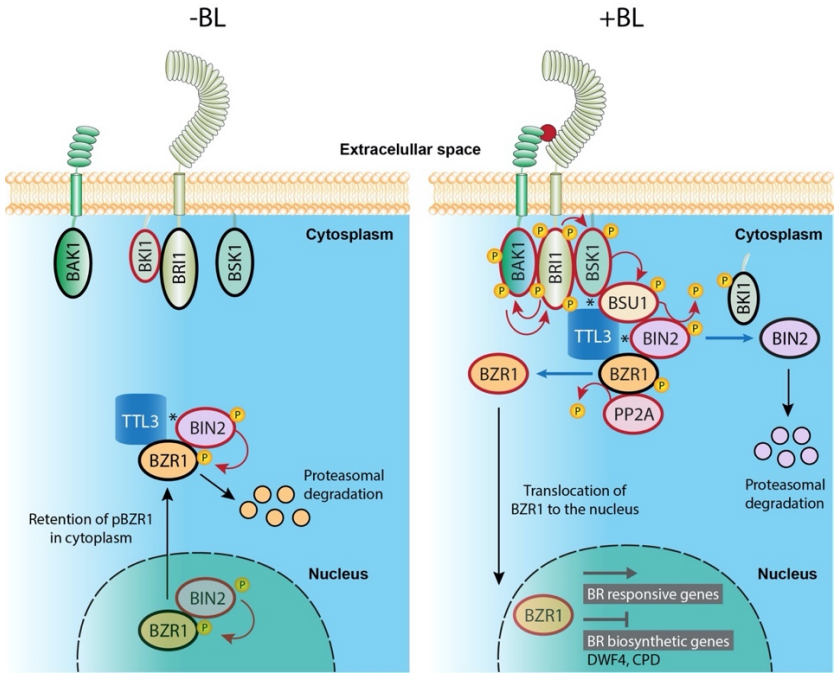

Figure 9. Model of TTL3 function in the BR signalling pathway. In BL absence, BIN2 is active and phosphorylates and inactivates BZR1 and also BES1 (not shown). In the presence of BL, BRI1 and BAK1 heterodimerise and are transphosphorylated. TTL3 relocalises to the plasma membrane and interacts with the phosphorylated BRI1 and thereby recruit the other BR signalling components including BSU1, BIN2 and phosphorylated BZR1. This scaffolding promotes inactivation of BIN2 and thus dephosphorylation of BZR1 through PP2A phosphatase. Finally, active BZR1 and BES1 (not shown) transcription factor are translocated into the nucleus to promote BR responses and inhibition of BR biosynthetic genes. Red protein outlines represent the active sate of a given BR signaling component, while de lack protein outlines represent the inactive state. Phosphorylated proteins are represented with a P in an orange circle. Asterisk represent that TTL3 associate with BSK1 and BIN2 but was not demonstrated if this interaction is or not direct interactions. TTL3, TETRATRICOPEPTIDE THIOREDOXIN-LIKE 3; BRI1, BRASSINOSTEROID INSENSITIVE 1; BAK1, BRI1-ASSOCIATED KINASE 1; BKI1, BRI1 KINASE INHIBITOR 1; BSK, BRI1 SUBSTRATE KINASE; BSU1, BRI1 SUPPRESSOR 1; BIN2, BRASSINOSTEROID INSENSITIVE 2; PP2A, PROTEIN PHOSPHATASE 2A; BZR1, BRASSINAZOLE-RESISTANT 1. Adapted from Amorim-Silva 2018 bioRxiv (doi: https://doi.org/10.1101/351056).

7.2 The TTL Gene Family and their Role During Adverse Conditions

As previously described, TTL1, TTL3 and TTL4, function as positive regulators of BRs signalling (Amorim-Silva et al., 2019). However, *TTL* genes were originally identified to have a role in salt tolerance. Indeed, mutations in *TTL1*, *TTL3*, and *TTL4* cause reduced growth under abiotic stresses such as salinity and drought that is characterized by reduced root elongation and impaired osmotic responses during seedling development (Rosado et al., 2006; Ceserani et al., 2009; Lakhssassi et al., 2012). This stress hypersensitivity is exacerbated in double and triple *ttl* mutants (Lakhssassi et al., 2012). *TTL2* is specifically expressed in pollen grains and does not have a role in stress tolerance, but it is important for male sporogenesis (Lakhssassi et al., 2012). Interestingly, phylogenetic analysis of sequenced genomes indicated that *TTL* genes are specific to land plants, specifically *TTLs* appeared in the Bryophytes group (Lakhssassi et al., 2012). However, cellulose synthase and other cellulose-related genes appeared before in evolution, specifically to the Charophytes and the Chlorophytes groups. Hence, *TTLs* could have appeared in evolution in land plants adaptation to face against the environmental conditions, such as the mentioned salt stress tolerance, in order to protect the integrity of the plant cell growth. *TTL* genes from *Arabidopsis*, and also from other land plant species, encode proteins with a common modular architecture containing six tetratricopeptide repeat (TPR) domains distributed in specific positions throughout the sequence and a C-terminal sequence with homology to thioredoxins (TRXL) (Rosado et al., 2006; Lakhssassi et al., 2012) (Fig. 10A). TPR domains are well-described protein–protein interaction modules. An *in silico* structural analysis of *Arabidopsis* TTL proteins predicts also the presence of an intrinsically disordered region (IDR) at the N terminus (Fig. 10A, Amorim-Silva et al., 2019). Prediction of TTL3 protein 3D structure using I-TASSER server (Zhang, 2008) and processed by PyMOL (Schrödinger), supports the presence of

an IDR at the N terminus with the rest of the protein forming a horseshoe-shaped structure composed of multiple helix-turn-helix motifs (Fig. 10B). This structure is consistent with TTL3 being involved in protein–protein interactions and the assembly of multiprotein complexes (Blatch and Lässle, 1999; D'Andrea and Regan, 2003; Yang et al., 2005).

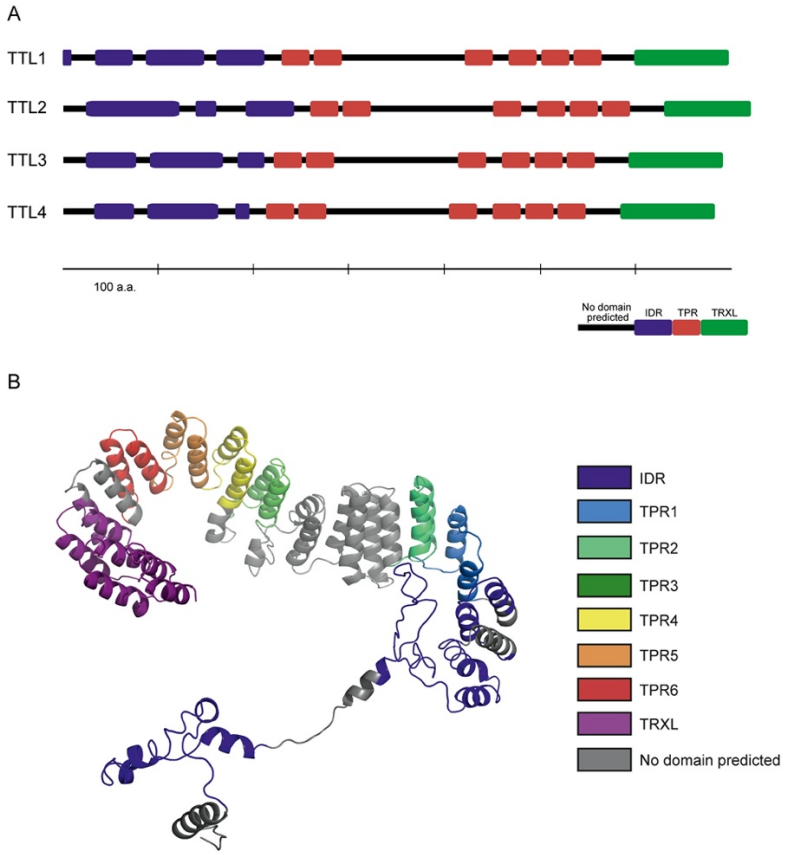

Figure 10. ***In silico*** **structural analysis of** ***Arabidopsis*** **TTL proteins. (A)** *TTL* genes contain an intrinsically disordered region (IDR) at the N terminus, six tetratricopeptide repeat (TPR) domains distributed in specific positions throughout the sequence and a C-terminal sequence with homology to thioredoxins **(B)** Structural model of TTL3 protein predicted in silico using I-TASSER server (Zhang, 2008) and processed by PyMOL (Schrödinger). C, C terminus; N, N terminus. Adapted from Amorim-Silva et al., 2019.

Although the molecular mechanism of how TTLs operate in BR signalling has been recently reported (Amorim-Silva et al., 2019), how TTL proteins function in stress tolerance remains elusive. Recent works revealed the

importance of BRs crosstalk with other hormones in mediating adaptation to abiotic stresses, such as drought, non-optimal temperatures and salinity (Nolan et al., 2017, 2020), which includes the appropriate integrity of the plant cell wall, during these adverse conditions, for a proper growth and development.

Whether the contribution of TTLs to the adaptation of the plant cell wall during salt stress episodes, is mediated by their role in BR signalling, in other signalling pathways, or as scaffolding components remains elusive. As mentioned, mutations in *TTL1*, *TTL3*, and *TTL4* cause reduced growth under abiotic stresses such as salinity and drought that are characterized by reduced root elongation and impaired osmotic responses during seedling development (Rosado et al., 2006; Ceserani et al., 2009; Lakhssassi et al., 2012). Similarly to *ttl* mutants, cellulose defective mutants typically displays an enhanced isotropic growth under salt stress conditions (Xu et al., 2008; Zhang et al. 2016; Kesten et al., 2019). Thereby, is plausible a possible connection between the maintenance of the plant cell wall integrity and the TTL function. Because *ttl* mutant growth is compromised during saline conditions, in this work we studied the role of TTL proteins in cellulose production, the major component of the plant cell walls and therefore, may have important biotechnological applications in crops.

Objectives

The main aim of this doctoral thesis is to investigate the role of TTL proteins in cellulose biosynthesis during adverse conditions.

Within this aim, includes specific objectives to achieve the main purpose of this work:

1. Characterization of cellulose-related phenotypes of *ttl* mutants in response to cellulose synthesis inhibitors: 4,5% sucrose, salt stress and isoxaben. This is included in Chapter 1.

2. Identify the molecular mechanism of TTL proteins in cellulose biosynthesis during adverse conditions. This is included in Chapter 1.

3. Genetic characterization of *TTL* genes relative to other pathways involved in cellulose biosynthesis. This is included in Chapter 2.

Material

and Methods

Table of contents

1. Plant Material

The Columbia (Col-0) ecotype of *Arabidopsis thaliana* was used in this study. The T-DNA insertions for *TTL* genes used in this study, have been described previously: *ttl1* (AT1G53300) Salk_063943; *ttl3* (AT2G42580) Sail_193_B05; *ttl4* (AT3G58620) Salk_026396; *ttl13*: *ttl1 ttl3* double mutant (Lakhssassi et al. 2012); *ttl134*: *ttl1 ttl3 ttl4* triple mutant (Lakhssassi et al. 2012). The *sos5-2* (SALK_125874) (Alonso et al., 2003) allele was obtained from the SALK T-DNA insertion collection. The *fei1*/*fei2* (Xu et al., 2008) and the *prc1-1* single mutant, which consist in a knock-out mutation in the *CESA6* gene (Desnos et al., 1996), were also used in this work. The Col *YFP-CESA6 TUA5-mCherry* and Col *TdT-CesA6* marker lines were provided by Clara Sanchez-Rodriguez (ETH Zurich) and subsequently crossed with *ttl13* to generate *ttl13 YFP-CESA6 TUA5-mCherry* and *ttl13 TdT-CesA6* lines.

2. PCR amplification and primers

Table 1. List of primers used for PCR amplification in this study.

Name	Sequence
FEI1 Topo Fw1	CACCATGATGGGCATCTGTGAGATGA
FEI1 Topo Rv1	ATCAGAGCTGGAATCATAAAATTCGC
FEI2 Topo Fw1	CACCATGGGCATCTGTCTAATGAAGC
FEI2 Topo Rv1	ATCGGAGCTGGAGTCGTAGA
FEI2-S5	ACAAATCGATATTGTGTGCAATGACAG
FEI2-A5	TCAATCGGAGCTGGAGTCGTAGAAG
LB *fei2-1*	TTACCCAACTTAATCGCCTTGCAGCACAT
FEI1-Sense	GAAGCTGGAAATGTTGAATGAAGA
FEI1-AS	TTAATCAGAGCTGGAATCATAAAATTC
LB-JMLB1	GGCAATCAGCTGTTGCCCGTCTCACTGGTG

eGFP Fw1	CGTGAACGGCCACAAGTTC
eGFP Rv1	CTCAGGTAGTGGTTGTCGGG
TdTomato dPCR Fw1	GGGCGAGGAGGTCATCAAAG
TdTomato dPCR Rv1	GATGACGGCCATGTTGTTGTC
SOS5 LP	GAAACTGGGAATAACCTTCGG
SOS5 RP	AGCTTCTCGAGACCAAACCTC
mCherry Fw1	TTGGATCCATGGTGAGCAAGGGCGAGGA
mCherry Rv1	GGTCCGGACTTGTACAGCTCGTCCATGC
TTL1DPCRF	TGGACTCACCACCACCACTA
TTL1DPCRR	ACCGAGTCTGCGAACAAGAT
TTL1-1_dPCR Fw1	TCACGAGATCCCCAATCTCTCT
TTL1-1_dPCR Rv1	TAGTGGTGGTGGTGAGTCCA
TTL1C_stop Fw1	AAAAAGCAGGCTCGATGCCCAAGTCAGTTAAACCCA
TTL1C_stop Rv1	AGAAAGCTGGGTGTTATCTAATAAGCAATAAGGCCAAACGGT
TTL3DF	AGAGAGCTGCGATGCTTGAT
TTL3DR	ATGCTCTCCTCCACATCCAC
SAIL_LB3	TAGCATCTGAATTTCATAACCAATCTCGATACAC
TTL3_3UTR Rv	AAAGCAAGCAGAGCCAAACTC
dPCR IDRremove Fw1	GTGAAGACACGGGAGCGAA
dPCR IDRremove Rv1	CAGCAACAAAACAAAAAGCCTCTC
IDRremove Fw1	GGAGGAACCAGCGGAAAG
IDRremove Rv1	CATCGTCGTCACTTCCTC
dPCR IDRremove TTL3-cDNA Fw1	CGGCGGATTTGTCCTACTCA
dPCR IDRremove TTL3-cDNA Rv1	CTTCTCCAGCGTCTGTAGCC
IDRremove TTL3-cDNA Fw1	GGAGGAACCAGCGGAAAGG
TTL3-cDNA Rv1	CATGGTGAAGGGGGCGGC
dPCR TTL3_IDR Fw	GTACTTGTTTCTGTCCGGCG
dPCR TTL3_IDR Rv	CGACTCACTATAGGGGATATCAGC
TTL3_IDR Fw1	AAGGGCGAATTCGACCCAGC
TTL3_IDR Rv1	TCCTCCGCCGCTGCGTAC
TTL4-1_dPCR Fw1	AGCTCGTGATGAACACTAAGAA
TTL4-1_dPCR Rv1	CTGAGAAGTGACAGCGGGTT
DT0-BsR2	ATATTATTGGTCTCAATCTCTTAGTCGACTCTACCAAT

TTL1-1-BsF	ATATATGGTCTCGATTGAGTTTGTCAGATTCAGAGATGTT
TTL1-1-F0	TGAGTTTGTCAGATTCAGAGATGTTTTAGAGCTAGAAATAGC
TTL3-1-BsF2	ATATTATTGGTCTCAAGATTGCCTGCTATAGATTCAATCACGTT
TTL3-1-F0	TGCCTGCTATAGATTCAATCACGTTTTAGAGCTAGAAATAGC
TTL4-1-R0	AACACGAGACGATGACGTCATCACAATCACTACTTCGTCTCTAACCAT
LBb 1.3	ATTTTGCCGATTTCGGAAC
U6-26p-F	TGTCCCAGGATTAGAATGATTAGGC
U6-29p-R	AGCCCTCTTCTTTCGATCCATCAAC
U6-29p-F	TTAATCCAAACTACTGCAGCCTGAC
U6-1p-R	TATGCAAGTCTCACTCACACTCACG
U6-29t-F	CGTGTTTCAGCTCTCATGATCCTTG
FEI1-C2	CACCATGAAAAAGCTTGGTAGAGTTGAG
TTL3-1_dPCR Fw1	TCAGGGAGATAAATCCGTAATCTT
TTL3-1_dPCR Rv1	AGCCATCTGAGAACTCACCG

PCR amplification design was specific for each experiment and primers listed in Table 1 were used for different purposes as follows:

(1) Diagnostic PCR. Diagnostic PCR was performed mainly in uniplex but also as multiplex (more than 2 primers per reaction). Reactions (50 µL; 0.2 mL microtube) were prepared as follows: ~1 µg DNA, 1 µM of each primer, 0.2 mM of dNTP mix (Promega), 2 mM of $MgCl_2$, 10 µL 5x Green GoTaq Reaction Buffer (Promega) and 0.25 µL of GoTaq DNA polymerase (Promega). PCR steps: (1) denaturation for 3 min at 95°C; (2) 35 cycles of denaturation for 45 s at 94°C, annealing for 30 s at 60°C, extension for 1 min per kb at 72°C; (3) final extension of 10 min at 72°C.

(2) *Escherichia coli* colony PCR. Reactions (25 µL; 0.2 mL microtube) were performed as follows: one *E. coli* colony was resuspended in 10 µL H_2O, mixed in a solution containing; 1 µM of each primer, 0.2 mM of dNTP mix (Promega), 2 mM of $MgCl_2$, 5 µL of 5x Colourless Go Taq Reaction Buffer (Promega) and 0.25

μL of GoTaq DNA Polymerase (Promega). PCR steps: (1) denaturation for 5 min at 95°C; (2) 35 cycles of denaturation for 45 s at 95°C, annealing for 30 s at 60°C, extension for 1 min/kb at 72°C; (3) final extension of 10 min at 72°C.

(3) ***Agrobacterium*** **colony PCR**. Reactions (25 μL; 0.2 mL microtube) were performed as follows: one *Agrobacterium* colony was resuspended in 10 μL H_2O, mixed in a solution containing; 1 μM of each primer, 0.2 mM of dNTP mix (Promega), 2 mM of $MgCl_2$, 5 μL 5x Colourless GoTaq Reaction Buffer (Promega) and 0.25 μL of GoTaq DNA Polymerase (Promega). PCR steps: (1) denaturation for 5 min at 95°C; (2) 35 cycles of denaturation for 45 s at 95°C, annealing for 30 s at 60°C, extension for 1 min/kb at 72°C; (3) final extension of 10 min at 72°C.

(4) Gateway cloning. PCR for Gateway cloning was performed in 50 μL Reactions as follows: ~1 μg DNA, 1 μM of each primer, 0.2 mM of dNTP mix (Promega), 2 mM of $MgCl_2$, 10 μL 5x Green GoTaq Reaction Buffer (Promega) and 0.25 μL of GoTaq DNA polymerase (Promega). PCR steps: (1) denaturation for 3 min at 95°C; (2) 35 cycles of denaturation for 45 s at 94°C, annealing for 30 s at 60°C, extension for 1 min per kb at 72°C; (3) final extension of 10 min at 72°C. Then, PCR product was purified from an 1% agarose gel using the Wizard® SV Gel and PCR Clean-Up System (Promega).

3. Site-specific Mutagenesis of Plasmid DNA

The truncated versions TTL3ΔIDR promoter::genomicDNA vectors were generated using the Q5 Site-Directed Mutagenesis Kit (New England Biolabs). Primers were designed using the NEB online primer design software NEBaseChanger™ (ww.NEBaseChanger.neb.com). PCR amplification of the desired sequence was performed as follows in Table 2 and Table 3.

Table 2. PCR mix for a Site-specific Mutagenesis reaction.

Reactive	25 µL Reaction	Final concentration
Q5 Hot Start High-Fidelity 2X Master Mix	12.5 µL	1X
10 µM Forward Primer	1.25 µL	0.5 µM
10 µM Reverse Primer	1.25 µL	0.5 µM
Template DNA (pTTL3::gTTL3 pENTR)	1 µL	1-25 ng
dH_2O	9 µL	

Table 3. PCR programme for a Site-specific Mutagenesis reaction.

Step	Temperature	Time
Initial Denaturation	98° C	30 seconds
25 Cycles	98° C	10 seconds
	60° C	30 seconds
	72° C	30 seconds
Final Extension	72° C	2 minutes
Hold	16° C	

PCR product generated was then incubated with the KLD Enzyme Mix at room temperature for 5 min. Then, KLD mix was transformed in *E. coli* and pENTR generated was confirmed by PCR amplification, digestion and sequencing.

4. Plant DNA Miniprep

Genomic DNA was extracted as described previously (Edwards et al. 1991) with some modifications. One leaf of 3 weeks-old *Arabidopsis* plants was grinded in extraction buffer (200 mM Tris-HCl pH 7.5, 250 mM NaCl, 25 mM EDTA, 0.5% SDS) using the Tissue Lyser II (Qiagen). Supernatant was transferred to a new tube and then centrifuged at 14000 rpm for 5 min. 300 µL of clarified supernatant was placed in a new tube and mixed with 300 µL of Isopropanol in order to precipitate nucleic acids, vortexed and centrifuged at 14000 rpm for 5 min. DNA pellet was washed with 500 µL of 70% ethanol and centrifuged for 2 min. Supernatant was discarded and pellet was resuspended in 50 µL of dH_2O.

5. Growth conditions

Seeds were surface sterilized using the chlorine gas method (Lindsey et al., 2017) and cold treated for 2-4 days at 4°C for stratification. For root elongation assays, seeds were sowed onto half-strength Murashige and Skoog (MS) agar solidified medium (0.6% [w/v] agar for horizontal growth and 1% [w/v] for vertical growth) containing 1.5% and 4.5% [w/v] sucrose as indicated in each figure legend and subsequently grown under cool-white light (at 120 µmol photon m^{-2} s^{-1}) with a long-day (at 16 h light/8 h dark cycle) or short-day photoperiod (at 8 h light/16 h dark cycle). For etiolated hypocotyl experiments, seeds were plated on media containing 1.5% sucrose, stratified for 2-4 days, exposed to light for 3 h and subsequently grown in dark conditions at 22°C for 4 days.

6. Treatment with Cellulose Synthesis Inhibitors

For *in vitro* assays, seeds were sowed in half-strength MS agar-solidified medium supplemented both with 4.5% sucrose [w/v] and with 1.5% sucrose plus 1 nM and 2 nM Isoxaben (Santa Cruz Biotechnology) and photographed either 4 days for etiolated seedlings or 7 days later for light-grown seedlings. For salt stress, seedlings were transferred from 1.5% sucrose plates to MS 1.5% sucrose plates supplemented with NaCl. Seedlings were transferred to NaCl plates after 2 days (etiolated seedlings) or 3 days (light-grown seedlings) and photographed 3 days or 7 days later, respectively. For confocal microscopy, 3-day-old etiolated seedlings were incubated in half-strength MS liquid medium supplemented both with 4.5% sucrose [w/v] or with 1.5% sucrose plus 200 mM NaCl.

7. Cell wall analysis

Cell wall analysis was performed as previously described (Kesten et al., 2019; Yeats et al., 2016) with some modifications . Plants were grown and treated as described in "Growth Conditions" and "Treatments with cellulose synthesis inhibitors" sections (Sections 5 and 6, repectivelly). Light-grown seedlings were covered from light 24 h before harvesting in order to avoid starch synthesis (Sorek et al., 2015) that contribute to glucose quantified in the analysis of the plant cell wall material. Tissue was harvested in 50 mL falcon tubes containing 70% ethanol until chlorophyll was completely depleted. Then, seeds were removed by hand as seeds produce its own cell wall and interferes in the analysis. Ethanol was drained at 60°C from tissue until was completely evaporated and resulting tissue was frozen and grinded (in 2 mL tubes Safe-Lock tubes, Eppendorf) with glass beads using the Tissue Lyser II (Qiagen). Alcohol-insoluble residue (AIR) was resuspended in chloroform:ethanol solution (1:1) and incubated at 4°C for 2

h using a regular rotator. Subsequently, solution was centrifuged at 14000 rpm for 10 minutes at room temperature. Pellet was washed with acetone for 30 min at room temperature and later centrifuged at 14000 rpm for 10 min at room temperature. Then, acetone was removed from AIR at 60°C overnight. One mg of remaining AIR was hydrolysed at 121°C with 4% sulfuric acid for Matrix Hydrolysis. For Saeman Hydrolisis, 1 mg of AIR was incubated with 72% sulfuric acid for 1 h at room temperature plus vortexing and incubated at 121°C for 1h with 4% sulfuric acid, afterwards. Crystalline cellulose content was the result of subtract glucose released by weak "matrix hydrolysis" from glucose released by strong "Saeman hydrolysis". Preceding to hydrolysis, 150 μg of sedoheptulose (CarboSynth, Item Number MS139006) was added to each sample as an internal standard. 10 μl of 1:10 dilutions of hydrolysed samples was measured on a Dionex ICS- 5000 using a ThermoFischer Scientific CarboPac PA20 column (3 × 150 mm, Product Number 060142) and accompanying CarboPac PA20 guard column (3 × 30 mm, Product Number 060144). Conditions for HPLC Eluents were performed as described in Kesten et al. 2019. All standard curve and hydrolysis sample peaks were integrated using Chromeleon 8.0 software.

8. CRISPR-Cas9-Mediated Mutations in *TTL* genes

Mutations in *TTL* genes were generated using the CRISPR-Cas9 system (Wang et al. 2015; Xing et al. 2014). All single guides RNAs (sgRNAs) were designed using the Cas Designer tool (http://www.rgenome.net) with a maximum nucleotide length of 20 (without the PAM sequence). sgRNAs were selected according to the Cas-OFF Finder tool (http://www.rgenome.net) analysis, in order to check off-targets genes in the *Arabidopsis* genome. Using pCBC-DT1DT2 and pCBC-DT2DT3 vectors (Xing et al., 2014) and sgRNA-containing primers, PCR amplification was performed as described in "PCR

amplification and primers" section. PCR product generated was cloned into the destination vector pHEE401 (Wang et al., 2015) using the golden gate system detailed in "PCR amplification and primers" section (Section 2). CRISPR-Cas9 construct was confirmed by PCR amplification and sequencing. Then, CRISPR-Cas9 vector generated was transformed in *A. thaliana* and transgenic plants were selected as described in "Generation of stable lines in *A. thaliana*" section (Section 10).

To genotype these mutant lines, T2 transgenic lines were sowed half-strength MS agar-solidified medium supplemented with 4.5% sucrose [w/v] in order to seek dramatic isotropic phenotypes in 7-days-old light-grown seedlings. Then, total DNA was extracted from T2 transgenic plants and fragments containing the target sites were amplified by PCR using gene-specific primers described in "PCR amplification and primers" section (Section 2) and confirmed by sequencing.

9. Plasmid constructs

The genomic and coding sequence for each gene were amplified as detailed in "PCR amplification and primers" section (Section 2). Subsequently, PCR products were introduced into the pENTR/D-TOPO vector using the pENTR Directional TOPO cloning kit (Invitrogen). Expression clones were obtained by Gateway LR-reaction (Invitrogen) using an expression clone for each gene of interest. All plasmid constructs used in this work were further confirmed by PCR amplification, digestion and sequencing.

The pGWB4 and pGWB5 vectors, from the pGWB vector series, were provided by Tsuyoshi Nakagawa (Department of Molecular and Functional

Genomics, Shimane University; Nakagawa et al., 2007) and were used as pDEST for either transient expression in *Nicotiana benthamiana* or generating stable lines in *A. thaliana*. For Bimolecular Fluorescence Complementation (BiFC) assays, pDEST- GW-VYNE and pDEST-GW-VYCE (Gehl et al. 2009) were used. Finally, the pGADT7(GW) and pGBKT7(GW) destination vectors were provided by Salomé Prat (Centro Nacional de Biotecnología-Consejo Superior de Investigaciones Científicas) and were used for generating the different TTL versions in order to perform the yeast two-hybrid assay. The prey and bait N- and I-domains vectors of cellulose synthases were provided by Clara Sánchez-Rodríguez (ETH Zúrich, Switzerland). The pCBC-DT1T2 and pCBC-DT2T3 were a gift from Qi-Jun Chen (Addgene plasmid #50590; http://n2t.net/addgene:50590; RRID:Addgene 50590). The pHEE401 was a gift from Qi-Jun Chen (Addgene plasmid # 71286; http://n2t.net/addgene:71286; RRID:Addgene 71286).

10. Generation of stable lines in *A. thaliana*

Expression clones were transformed into *Agrobacterium tumefaciens* strain GVG3101::pMP90 through electroporation and then confirmed by diagnostic PCR. The pGWB4 harbouring the truncated line *TTL3p::ΔIDR-TTL3g-GFP* construct was transformed into *Arabidopsis* plants by floral dipping (Clough and Bent, 1998) to generate stable transgenic plants. *TTL3p::ΔIDR-TTL3g-GFP* line was transformed into the *ttl13* double mutant. Seeds obtained were sowed in half-strength MS agar-solidified medium supplemented with 1.5% sucrose [w/v] and with 50 μg/mL Hygromycin B (Duchefa). T3 or T4 homozygous transgenic plants were used in this study.

11. Transient expression in *N. benthamiana*

Transient expression in *N. benthamiana* was performed following the protocol described by (Y. Yang, Li, and Qi 2000). *A. tumefaciens* (GV3101::pMP90) carrying the different constructs was used together with the p19 strain. Cultures were grown overnight in Luria-Bertani (LB) medium containing rifampicin (50 mg/mL), gentamycin (25 mg/mL) and antibiotic specific for the positive selection of colonies carrying the plasmid construct. Individual agrobacteria colonies were used for inoculation on LB for a given construct. After overnight culture incubation at 28°C, *Agrobacterium* cells were collected by centrifugation (15 min at 3000g in 50-mL falcon tubes) at room temperature and pellets were resuspended in agroinfiltration solution (10 mM MES, pH 5.6, 10 mM $MgCl_2$ and supplemented with 100 μM acetosyringone) afterwards. Subsequently, cultures were incubated for 2-4 h at room temperature in dark conditions. Bacterial suspension was adjusted at OD_{600} of 0.8 for the constructs and 0.2 for the p19 strain to reach a final OD_{600} of approximately 1 for agroinfiltration. For double infiltration experiments, Agrobacterium strains were infiltrated at OD_{600} of 0.4 for each construct and at OD_{600} of 0.2 for the p19 strain. Cultures were infiltrated in 4-week-old *N. benthamiana* leaves using 1mL syringes (BD Plastipak) at the abaxial side of the leaf. After infiltration, all plants were kept in the greenhouse and analysed 2 days later.

12. General extraction of Total Protein from *Arabidopsis*

Arabidopsis tissue was collected in 2 mL Safe-Lock tubes (Eppendorf), three 3 mm diameter stainless steel beads were added to the tubes and then tissue was ground to a fine powder in liquid nitrogen using the Tissue Lyser II (Qiagen). Approximately 100 mg of ground tissue per sample was used for protein

extraction. Plant material was subsequently homogenized and incubated in 200 mL of 2X Laemmli buffer (125 mM Tris-HCl, pH 6.8, 4% [w/v] SDS, 20% [v/v] glycerol, 2% [v/v] β-mercaptoethanol, and 0.01% [w/v] bromophenol blue) for 5 min at 95°C, centrifuged (5 min at 20000g) at room temperature. Finally, total proteins from supernatant were separated in a 10% SDS-PAGE gel and analysed as described in the "Western blot and image analysis" section (Section 13).

13. Western blot and image analysis

Protein extraction was performed as previously described in Laemmli ,1970 and in the "General extraction of Total Protein from *Arabidopsis*" section (Section 12). SDS-PAGE polyacrylamide gel was placed in an electrophoresis cuvette in constant electromotive force (80V). SDS-page gels were electroblotted using Trans-blot Turbo Transfer System (Bio-Rad) onto polyvinylidene difluoride (PVDF) membranes (Immobilon-P, Millipore) using the preprogramed protocols and set specifically for each protein size. PVDF membranes, were then incubated with the appropriate either primary or secondary peroxidase-conjugated antibody. In this work, the following primary antibodies were used for detection of epitope-tagged proteins: mouse monoclonal anti-GFP clone B-2 (1:600, catalog no. sc-9996, lot no. C0619, Santa Cruz Biotechnology), and mouse monoclonal anti-HA clone HA-7 (1:3000, catalog no. H3663, Sigma-Aldrich). The secondary antibodies used in this study were as follows: anti-mouse IgG whole molecule-Peroxidase (1:80,000; catalog no. A9044, lot no. 031M4752, Sigma-Aldrich). Proteins electroblotted in PVDF membranes were detected using either the Clarity ECL Western Blotting Substrate or SuperSignal West Femto Maximum Sensitivity Substrate according to the manufacturer's instructions, and images of different time exposures were acquired using the Chemidoc XRS1 System (Bio-Rad). PVDF membranes were

stained with colloidal Coomassie Brilliant Blue R 250 (Neuhoff et al., 1988) as loading control for the different samples in a given experiment.

14. Protein Extraction and Co-IP in *N. benthamiana*

Protein extraction and Co-IP in *N. benthamiana* were performed as described previously (Kadota et al., 2016) with some modifications. Briefly, 4-week-old *N. benthamiana* plants were used for transient expression assays as described in "Transient Expression in *N. benthamiana*" section (Section 11). *N. benthamiana* leaves were mainly ground to fine powder in liquid nitrogen. Approximated 0.5 g of ground leaves per sample was used, and total proteins were then extracted with extraction buffer (50 mM Tris-HCl, pH 7.5, 150 mM NaCl, 10% glycerol, 10 mM EDTA pH8, 1 mM NaF, 1 mM $Na_2MoO_4 \cdot 2H_2O$, 10 mM DTT, 0.5 mM PMSF, 1% [v/v] P9599protease inhibitor cocktail [Sigma-Aldrich]); Nonidet P-40, CAS: 9036-19-5 [USB Amersham Life Science] 0.5% (v/v), added at 2 mL/g powder using an end-over-end rocker for 30 min at 4°C. Samples were centrifuged 20 min at 4°C and 9000 rpm (9056 g). Supernatants (approx. 4 mg/mL protein) were filtered by gravity through Poly-Prep chromatography columns (731-1550, Bio-Rad), and 100 μL was used as input. The remaining supernatants were incubated for 2h at 4°C with 15 μL of GFP-Trap coupled to agarose beads (Chromotek) in an end-over-end rocker. During incubation of protein samples with GFP-Trap beads, the final concentration of detergent (Nonidet P-40) was adjusted to 0.2% (v/v) in all cases in order to avoid unspecific binding to the matrix as recommended by the manufacturer. Subsequent incubation, beads were collected and washed four times with the wash buffer (similar to extraction buffer but without detergent). Finally, beads were resuspended in 75 mL of 2X concentrated Laemmli sample buffer and heated at 70°C for 20min to dissociate immunocomplexes from the beads. Total (input),

immunoprecipitated (IP), and CoIP proteins were separated in a 10% SDS-PAGE gel and analysed as described in the section "Immunoblot".

15. Confocal Imaging of *N. benthamiana*

All confocal images were obtained using a Zeiss LSM880 confocal microscope, without the airyscan unit, equipped with a 488-nm argon laser for GFP and YFP. For confocal imaging of *N. benthamiana* leaves in coexpression and BiFC experiments, GFP or YFP fluorescence of the lower epidermis of the leaf was visualized with the confocal 2 d after infiltration.

16. Spinning disc confocal microscopy

GFP-tagged proteins were imaged with a CSU-X1 Yokogawa spinning disc head fitted to a Nikon Ti-E inverted microscope with a CFI APO TIRF ×100 N.A. 1.47 oil immersion objective, an evolve charge-coupled device camera (Photometrics Technology, USA), and a ×1.2 lens between the spinning disc and camera. The 3-day-old dark grown seedlings were mounted on the microscope stage as described by Gutierrez et al. (2009) and analysed by the FIJI software (Schindelin et al., 2012). Drifts were corrected by using the plugin StackReg. Backgrounds were subtracted by the "Subtract Background" tool (rolling ball radius, 50 pixels).

17. Bimolecular Fluorescence Complementation (BiFC) Assays in *N. benthamiana*

Leaves were co-agroinfiltrated as described in "Transient Expression in *N. benthamiana*" (Section 11) with the *Agrobacterium* strain harbouring a construct to express a given protein fused to the N-terminal half of YFP and the BiFC partner protein fused to the C-terminal half of YFP, and vice versa to test both BiFC directions. Leaves were observed using a confocal microscope 2 d after infiltration, as described in the section "Confocal Imaging of *N. benthamiana*" (Section 15).

18. Image analysis and processing

For confocal experiments, images were processed as detailed in "Confocal Imaging of *N. benthamiana*" (Section 15), using the FIJI software (Schindelin et al., 2012). For root and hypocotyl measurements, each seedling was measured independently through the "free hand" tool of FIJI software and data was processed and analysed using the Graphpad Prism® 8 software (GraphPad Software, www.graphpad.com), in order to perform the statistical analysis of a given experiment.

19. Stereo Microscopy of *Arabidopsis* Seedlings

Arabidopsis seedlings images were acquired using the ZEISS SteREO Discovery V12 with digital cam Axiocam 503 color (excitation wavelengths 488 nm and emission wavelengths 498 nm to 550 nm). Transgenic plants harbouring a given fluorescent tag were selected using the colour filters. WT Col-0 seedlings

were used as a negative control to subtract the chlorophyll fluorescence background.

20. Statistics

For statistical analysis, one-way analysis of variance (ANOVA) followed by: (1) Tukey's multiple comparison test ($P < 0.05$) for roots; (2) Fisher's Least Significant Difference (LSD) test for hypocotyls; were performed using Prism 8.00 for Mac (GraphPad Software, www.graphpad.com). Different lowercase letters in the graphs indicate significant differences between genotypes ($P \leq 0.05$). Data represent mean values and error bars are SEM.

21. *In Silico* Three-Dimensional Structural Model of TTL3

The *in silico* protein structure prediction for TTL3 protein was generated by submitting full-length primary sequences to the I-TASSER server (Zhang, 2008) and processed by PyMOL (Schrödinger). IDRs were predicted using GlobPlot 2 tool (http://globplot.embl.de/). TPR and thioredoxin-like (TPRX) domains were predicted using the SMART/Pfam server and were described previously (Lakhssassi et al., 2012).

22. Accession Numbers

Sequence data from this thesis can be found in the EMBL/GenBank data libraries under the following accession numbers: AT1G53300 for *TTL1*, AT3G14950 for *TTL2*, AT2G42580 for *TTL3*, AT3G58620 for *TTL4*, AT4G32410 for *CESA1*, AT5G64740 for *CESA6*, AT5G05170 for *CESA3*, AT3G46550 for *SOS5*,

AT1G31420 for *FEI1*, AT2G35620 for *FEI2*, AT5G19780 for *TUA5*, AT1G45688 for *CC1*, AT5G42860 for *CC2*.

23. Yeast Two-Hybrid Assay (Y2H)

23.1 Yeast Transformation

The Yeast GAL4 Two-Hybrid System (Clontech Laboratories) was used for testing the interaction between TTL3 and TTL3 truncated version with different domains of cellulose synthases. The generation of bait and prey constructs are explained in the section "Plasmid Constructs" (Section 9). The bait and prey plasmids were transformed into *Saccharomyces cerevisiae* strain AH109_240719 as described previously (Gietz and Schiestl, 1995). *S. cerevisiae* preculture was incubated at 30°C overnight and subsequently inoculated and incubated at 30°C in 50-mL Yeast-Peptone-Dextrose-Adenine (YPDA) media at a final OD_{600} of 0.2. Culture was then centrifuged at 4000 rpm for 4 min once reached OD_{600} of 0.8-1. Pellet was washed with sterile $_{dd}H_2O$, centrifuged, washed with 0.1 M lithium acetate (LiAc) and finally centrifuged at 4000 rpm. Pellet was resuspended in 0.1 M AcLi and aliquoted 50 µL into microcentrifuge tubes containing: 50% polyethylene glycol (PEG), 36 µL 1 M AcLi, 2 µL of binding domain (BD) and 2 µL of activation domain (AD) of Gal4 vectors and sterile $_{dd}H_2O$. Tubes were incubated at 30°C for 30 min and then incubated at 42°C for 30 min. Cells were centrifuged at 4000 rpm for 3 min and pellet was resuspended in sterile $_{dd}H_2O$. 100 µL cells were sowed into plasmid-selective media plates: Yeast Nitrogen Base (YNB) media supplemented with Methionine (Met), Lysine (Lys), Uracil (Ura), Histidine (His) and Adenine (Ade). Plates were incubated at 28°C for 4 d.

23.2 Y2H Interaction Analysis

Independent colonies for each bait–prey combination, were resuspended in 200 mL of sterile water. Tenfold serial dilutions were made and 5 μL of each dilution were spotted onto three alternative interaction-selective medium: A: YNB, Met, Lys, Ura, 2 mM 3-amino-1,2,4-triazole (3-AT); B: YNB, Met, Lys, Ura, Ade; C: YNB, Met, Lys, Ura, Ade, 2mM 3-AT. Plates were incubated at 28°C and photographed 3 or 7 d later.

Chapter 1

TTL proteins stabilize the Cellulose Synthase Complex during adverse conditions

Table of contents

1. Introduction

Changes in environmental conditions have a detrimental impact on plant growth leading to reduced biomass production (Qin et al., 2011). Abiotic stresses, including drought, heat, cold, and salinity, are estimated to be the causative factor for up to 50% of yield loss for various crop species (Boyer, 1982). However, mechanisms that link salt stress and the biomass producing capabilities of plants remain tenuous.

Plant biomass is largely made up of plant cell walls, which provide the major sustainable resource for many human products including feed, food, and fuel (Somerville et al., 2010; McFarlane et al, 2014). Cellulose contributes the main bulk of plant cell walls and is the most abundant biopolymer on Earth. Cellulose is a paracrystalline structure of β-(1→4)-D-glucan chains synthesized by cellulose synthases (CESAs) complexes (CSCs). CSCs are typically arranged as hexameric rosettes (Mueller and Brown, 1980) and can crystallize into cellulose microfibrils connected by intra- and inter-molecular hydrogen bonds (McFarlane et al, 2014). These microfibrils provide the main cell wall tensile strength and are essential for plant development (Höfte and Voxeur, 2017). Because cellulose is the main load-bearing polymer of the cell wall, the length, angle, and crystallinity of cellulose microfibrils are important determinants of the physical properties of the cell wall (Nishiyama, 2009).

Plants cell walls contain two different types of cell walls; a primary wall that surrounds all growing cells and a secondary wall that provides support to specialized cells, located between the protoplasm and the primary cell wall (McFarlane et al., 2014; Meents et al., 2018). In some species, gelatinous layer walls are deposited between the plasma membrane and the secondary cell wall,

composed mainly composed of polysaccharides and capable of generating contractile forces, where cellulose contributes with the 85% of the composition and is deposited (Gorshkova et al., 2018; Anderson and Kieber, 2020). The CSCs are characterized to contain three distinct CESA subunits to form a functional complex (McFarlane et al., 2014; Kieber and Polko, 2019). Thus, the primary wall CSCs in *Arabidopsis* require *CESA1*, *CESA3*, and a *CESA6-like* gene such as *CESA6, CESA2* or *CESA5* to be functional (Thierry et al., 2007; Persson et al., 2007; Kieber and Polko, 2019). The CSCs are assumed to be assembled in the endoplasmic reticulum (ER) or Golgi and are transported to the cell surface where they are inserted into the plasma membrane adjacent to cortical microtubules (Gutierrez et al., 2009). The CESAs are also found in small post-Golgi-related compartments referred to SmaCCs (Gutierrez et al., 2009), or MASCs (Crowell et al., 2009), involved in either exo- or endocytosis of the CSCs (Crowell et al., 2009; Gutierrez et al., 2009).

According to the current model, cellulose biosynthesis correlates with the movement of CSCs at the plasma membrane (i.e. direction and speed) essential for deposition of nascent cellulose microfibrils (Gutierrez et al., 2009). The tracks of the moving CESAs co-align with the underlying cortical microtubules (MT), supporting that these cytoskeletal fibrils guide the CSCs while producing cellulose (Gutierrez et al., 2009; Kesten et al., 2019).

Salt stress has serious consequences for plant growth and crop production (Munns and Tester, 2008). Cellulose defective mutants are especially sensitive to saline conditions, mostly caused by a salt-induced impairment of the microtubule cortical array (Endler et al., 2015). In fact, microtubules are disassembled rapidly after exposure to salt and other osmotic stresses (Komis et al., 2002) and the subsequent repolymerization is required for plant cells adaptation to stress episodes (Wang et al., 2007). In *Arabidopsis*, several *CESA*

genes have been predicted to be involved in salt stress responses by *in silico* analyses (Heyndrickx and Vandepoele, 2012). In fact, salt treatment negatively affects CESA trajectories at the plasma membrane, due to microtubule depolymerization, leading to defective cellulose deposition (Paredez et al., 2006). Furthermore, mutations in the companion of cellulose synthase (CC) proteins cause a permanent decrease of CSC density in the plasma membrane during salt stress episodes (Endler et al., 2015; Kesten et al., 2019). According to that, authors underline a mechanism about how integral CSC components to sustain cellulose biosynthesis during adverse conditions.

Plant growth is achieved mostly by cell expansion. To achieve directional growth, the deposition of cellulose microfibrils perpendicular to the axis of growth is important for cellular anisotropic expansion (McFarlane et al., 2014). Therefore, the inhibition of cellulose biosynthesis caused by salt stress leads to a decrease in growth anisotropy in cellulose-defective mutants (Kesten et al., 2019; Kieber and Polko, 2019).

In *Arabidopsis*, the *TETRATRICOPEPTIDE THIOREDOXIN-LIKE (TTL)* gene family is composed of four members (*TTL1* to *TTL4*). The *TTL1* gene was originally identified to have a role in salt tolerance (Rosado et al., 2006). Later it was found that mutations in *TTL3*, and *TTL4* also cause reduced growth under abiotic stresses such as salinity and drought that is characterized by reduced root elongation and impaired osmotic responses during seedling development (Rosado et al., 2006; Ceserani et al., 2009; Lakhssassi et al., 2012). However, the mechanism that described the role of TTL proteins in the adaptative response to salt stress remains unknown. Because salt stress negatively affects the plant cell wall integrity, causing an isotropic growth in *ttl* mutants, in this work we studied the role of TTL proteins in cellulose production, the major component of the plant cell walls.

2. Results

2.1 Mutants in *TTL* Genes Show Phenotypes Typical of Mutants Deficient in Cellulose Biosynthesis

Mutations in *TTL* genes cause decreased root growth and isotropic cell expansion at high concentrations of NaCl but not during standard growth conditions (Rosado et al., 2006; Lakhssassi et al., 2012). Because disruption of anisotropic cell expansion is a hallmark of mutants that show defects in the synthesis or organization of cellulose microfibrils (Xu et al., 2008; Endler et al., 2015; Zhang et al., 2016), we investigated a possible role of *TTL* genes in cellulose biosynthesis.

Genes that have a role in cellulose biosynthesis are often transcriptionally co-expressed with the *CESA* genes (Persson et al., 2005; Endler et al., 2015; Sánchez-Rodríguez et al., 2017). Therefore, we determined the co-expression of *TTL* genes together with *CESA1* using GeneMANIA (Heyndrickx and Vandepoele, 2012). Remarkably, *TTL1*, *TTL3*, and *TTL4* show co-expression with most of the *CESAs* involved in primary cell wall such as *CESA1*, *CESA3*, and *CESA6-like* genes (*CESA6, CESA2* and *CESA5)*, and with *CSI1* (Fig. 1), supporting an involvement of *TTL* genes in cellulose production.

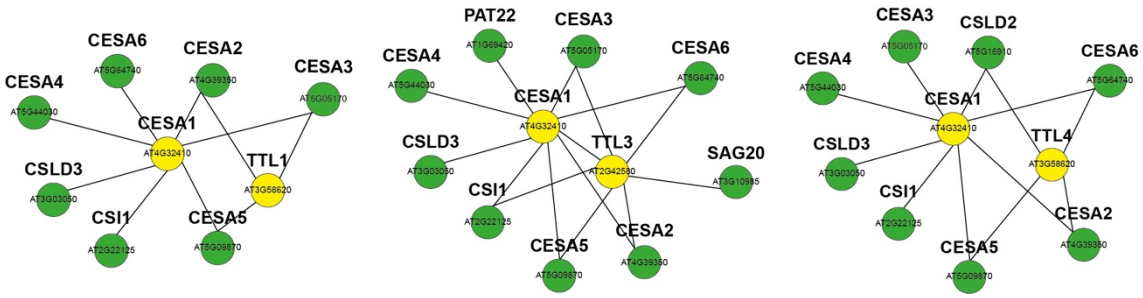

Figure 1. *TTL* genes co-express with the primary *CESA* genes. Truncated co-expression network for primary wall cellulose-related genes using the GeneMANIA tool (Heyndrickx and Vandepoele, 2012). Yellow balls represent genes used as inputs. Green balls represent co-expressed genes in the network. Black lines indicate direct coexpression.

Next, we determined whether single *ttl* mutants phenocopy mutants that are defective in cellulose biosynthesis. We started by analysing the response of individual *ttl* mutants to MS media supplemented high sucrose (4.5%) that is known to exacerbate the isotropic cell expansion characteristic of cellulose-defective mutants (Fagard, 2000; Xu et al., 2008). In fact, identification and analysis of new mutants affected in cellulose have been performed in medium supplemented with high concentrations of sucrose (Fagard, 2000; Polko et al., 2018; Yang et al., 2015). In these conditions, both *ttl1* and *ttl3* showed shorter roots and exhibited a strong radial expansion of root tips compared to WT seedlings (Fig. 2A-B), while in contrast, roots of *ttl2* and *ttl4* were similar to WT. We then investigated the redundancy of *TTL1*, *TTL3*, and *TTL4* in sucrose responses by analysing the growth of a *ttl1 ttl3* double mutant (*ttl13*) and a *ttl1 ttl3 ttl4* (*ttl134*) triple mutant under 4.5% sucrose. No obvious differences among on root swelling were found between *ttl13* and *ttl134*, but both displayed additive isotropic growth than either *ttl1* or *ttl3* single mutants (Fig. 2A-B). Further quantification indicated that *ttl13* and *ttl134* root growth were similar to WT in control conditions, while both mutants showed a similar reduction in root length and isotropic growth compared to WT roots under 4.5% sucrose (Fig. 2C, D, F). In addition to root growth defects, components involved in cellulose biosynthesis usually show defective hypocotyls (Endler et al., 2015; Yang et al., 2015). We

found that *ttl13* and *ttl134* show a similar reduction in hypocotyl length relative to the WT under 4.5% sucrose (Fig. 2E). Taken together, this data indicates that *TTL1* and *TTL3* play an important role in maintaining proper root and hypocotyl growth under high sucrose.

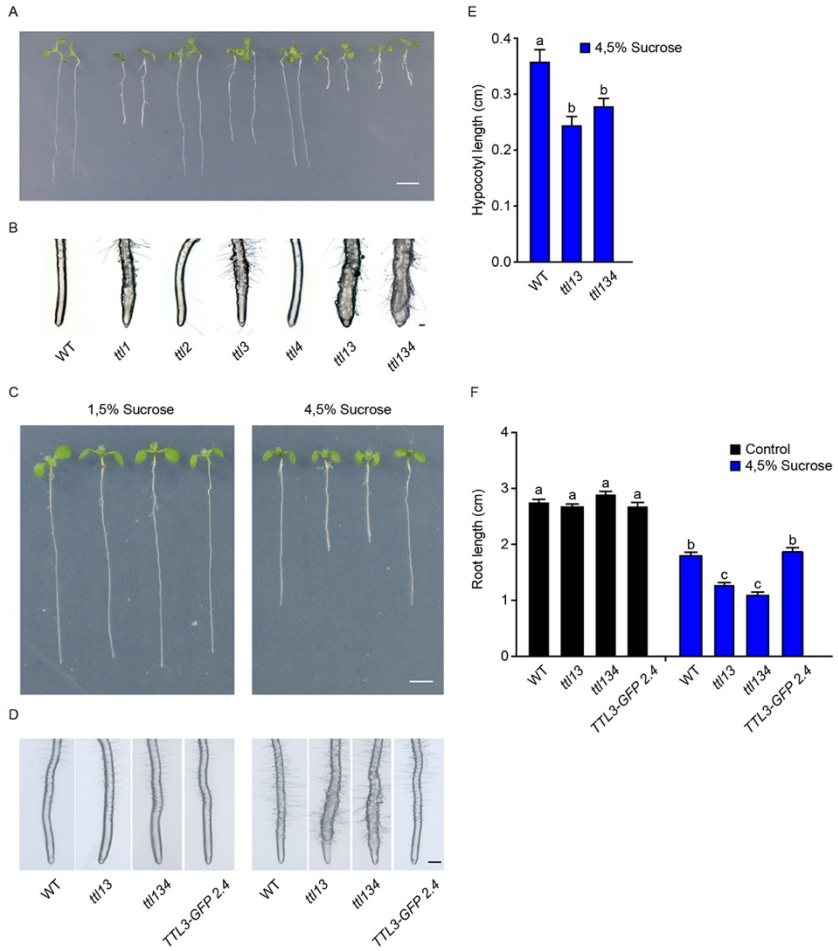

Figure 2. *TTL1* and *TTL3* genes are essential for maintaining an appropriate plant growth in presence of high levels of sucrose. (A) Root phenotype of *ttl* single, double and triple mutant roots in 4.5% sucrose. Seedlings were germinated in half-strength MS agar solidified medium supplemented with 4.5% sucrose and photographed 8 days later. Bar = 5 mm **(B)** Close-ups of root tips from seedlings represented in (A). Bar = 200 μm. **(C)** *TTL4* mutation do not contribute to the *ttl134* seedlings phenotype and *TTL3* expression results crucial to complement the *ttl13* mutation. Seedlings were germinated in half-strength MS agar solidified medium supplemented with either 1.5% sucrose or 4.5% sucrose and photographed 8 days later. Bar = 3 mm. **(D)** Close-ups of root tips from seedlings represented in (D). Bar = 300 μm. **(E)** Defective hypocotyl elongation in *ttl* mutants. Quantification of etiolated seedlings germinated in half-strength MS

agar solidified medium supplemented with 4.5% sucrose and photographed 4 days later. **(F)** Quantification of root elongation from (D). Data were analysed first with two-way ANOVA and then with Tukey's multiple comparison test; $P < 0.05$. Data represent mean values, error bars are SEM, n = 30 seedlings per experiment. The experiment was repeated three times with similar results.

2.2 Generation of New Alleles Using the CRISPR/Cas9 System

T-DNA insertion in *Arabidopsis* mutants can originate transcripts that could encode for truncated protein version that partially preserve its biological function in some cases (Wang and Wang, 2008). In order to validate that *ttls* T-DNA Salk lines previously described as complete knock-out mutants (Lakhssassi et al., 2012), we generated new *ttls* mutant alleles using CRISPR/Cas9 system. Thereby, we designed one single guide RNA (sgRNA) for *TTL1*, *TTL3* and *TTL4* genes, located near the sequence encoding the IDR of the TTL proteins (Fig. 3A). After transformation of Cas9-sgRNAs plasmid harbouring the three sgRNA into WT plants by floral dipping we selected a total of 94 hygromycin resistant lines. T2 segregating lines were then germinated in 4.5% sucrose analysed for isotropic root growth. In seven independent transgenic lines at least, one seedling displayed isotropic growth. Interestingly, in line #42 almost 90% of the seedlings presented isotropic growth, while in three other lines (#43, #41 and #49) presented a 50% of seedlings with isotropic growth. In addition, in lines #3, #7 and #93, a 10% of the seedlings presented isotropic growth (Fig. 3B). Because new CRISPR mutants showed an identical altered growth pattern when compared with the *ttl13* and *ttl134* T-DNA mutants, we confirmed that previously described TTL T-DNA Salk lines cause a knock-out mutation in the *TTL* genes analysed.

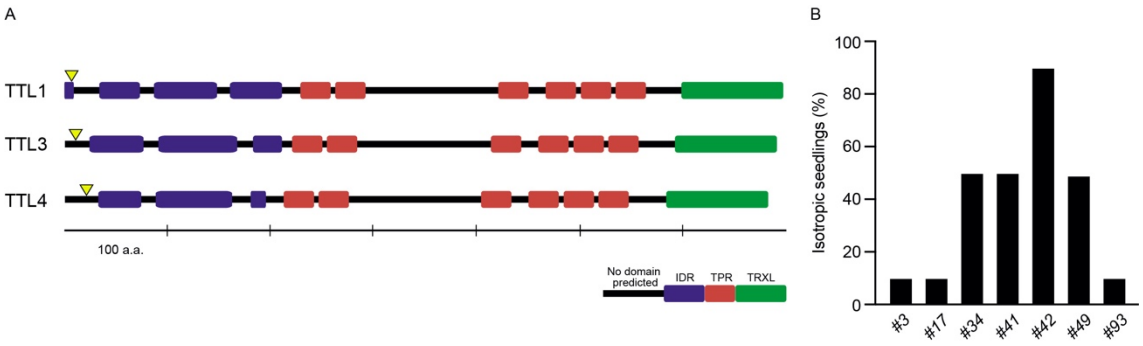

Figure 3. *ttl134* mutant generated using CRISPR present altered root growth in 4.5% sucrose. **(A)** Schematic representation of the spatial location of the target site of the single guides RNA (sgRNA) for *TTL1* (a.a. position 7), *TTL3* (a.a position 11) and *TTL4* (a.a position 21). Yellow arrowheads represent the respective target site of the sgRNA. **(B)** Mutations generated by CRISPR/Cas9 in the N-terminal region of TTLs cause isotropic root growth in seedlings. T2 seeds were germinated in half-strength MS medium supplemented with 4.5% sucrose and isotropic growth within the respective line was analysed 8 days later. In the graph, only T2 lines that showed at least one isotropic seedling are represented. 94 hygromycin-selected independent lines were tested in this study.

Cellulose deficiency mutants show hypersensitive growth under salt stress (Endler et al., 2015; Zhang et al., 2016), a phenotype previously described for *ttl* mutants (Rosado et al., 2006; Lakhssassi et al., 2012). Although no significant differences in hypocotyl length between *ttl13* and WT were found in control conditions or after NaCl treatment (Fig. 4A), *ttl13* displayed a marked isotropic hypocotyl expansion compared to WT after NaCl treatment (Fig. 4B-C). Surprisingly, increased isotropic expansion of *ttl13* relative to WT was also evident at control conditions (Fig. 4B-C). Moreover, while *ttl13* was indistinguishable from the WT on control medium, it showed decreased root growth and radially swollen roots after 4 days of transfer to plates containing 50 mM and 100 mM NaCl (Fig. 4D-F).

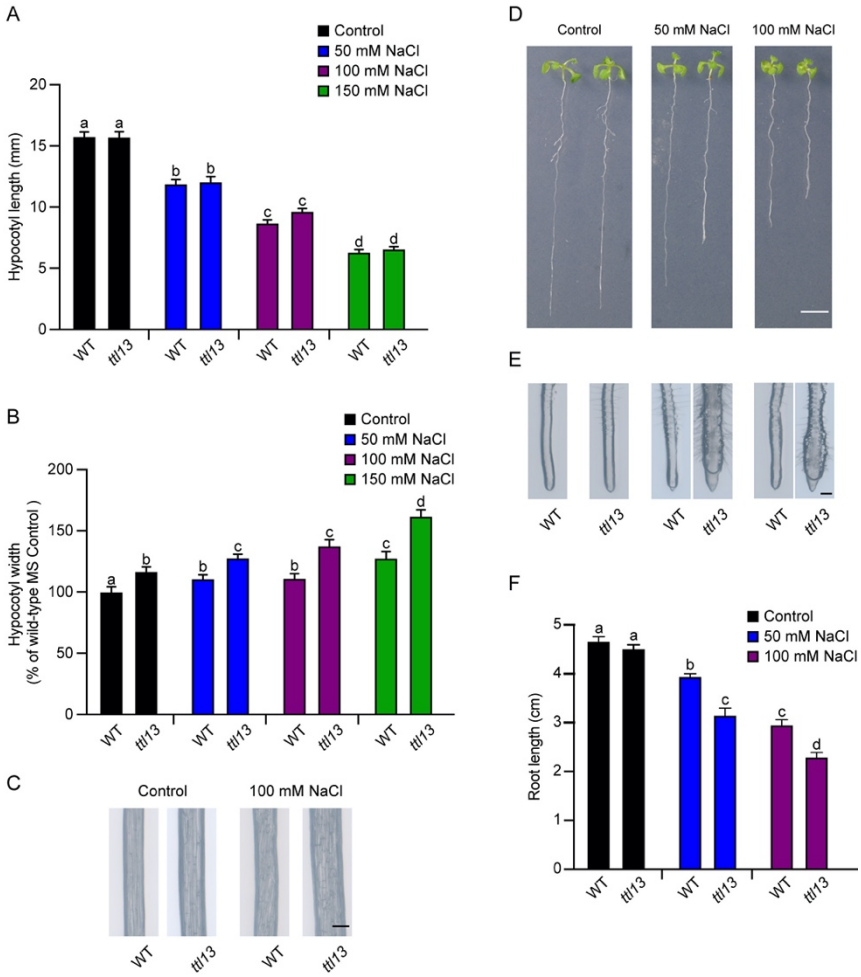

Figure 4. *ttl13* double mutant shows defects in plant adaptation to saline conditions. (A) *ttl13* hypocotyl growth is negatively affected during salt stress. Hypocotyl length quantification of seedlings that were germinated and grown for 2 days on MS agar-solidified medium (1.5% sucrose) and transferred to MS agar-solidified medium (1.5% sucrose) supplemented without and with 50, 100 150 mM NaCl and grown for an additional 3 days in dark. **(B)** Hypocotyl width quantification of seedlings grown as described in (A). **(C)** Close-ups of hypocotyls of seedlings grown as described in (A and B) using stereo microscopy. Bar = 200 μm**. (D)** *ttl13* roots show hypersensitivity to salt stress. Light-grown (long-day photoperiod) seedlings were germinated and grown for 3 days on MS agar-solidified medium (1.5% sucrose) and transferred to MS agar-solidified medium (1.5% sucrose) supplemented without and with 50, 100 mM NaCl and grown for an additional 7 days. Bar = 5 mm. **(E)** Close-ups of root tips of seedlings showed in (D) using stereo microscopy. Bar = 200 μm. **(F)** Root length quantification of seedlings as described in (D). Data were first analysed with two-way ANOVA and then with Fisher's test (Hypocotyls) or Tukey's multiple comparison test (Roots); $P < 0.05$. Data represent mean values, error bars are SEM, n = 30 seedlings per experiment. The experiment was repeated three times with similar results.

Isoxaben inhibits cellulose synthesis through the inhibition of CESA6 activity (Desprez et al., 2002), which results in radial swelling of actively growing cells (Heim, 1990). We investigated the effect of isoxaben in *ttl13* relative to WT by germinating and growing seedlings on control medium and medium supplemented with 1 nM isoxaben. While no differences were found in hypocotyl length between *ttl13* and WT in control conditions, *ttl13* presented shorter hypocotyls than WT in the presence of 1 nM isoxaben (Fig. 5A-C). Isoxaben also caused increased swelling in both WT and *ttl13* hypocotyls (Fig. 5D). Altogether, the defective growth shown for *ttl* mutants shown above strongly support that *TTL* genes play a role in cellulose biosynthesis.

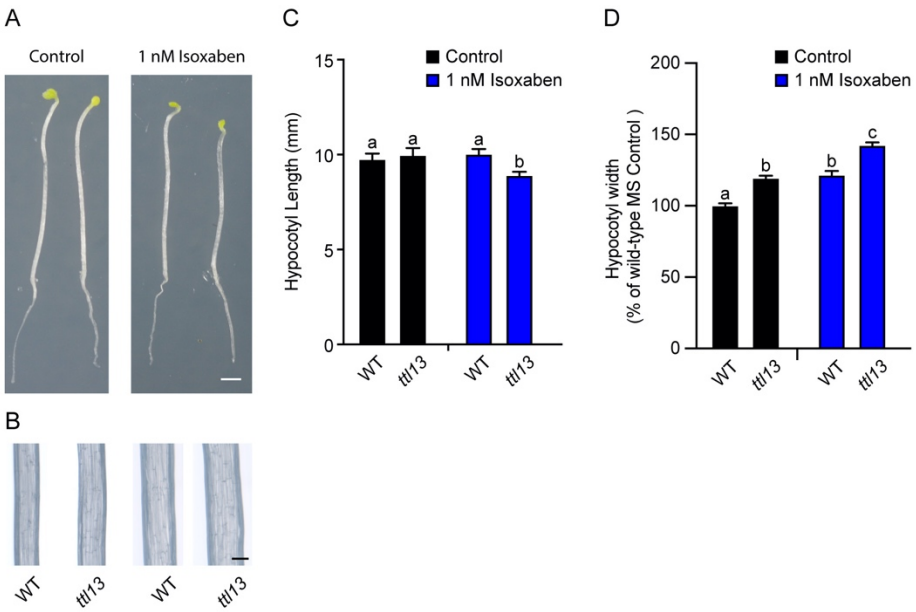

Figure 5. Isoxaben cause altered growth in *ttl13* hypocotyls. (A) Seedlings germinated on MS agar-solidified medium (1.5% sucrose) supplemented with or without 1 nM isoxaben and photographed 4 days later. Bar = 1 mm. **(B)** Close-ups of hypocotyls from seedlings grown as described in (A, B) using stereo microscopy. Bar = 200 μm**. (C-D)** Quantification of hypocotyl length (C) or hypocotyl width (D) of seedlings shown in (A-B). Data were first analysed with two-way ANOVA and then with Fisher's test; $P < 0.05$. Data represent mean values, error bars represent SEM, n = 30 seedlings per experiment. The experiment was repeated three times with similar results.

2.3 Impaired Cell Growth in *ttl* Mutants is not Correlated With The Crystalline Cellulose Content

We have shown that mutations in *TTL* genes present growth defects both in hypocotyl and root plant growth that are consistent with a role in cellulose biosynthesis. Hence, we performed a cell wall analysis of 5-days-old etiolated WT and *ttl13* mutants to investigate their cellulose amount when grown in the presence of 1.5% and 4.5% sucrose. A treatment of 4.5% sucrose cause approximately a 41% reduction in the content of crystalline cellulose, but surprisingly, the content of crystalline cellulose in *ttl13* was comparable to that of WT (Fig. 6A). As a control, we included in the analysis the *prc1-1* mutant, a loss of function of the *CESA6* that show a 54% reduction of crystalline cellulose (Fagard, 2000) (Fig. 6A). We also examined the amount of non-crystalline cellulose or amorphous cellulose (Fig. 6B). Again, no differences between *ttl13* and WT seedlings were found at 1.5% or 4.5% sucrose while *prc1-1* showed a drastic increase (Fig. 6B). Other cell wall sugars were analysed, including xylose, fucose and galacturonic acid that provide information about xyloglucans and pectins. We did not find for any of the genotypes analysed significative differences in sugar composition, suggesting that *ttl13* is not altered in other cell wall components (Fig. 6D-E).

We then performed a similar cell wall analysis of 8-days-old WT and *ttl13* root seedlings. In these conditions the isotropic phenotype of *ttl13* roots was evident when compared with the WT seedlings that presented a clear anisotropic root growth. Interestingly, in this case we found a significative decrease on the crystalline cellulose content when compared with WT, in contrast to the analysis in etiolated seedlings (Fig. 6F). Unexpectedly, WT roots showed higher amorphous cellulose content compared to *ttl13* mutant (Fig. 6G). In addition,

lower levels of total glucose were detected in *ttl13* roots (Fig. 6H) in 4.5% sucrose, in contrast to etiolated seedlings (Fig. 6C), which could explain the differences in the crystalline and non-crystalline content in comparison to WT roots. The content of other cell wall sugars was similar between WT and *ttl13* roots (Fig. 6I-J), suggesting that the structure of cellulose rather than the total content of cellulose is affected in *ttl13*.

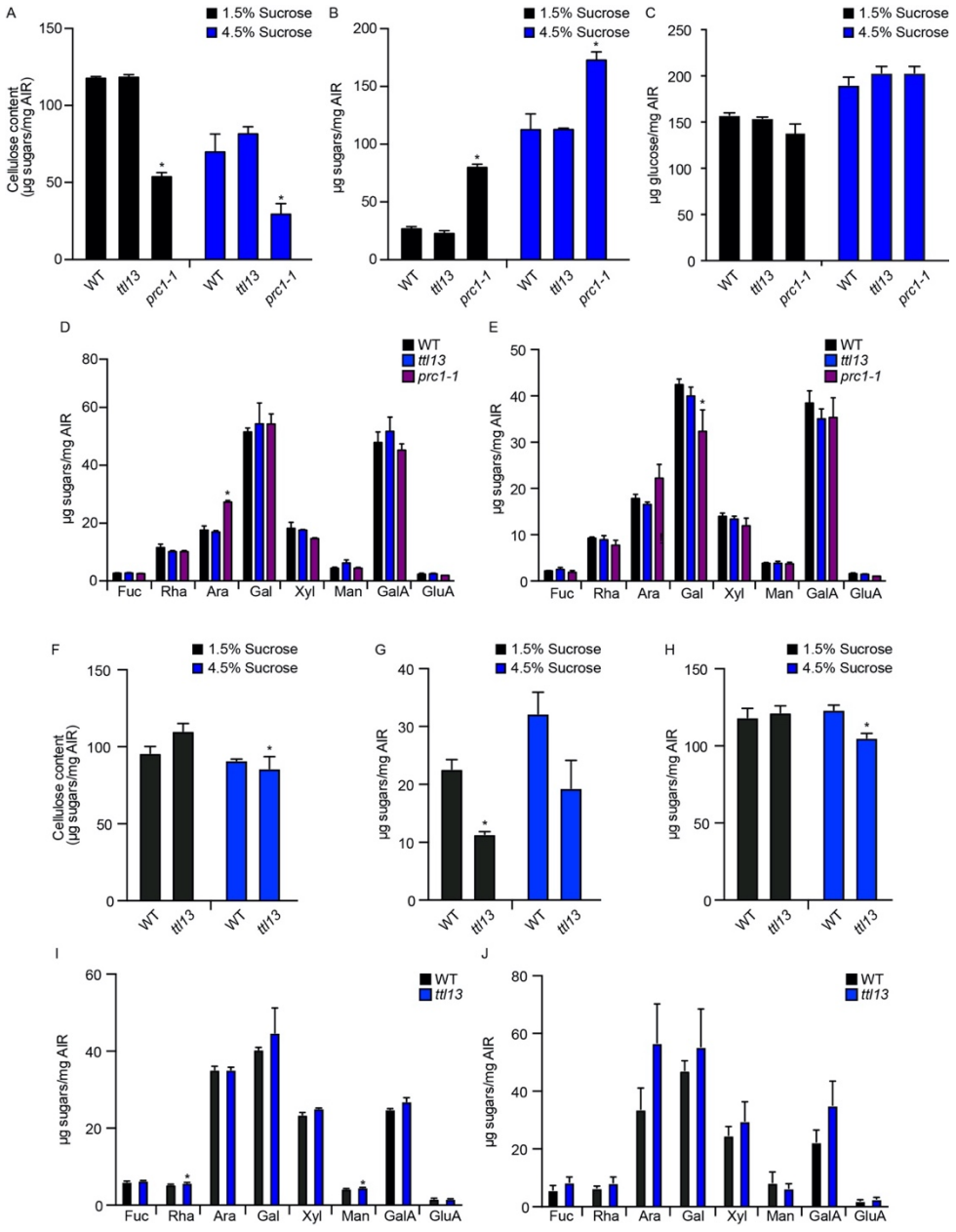

Figure 6. *ttl13* mutant displays decreased levels of crystalline cellulose in roots, but not in hypocotyls when grown in presence of high levels of sucrose. (A-E) *ttl13* etiolated seedlings

showed similar cellulose content respect to WT levels. **(A)** Crystalline cellulose content in 5-day-old etiolated seedlings germinated in both, half-strength MS agar-solidified medium and half-strength MS agar-solidified medium supplemented with 4.5% sucrose, was measured by HPLC analysis. **(B)** Glucose matrix of etiolated seedlings from etiolated seedlings grown as described in (A). **(C)** Total glucose content of etiolated seedlings grown as described in (A). **(D-E)** Monosaccharide content of etiolated seedlings in control (D) l and 4.5% sucrose (E) grown as described in (A). **(F-J)** *ttl13* roots displays decrease cellulose content compared with WT in presence of 4.5% sucrose. **(F)** Crystalline cellulose content in 8-day-old light-grown roots germinated in both, half-strength MS agar-solidified medium and half-strength MS agar-solidified medium supplemented with 4.5% sucrose, was measured by HPLC analysis. **(G)** Glucose matrix of roots from etiolated seedlings grown as described in (F). **(H)** Total glucose content of roots from seedlings grown as described in (F). **(I-J)** Monosaccharide content of roots in control (D) and 4.5% sucrose (E) of roots from seedlings grown as described in (F). Asterisks indicate statistical differences between mutant versus WT determined by the unpaired t test (*P ≤ 0.05). Data represent mean values, error bars represent SEM, 1 mg of respective tissue was used per experiment. The experiments were repeated three times with similar results.

2.4 Genetic Analysis Indicates that *TTL* Genes Function Independent of the *FEI1*/*FEI2*-*SOS5* Pathway and Confirm the Role of *TTLs* in Cellulose Biosynthesis Based on the Analysis of *ttl13 prc1-1*

Several regulators have been identified that play a role in cellulose biosynthesis during adverse growth conditions. Glycosyl phosphatidylinositol (GPI)-anchored proteins, such as the *Salt-Overly Sensitive 5* (*SOS5*) gene, encode an AGP-like and fasciclin-like domains and mutation in this gene leads to cell swelling and growth inhibition in the root tip upon 100 mM NaCl (Shi et al. 2003). To investigate the genetic interaction analysis between *TTLs* and the *SOS5*, we generated a homozygous *ttl13 sos5-2* triple mutant by crossing the *ttl13* with *sos5-2*. Five-day-old etiolated *ttl13* and *sos5-2* single mutants were indistinguishable from the WT when growing in control conditions, but surprisingly the *ttl13 sos5* double mutant presented a reduction in hypocotyl length and a slight isotropic growth compared with the parental lines (Fig. 7A-D). This reduced growth of

ttl13 sos5-2 was also observed in the rosette and shoot size of plants growing in soil (Fig. 7H-I) and suggest that while both proteins have a role in cellulose biosynthesis during normal growth they compensate for loss of the other. Upon 100 mM NaCl treatment, *ttl13* and *sos5* showed a reduced growth when compared to WT seedlings, whereas the double *ttl13 sos5-2* mutant presented extreme reduction of hypocotyl length and a wider growth that resulted in dwarfism (Fig. 7A-D). After 7 days of 100 mM NaCl treatment, the roots of *ttl13 sos5-2* were shorter and a massive isotropic growth was observed when compared with the *ttl13* and *sos5-2* mutants (Fig. 7E-G). Extreme growth defects for the *ttl13 sos5* double mutant were also observed in high sucrose indicating that these phenotypic responses are not specific to NaCl (Fig. 8). Overall, our data indicate that *ttl* and *sos5* mutations have an additive effect suggesting that they act in a nonlinear manner.

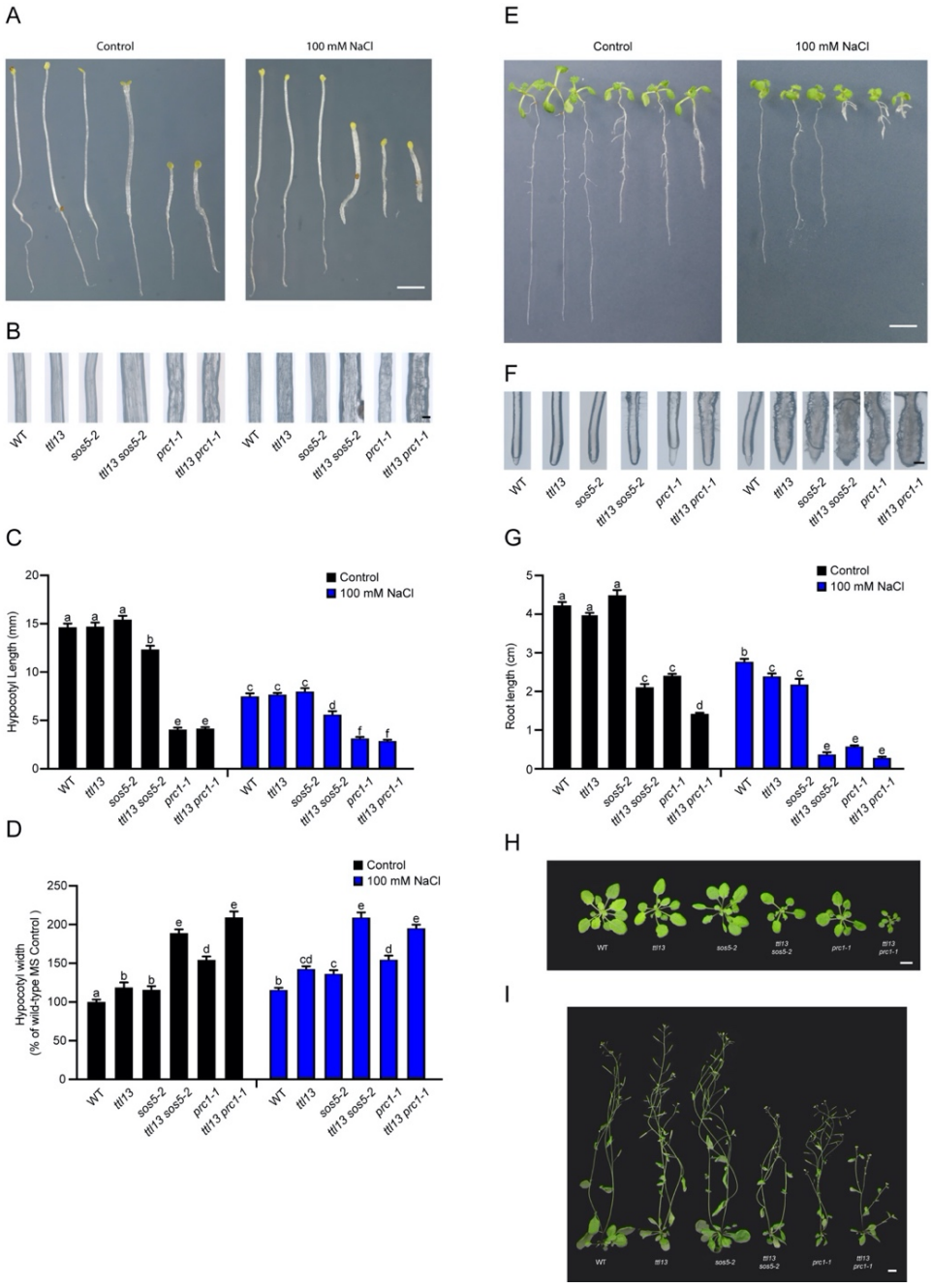

Figure 7. Absence of *TTL* genes enhanced the cellulose-related phenotypes in cellulose mutants. (A) *ttl13* mutations leads enhanced altered growth in cellulose mutants in dark conditions. Seedlings germinated and grown for 2 days on MS agar-solidified medium and transferred to MS agar-solidified medium supplemented without and with 100 mM NaCl and grown for an additional 3 days in dark. Bar = 5 mm. **(B)** Close-ups of hypocotyls of seedlings grown as described in (A) using stereo microscopy. Bar = 200 μm**. (C)** Hypocotyl length quantification of seedlings gown as described in (A). **(D)** Hypocotyl width quantification of seedlings shown in (B). **(E)** *ttl13* cause and additive affect in roots in cellulose mutants. Light-grown seedlings were germinated and grown for 3 days on MS agar-solidified medium and transferred to MS agar-solidified medium supplemented without and with 100 mM NaCl and

grown for an additional 7 days. Bar = 5 mm. **(F)** Close-ups of root tips of seedlings showed in (E) using stereo microscopy. Bar = 200 μm. **(G)** Root length quantification of seedlings shown in (E). **(H-I)** Absence of *TTL1* and *TTL3* genes cause an additive effect in cellulose mutants in adult plants. Morphological phenotypes of 5-week-old plants grown in either short days (H) or long days (I). Bar = 1 cm. Data were first analysed with two-way ANOVA and then with Fisher's test (Hypocotyls) or Tukey's multiple comparison test (Roots); $P < 0.05$. Data represent mean values, error bars represent SEM, n = 30 seedlings per experiment. The experiment was repeated two times with similar results.

Mutations and stresses that disrupt cellulose biosynthesis can act additively to influence the synthesis of cellulose (Kieber and Polko, 2019). Plant response to salt stress depend on the appropriate activity of the cellulose synthase complex, and a loss-of-function mutation in *CESA6*, such as *prc1-1* mutant leads to an abnormal root growth under salt (Zhang et al., 2016).

Next, we investigated the effect that decreased the cellulose content had on *ttl13* using a genetic strategy. For this, we introduced into *ttl13* the *prc1-1* mutation, a loss-of-function allele of *CESA6* (Fagard, 2000). Five-day-old etiolated *ttl13 prc1-1* seedlings showed increased radial expansion of the hypocotyls than *ttl13* and *prc1-1* in both, control conditions and after NaCl (Fig. 7A-D). This additive effect of *ttl13* mutation in *prc1-1* plants was evident in plants growing in soil, that showed a dwarf phenotype (Fig. 7H-I). *prc1-1* showed a similar reduction in root growth and isotropic cell expansion than *ttl13 sos5-2* (Fig. 7E-G), while *ttl13 prc1-1* mutant showed additive defects in root growth than *ttl13* and *prc1-1* in control conditions (Fig. 7E-G). Although the root length of *ttl13 prc1-1* and *prc1-1* were not statistically different, *ttl13 prc1-1* seedlings seemed more affected than *prc1-1* in high NaCl (Fig. 7E-G). This lack of differences in root growth might be due to the severe phenotype already shown by *prc1-1* under NaCl (Fig. 7E-G). In fact, under sucrose stress, *ttl13 prc1-1* showed decreased root growth and enhanced isotropic root growth compared to

prc1-1 Fig, 8A-C), likely because the effect of 4.5% sucrose is milder in *prc1-1* than 100 mM NaCl. Overall, the additive phenotype displayed in the *ttl13 prc1-1* mutant relative to *ttl13* and *prc1-1* support the crucial role of *TTL1* and *TTL3* genes in cellulose biosynthesis.

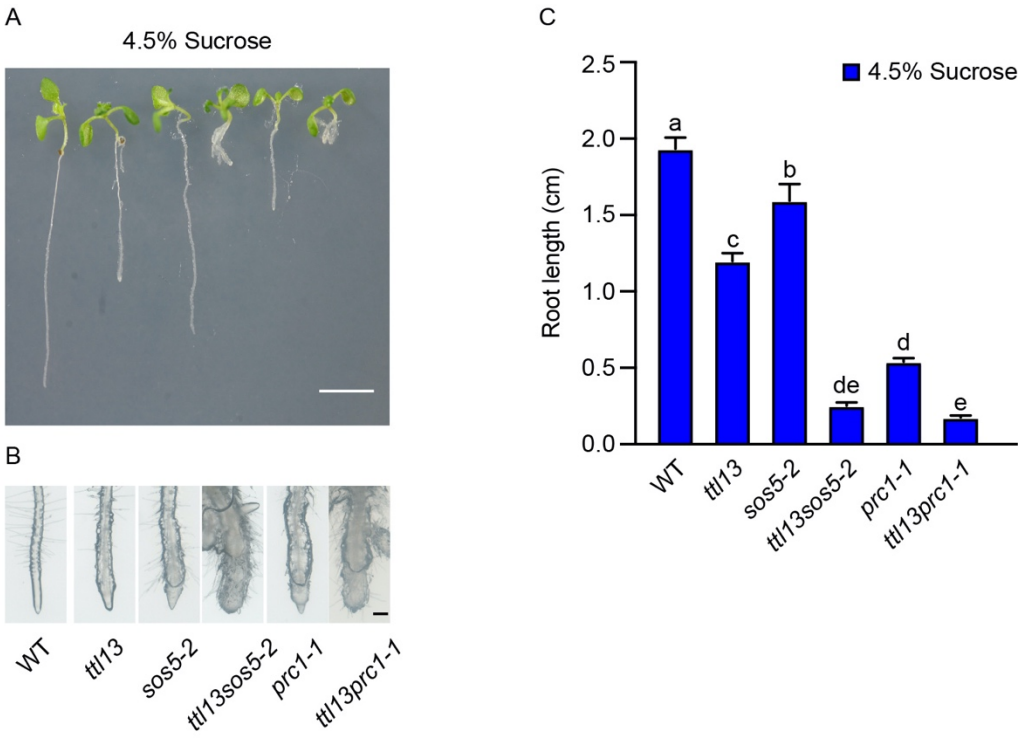

Figure 8. Mutations in both *TTL1* and *TTL3* genes lead to additive effects in cellulose mutants in presence of high sucrose. (A) Seedlings were germinated in half-strength MS agar-solidified medium supplemented with 4.5% sucrose and photographed 8 days later. Bar = 5 mm. **(B)** Close-ups of root tips from seedlings represented in (A). Bar = 250 μm **(C)** Quantification of root elongation from seedlings gown as described in (A). Data were analysed first with two-way ANOVA and then with Tukey's multiple comparison test; $P < 0.05$. Data represent mean values, error bars are SEM, n = 30 seedlings per experiment. The experiment was repeated three times with similar results.

2.5 TTL3 Tracks Together With the Cellulose Synthase Complex at the Plasma Membrane

We have previously shown that the defective BR responses of the *ttl134* mutant can be complemented by a genomic *TTL3* fragment with a *GFP* gene transcriptionally fused at the C-terminus of TTL3 (Amorim-Silva et al., 2019). Hence, we investigated if *TTL3-GFP* could also complement the cellulose deficiency defects shown by the *ttl* mutants. This line could indeed recover growth of *ttl* mutants to WT levels under high sucrose and salt stress (Fig. 2C-D; Fig. 9). It further indicates that the fusion protein complements the function of both TTL1 and TTL3 (Fig. 9).

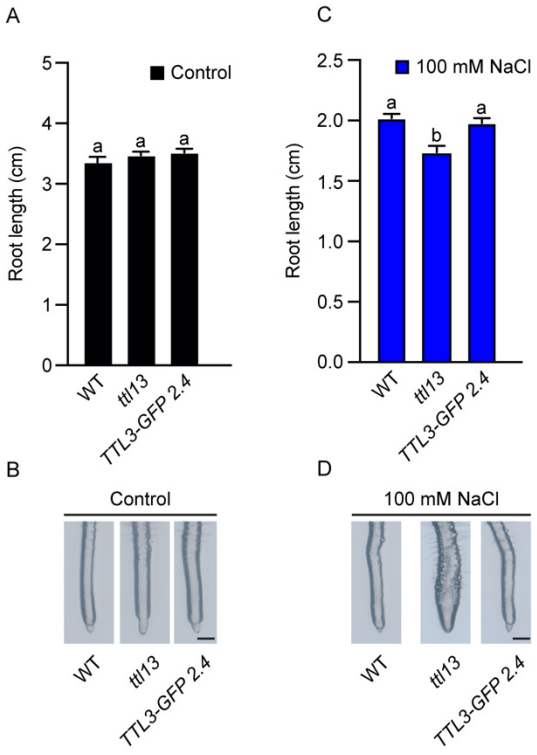

Figure 9. *TTL3* gene expression complements the *ttl13* mutations upon salt stress conditions. **(A)** Root length quantification of seedlings that were germinated and grown for 3 days on half-strength MS agar-solidified medium and transferred to half-strength MS agar-solidified medium for an additional 7 days in long-day photoperiod. **(B)** Close-ups of root tips of seedlings showed in (A) using stereo microscopy. Bar = 200 μm. **(C)** Root length quantification of seedlings

germinated and grown for 3 days on half-strength MS agar-solidified medium and transferred to half-strength MS agar-solidified medium supplemented with 100 mM NaCl for an additional 7 days in long-day photoperiod. Bar = 200 μm. Data were first analysed with two-way ANOVA and then with Tukey's multiple comparison test; $P < 0.05$. Data represent mean values, error bars represent SEM, n = 30 seedlings per experiment. The experiment was repeated two times with similar results.

To investigate the subcellular localization of TTL3, we imaged the corresponding GFP-tagged line in interphase cells of etiolated hypocotyls (Fig. 10A). Spinning disk confocal microscopy revealed a major localization of TTL3-GFP in the cytosol, consistent with data previously published by our group (Amorim-Silva et al., 2019). In addition, we could also discern weak signals of motile foci in the plasma membrane that were obscured by the high cytosolic background (Fig. 10A). In collaboration with Christopher Kesten (Sánchez-Rodriguez's Lab, ETH Zurich) we developed an image modification workflow that allowed us to remove most of the background signal and extract these mobile particles localized at the plasma membrane (Fig. 10B). Interestingly, the localization and behaviour of these particles was similar to what has been previously reported for the CSC (Paredez et al., 2006), indicating that TTL3 might track together with the CSC. We therefore generated a dual labelled TTL3-GFP and tdTomato (tdT)-CESA6 (Sampathkumar et al., 2013) lines in the *ttl13* double mutant background and observed that the differentially labelled plasma membrane localized foci indeed migrated together (Figure 10B-C,E-F). To substantiate the TTL3-CESA co-localization, we confirmed that TTL3-GFP moves bi-directionally with an average speed of 271 ± 86 nm/min, very similar to 267 ± 93 nm/min, the one measured for tdT-CESA6 (Fig. 10D).

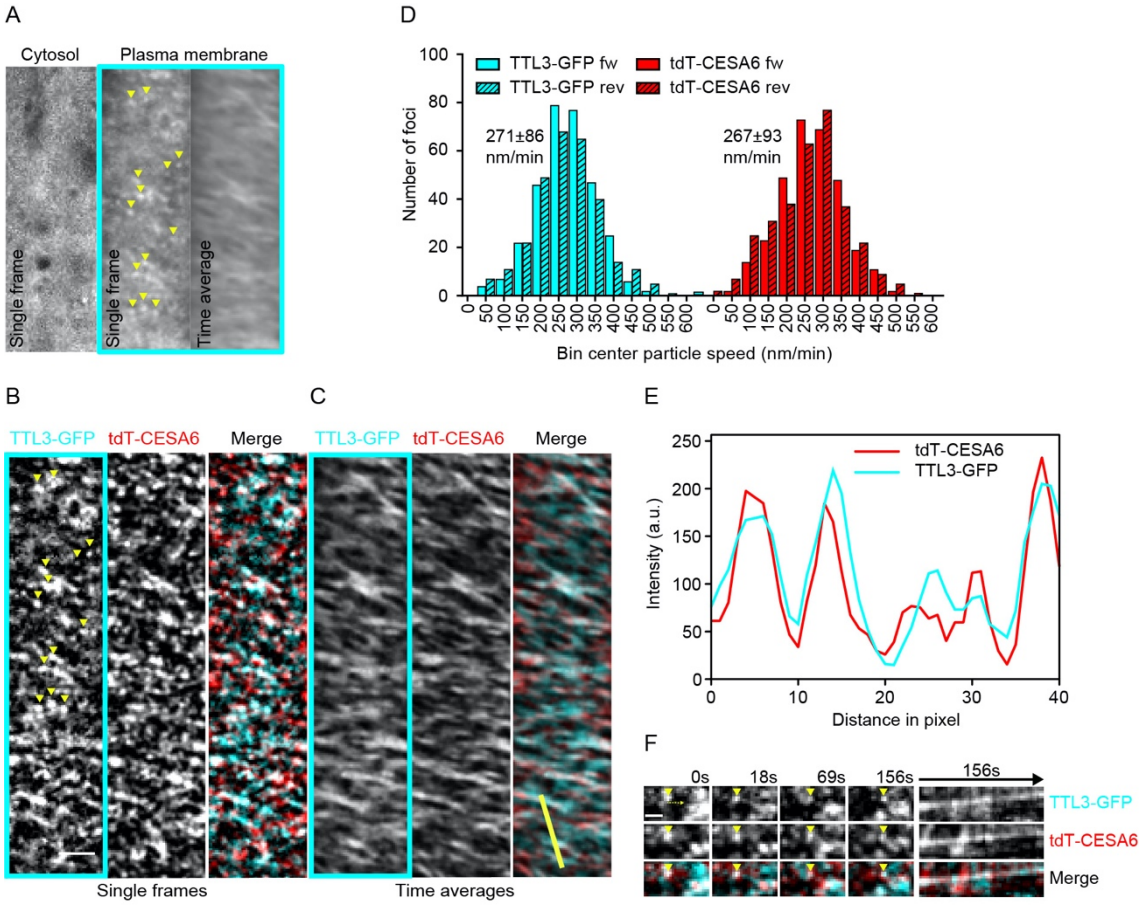

Figure 10. TTL3 co-migrates with the cellulose synthase complex. (A) TTL3-GFP is mainly located in cytoplasm and barely located in the plasma membrane. Imaging of *TTL3-GFP 2.4* was done in 3-day-old etiolated seedlings in hypocotyl cells using spinning disk microscopy. Yellow arrowhead represents TTL3-GFP particles. **(B)** TTL3-GFP and tdT-CESA6 co-localize at foci in the plasma membrane. Single frames of 3-day-old etiolated seedlings of TTL3-GFP and tdT-CESA6 from (A). Cytosolic signal was subtracted from images to clarify the plasma membrane localization. Bar = 2,5 μm. **(C)** Time-average projections of TTL3-GFP and tdT-CESA6 from (B) reveal co-migration of the fluorescent foci. **(D)** TTL3-GFP mobility in the plasma membrane is comparable to that of the tdT-CESA6 protein. Particle speed of focis was calculated from (B-C) using the FIESTA software. **(E)** TTL3-GFP co-localize with tdT-CESA6. Intensity plot of TTL3-GFP and tdT-CESA6 from transect in (C). **(F)** TTL3 co-migrates with tdT-CESA6 in the plasma membrane. Time frames of individual plasma membrane-located fluorescent TTL3-GFP and tdT-CESA6 foci. Yellow arrowhead represents particle mobility. Kymographs of 156 s movies of TTL3-GFP and tdT-C6 expressing cells from single frames. Bar = 1 μm. The experiments were repeated three times with similar results. Imaging was performed by Christopher Kesten (Sánchez-Rodriguez's Lab, ETH Zurich).

2.6 TTL3 is a New Member of the Cellulose Synthase Complex

Since TTL3-GFP colocalize dynamically with the CSC complex, we investigated whether TTL3 can directly interact with the CESA1, CESA3, and CESA6 proteins using yeast two-hybrid (Y2H) assays. We have previously shown that the full-length TTL3 protein is not stable in yeast (Amorim-Silva et al., 2019). Therefore, we used as preys (AD) the N-terminal region of TTL3 that contained the Intrinsic Disorder Domain (IDR) and the first two TPRs (TTL3-N) and TTL3 C-terminal region that contained all six TPRs and the TRLX motif (TTL3-C) (Fig. 11A). As baits (BD), we used the cytosolic N-terminal domain (N-domain) and the cytosolic Interacting domain (I-domain) from CESA1, CESA3, and CESA6 (McFarlane et al., 2014).

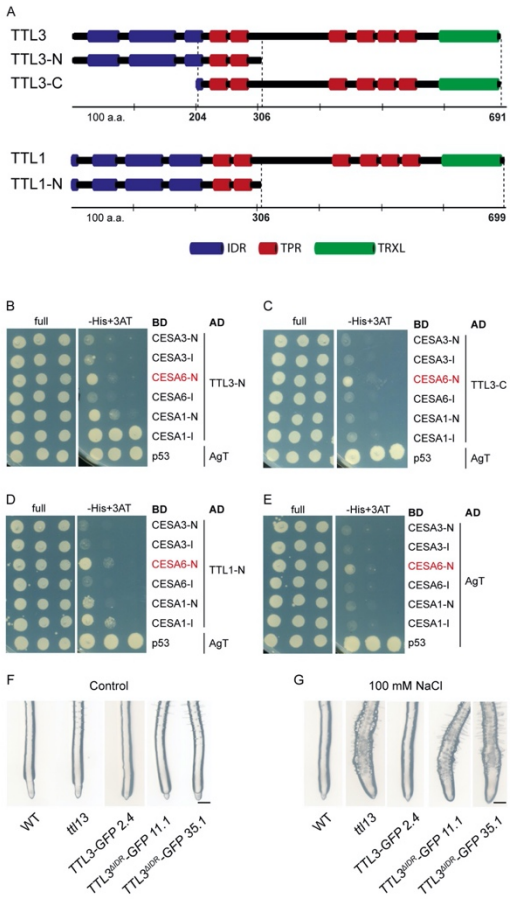

Figure 11. The IDR of TTL proteins interacts with the catalytic loop of CESA1. (A) Schematic representations of full-length and different truncated versions of TTL3 and TTL1 proteins.

Numbers indicate first and last amino acids (a.a.) of TTL truncated proteins. **(B-E)** TTL1 and TTL3 interacts with CESA1-I through the IDR domain of TTLs. Yeast two-hybrid assays to determine the interaction of the TTL3 fragment TTL3-N (amino acids 1 to 306) (B), the TTL3 fragment TTL3-C (amino acids 204 to 691) (C), and the TTL1 fragment TTL1-N (D) with the different domains of CESA1, CESA3 and CESA6. (E) Positive (AgT-p53) and negative controls (AgT-CESAs) for the yeast two-hybrid assays. Growth on non-selective media (left column) and interaction-selective media (lacking histidine [-his] and supplemented with 3-amino-1,2,4-triazole [+3AT], right column) are shown. -N, N-terminal region of CESAs; -I, catalytic cytosolic loop of CESAs. Y2H performed by Araceli Castillo, University of Malaga. **(F-G)** The IDR of TTL3 is essential to complement the isotropic phenotype during adverse conditions. Close-ups of root tips of seedlings that were germinated and grown for 3 days on MS agar-solidified medium and transferred to MS agar-solidified medium without (F) and supplemented with 100 mM NaCl (G) for an additional 7 days in long-day photoperiod, using stereo microscopy. Bar = 200 μm.

Y2H analyses indicated that TTL3-N interacted steadily with CESA1-I and weakly with CESA1-N (Fig. 11B). Because the TTL3-C construct shares the first two TPRs with TTL3-N and did not interact with any of the CESAs assayed (Fig. 11C), suggested that the TTL3 IDR domain found in TTL3-N is the main determinant for the interaction. No interactions were found between TTL3-N and TTL3-C constructs with any of the CESA3 or CESA6 domains (Fig. 11B-C), indicating that the interaction between TTL3 and the CSC complex was specific for CESA1. It is worth mentioning that BD-CESA6-N autoactivated the reporter HIS gene (Fig. 11E) and therefore the results from the interactions assayed with CESA6-N are not conclusive. In addition to *TTL3*, the *TTL1* gene has also an important role in cellulose biosynthesis. Therefore, we generated a prey (AD) construct that contained the N-terminal region of TTL1 correspondent to TTL3-N, i.e. the IDR and the first two TPR domains (TTL1-N) (Fig. 11A). As shown in Fig. 11D, TTL1-N also interacted with CESA1-N and CESA1-I domain, that also correlates with the similar identity of the predicted TTLs IDR segments (Fig. 12A-B).

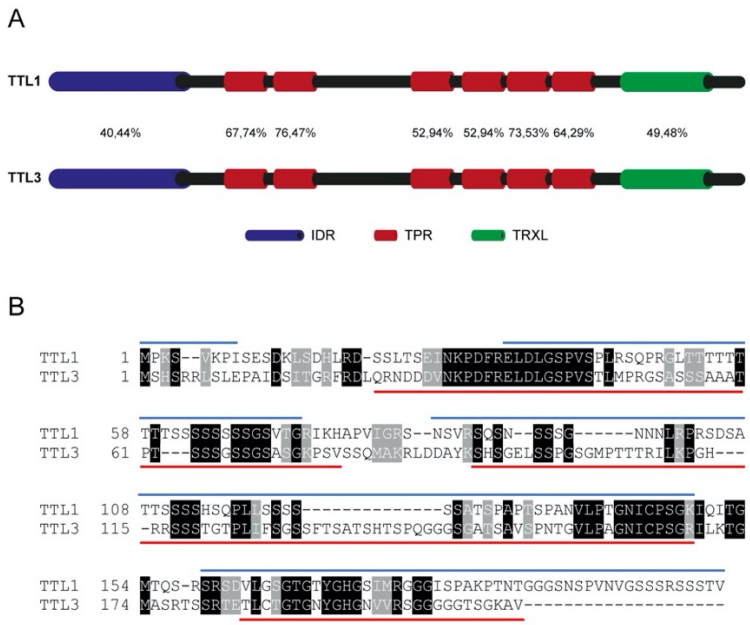

Figure 12. The identity of the IDR of TTL1 and TTL3 is highly similar. (A) *In silico* analysis of the identity percentage between the different domains of TTL1 and TTL3 proteins. **(B)** TTL1 and TTL3 sequence comparison indicates highly conserved residues in the IDR. The protein sequences of *A. thaliana* TTL1 (AT1G53300) and TTL3 (AT2G42580) were retrieved from the TAIR database. The TTL1 and TTL3 predicted IDRs are underlined in blue and red, respectively. Black and gray boxes highlight identical and similar amino acids, respectively.

The interaction of the N-terminal domain of TTL3 and TTL1 with CESA1 suggest an important role of the IDR for TTL function. To investigate the function of the IDR *in vivo*, a genomic *TTL3-GFP* construct lacking the IDR driven by the *TTL3* promoter (*TTL3:TTL3$^{\Delta IDR}$-GFP)* was generated (Fig. 13A). After transformation of this construct into the *ttl13* double mutant by floral dipping, we selected a total of 38 hygromycin resistant lines. Accumulation of TTL3$^{\Delta IDR}$-GFP protein in T2 segregating lines were compared with that of TTL3-GFP using immunoblot analysis with GFP antibodies (Fig. 13B). Based on protein accumulation levels and the presence of a single insertion we selected *TTL3$^{\Delta IDR}$-GFP 11.1* and *TTL3$^{\Delta IDR}$-GFP 35.1* lines for further analysis. We then investigated the root phenotypes of *TTL3$^{\Delta IDR}$-GFP 11.1* and *TTL3$^{\Delta IDR}$-GFP 35.1* lines together with the complementing *TTL3-GFP 2.4* line in the presence of high NaCl concentration. While all genotypes presented a WT root growth in control

conditions, *TTL3$^{\Delta IDR}$-GFP 11.1* and *TTL3$^{\Delta IDR}$-GFP 35.1* did not complemented the root swollen shown by *ttl13* (Fig.11F-G), supporting that the IDR of TTL3 (and likely TTL1) is important for its function, most likely through the interaction with CESA1.

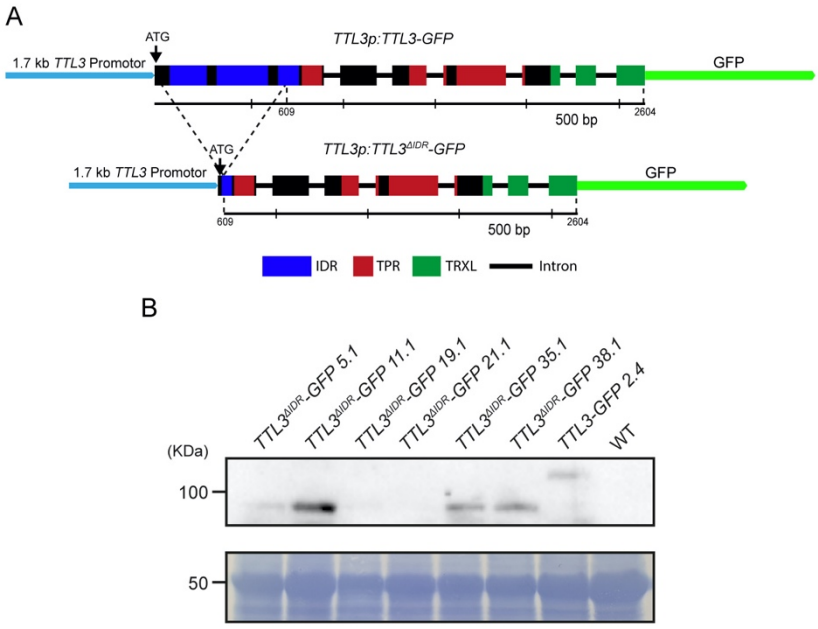

Figure 13. Generation of the *TTL3$^{\Delta IDR}$-GFP* transgenic line in *Arabidopsis*. (A) Schematic representations of the genomic TTL3 sequence and the deletion of its IDR. **(B)** Immunoblot analysis of the relative protein quantity of the different TTL3$^{\Delta IDR}$-GFP transgenic lines. TTL3-GFP 2.4 line that contains the IDR was also included into this analysis. Equal loading was confirmed by Coomassie blue staining (CBB) of total proteins.

2.7 TTL3-GFP Massively Relocalizes and Stabilizes the CSC at the Plasma Membrane Under Adverse Conditions

To get an understanding of how TTL proteins affect the cellulose synthase machinery upon salt stress, we generated a YFP-CESA6 and mCh-TUA5 dual labelled *ttl13* line. Three-day-old etiolated hypocotyls were imaged after 30 min and 1 to 32 h of 200 mM NaCl treatment. As previously shown before (Wang et al., 2007; Fujita et al., 2013; Endler et al., 2015; Kesten et al., 2019), the microtubule array in WT plants depolymerized approximately after 2 h and re-assembled

within 8 h of salt treatment, an observation that coincided with CESA dynamics at the plasma membrane (Fig. 14A-B). Remarkably, in *ttl13* mutants there was a rapid decrease of CESA density at the plasma membrane within 30 min of NaCl treatment and the CESAs never re-populated the plasma membrane in the course of the experiment, indicating a role for TTL proteins in CSC stabilization (Fig. 14A-B). The cortical microtubule array in *ttl13* mutant seedlings on the other hand did not fully de-polymerize within 2h as in WT seedlings and, after a brief re-polymerization phase within 8 h, collapsed within 28 h of NaCl treatment (Fig. 14A, C). Thus, these data indicate a prominent function of TTL proteins in the stability of the CSC and cortical microtubule array under salt stress acting as a safeguard of the complex.

We then investigated the molecular reason behind this observation. We treated 3-day-old etiolated seedlings hypocotyls of the *ttl13* TTL3-GFP and tdT-CESA6 dual-labelled line with 200 mM NaCl. This stress condition caused a massive re-localization of the TTL3-GFP signal to the plasma membrane of etiolated hypocotyls, with an almost complete depletion of the cytosolic background signal (Fig. 14D). Skewness is a measure for the asymmetry of an image histogram. Thereby, if the skewness score increases, it means that more pixel of high intensity in the image histogram are present. We reasoned that accumulation of TTL3-GFP in plasma membrane upon stress imposition, might result in an enhanced skewness due to signal-cluster formation, an observation that was also made for bundling of filaments (Higaki et al. 2010). Therefore, skewness can be used as a measure of plasma membrane localization of cytosolic proteins if a signal-cluster formation occurs in this instance. Thus, the rather evenly distributed cytosolic signal of TTL3-GFP in control conditions resulted in a low skewness of the histogram (Fig. 14D). However, the stress re-localization of TTL3-GFP from cytosol to the plasma membrane resulted in significantly enhanced skewness within 28 h of NaCl treatment, while the skewness of the

tdT-CESA6 signal remained mostly unaffected (Fig. 14D). In order to test whether TTL proteins are important for the delivery of CSCs to the plasma membrane, we performed FRAP experiments in the *ttl13* YFP-CESA6 line. After photobleaching, we observed comparable dynamics between the WT and *ttl13* mutant backgrounds, thus suggesting that TTLs are not involved in the CSC delivery to the plasma membrane, but rather function in plasma membrane stabilization.

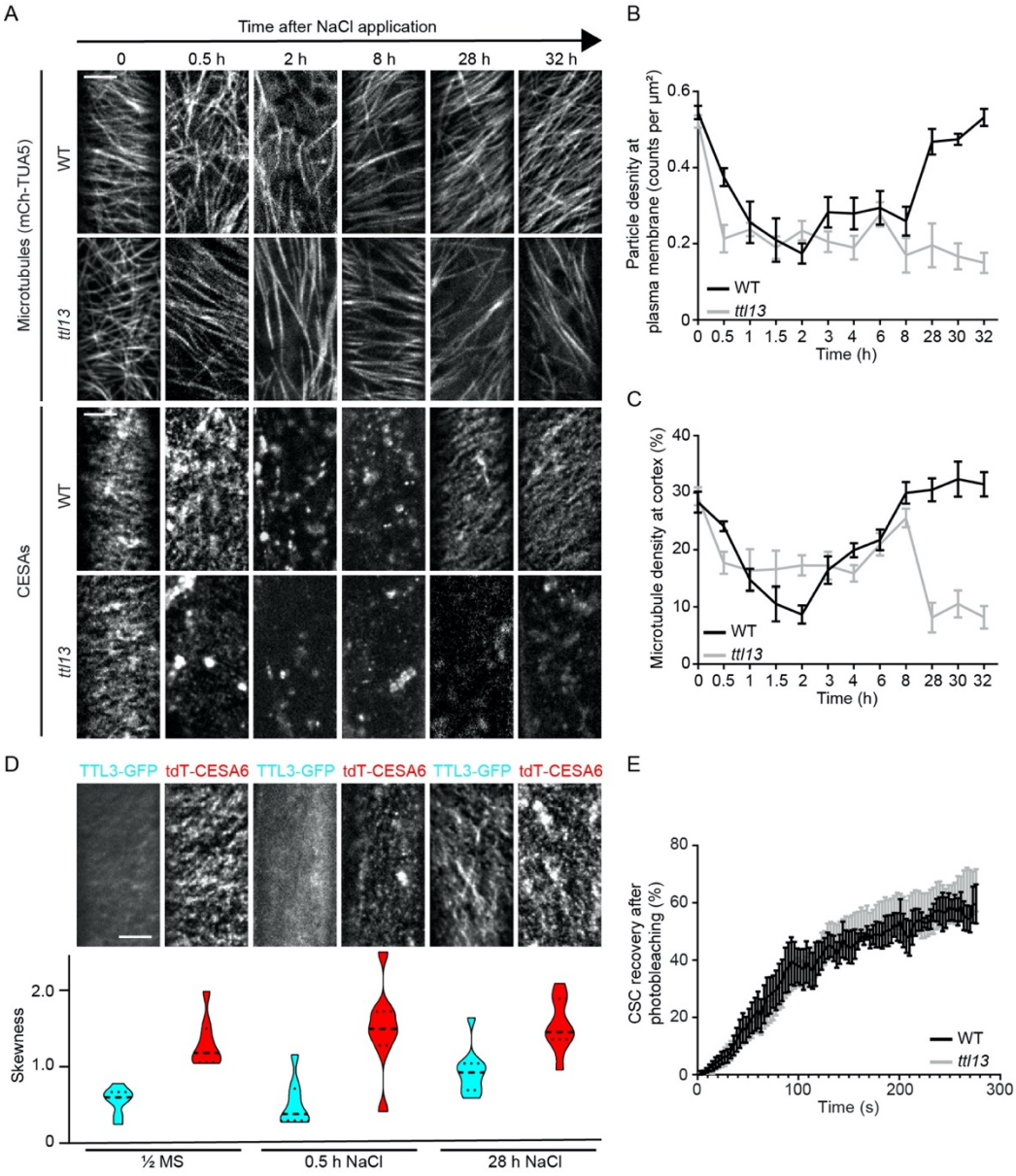

Figure 14. The TTL proteins safeguard the cortical microtubule array and CESA activity during salt stress. (A) Microtubule and CESA array at the cell cortex and plasma membrane,

respectively, in 3-day-old mCherry-TUA5 and YFP-CESA6 expressing etiolated seedlings after exposure to 200mM NaCl for times indicated. T = 0 indicates time just prior to salt exposure. Bar = 5 μm. **(B)** Quantification of CESA coverage at the plasma membrane, from experiment showed in (A). **(C)** Quantification of microtubule coverage at the cell cortex from experiment showed in (A). Data represent mean values, error bars are SEM, n = 9 seedlings and 27 cells per timepoint were analysed per experiment. **(D)** TTL3-GFP relocates to plasma membrane after 28 h salt stress exposure. Single frames of 3-day-old etiolated seedlings expressing TTL3-GFP and tdT-CESA6 in half-strength MS medium supplemented with 200 mM NaCl for times indicated. Quantification of the skewness of TTL3-GFP particles were calculated from images. Data represent mean values (dashes) and quartiles (dots). Bar = 5 μm. n = 8 seedlings and 18 cells per timepoint were analysed per experiment. **(E)** TTL proteins do not contribute to the CSC recovery in the plasma membrane. FRAP of 3-day-old WT or *ttl13* hypocotyl cells expressing YFP-CESA6. Data represent mean values, error bars represent SEM, n = 8 seedlings and 18 cells per timepoint were analysed per experiment. The experiments were repeated three times with similar results. Imaging was performed by Christopher Kesten (Sánchez-Rodriguez's Lab, ETH Zurich).

As showed in Fig. 2, high sucrose levels resulted in severe phenotype of *ttl13* when compared to WT. Therefore, in order to investigate the dynamics of TTL3-GFP at the cellular level, we treated 3-day-old etiolated seedlings of the *ttl13* TTL3-GFP and tdT-CESA6 dual-labelled line with 4.5 % sucrose and analyzed the dynamics using spinning disk confocal microscopy (Fig. 15A-B). Similarly, we observed an enhanced re-localization of the TTL3-GFP signal to the plasma membrane during after high sucrose exposure (Fig. 15A-B), where we observed an enhanced skewness due to TTL3-GFP signal-cluster formation, in contrast to control conditions (Fig. 15C). Next, the density of both TTL3-GFP and tdT-CESA6 at the plasma membrane under control and high sucrose conditions was determined. The particle density of both proteins was identical under mock conditions and did not change upon treatment with 4.5% sucrose (Fig. 15D), indicating that high sucrose treatments cause the accumulation of TTL3-GFP due to its re-localization from the cytosol to the plasma membrane. In order to analyse how a deletion of TTL activity affected the cellulose synthesis machinery in 4.5% sucrose, we tested the YFP-CESA6 and mCh-TUA5 dual labelled in the *ttl13* line

(Fig. 15E-F). Consistent with the phenotypic analyses, both the speed and density of the CSC under control conditions were indistinguishable between WT and *ttl13* plants (Fig. 15G-H). However, treatment with 4.5 % sucrose resulted in a decrease of CSC speed at the plasma membrane in WT plants but not in *ttl13* mutants, while CSC density remained at control levels in both genotypes (Fig. 15G). This indicated that spatial organization of cellulose microfibrils could be altered in *ttl* mutants, as CSC catalytic activity directly correlates with CSC mobility (Morgan et al., 2013).

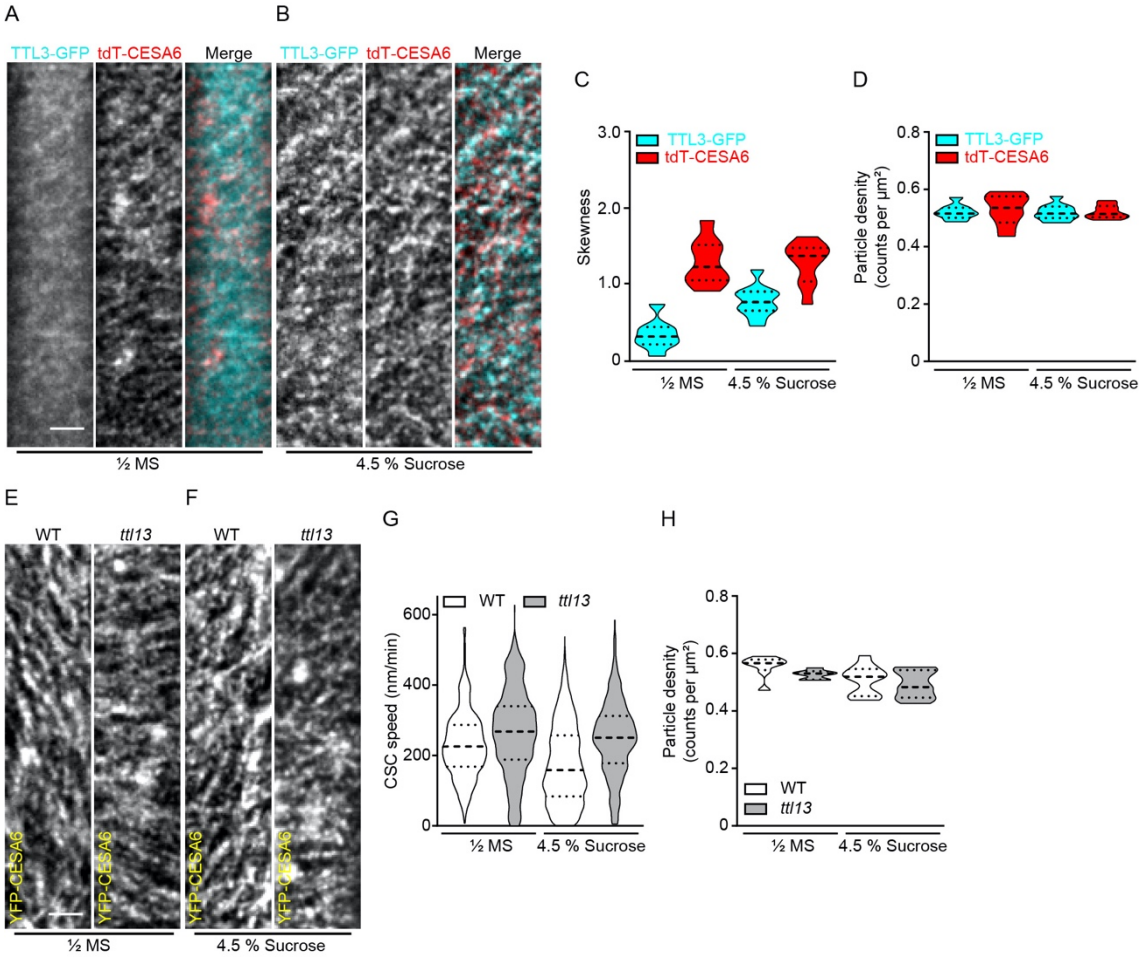

Figure 15. TTLs are essential for the appropriate activity of the cellulose synthase complex. (A) TTL3 experiments a massive relocation to plasma membrane in presence of high sucrose. Single frames of 3-day-old etiolated seedlings of TTL3-GFP and tdT-CESA6 using spinning disk microscopy. Bar = 2,5 µm. **(B)** Time-average projections of TTL3-GFP and tdT-CESA6 from (A). **(C)** Quantification of the skewness of TTL3-GFP particles from (A-B). Data represent mean values (dashes) and quartiles (dots), n = 8 seedlings and 25 cells per treatment were analysed per

experiment. **(D)** Quantification of CESA coverage at the plasma membrane, from experiment showed in (A-B). Data represent mean values (dashes) and quartiles (dots). Error bars are SEM, n = 8 seedlings and 66 cells per treatment were analysed per experiment. **(E-H)** CSC density in plasma membrane is not affected in *ttl13* mutant, but CSC speed is altered in presence of 4.5% sucrose. **(E-F)** Single frames of 3-day-old etiolated seedlings of TTL3-GFP and tdT-CESA6 in half-strength MS media without (E) and supplemented with 4.5% sucrose (F). Bar = 2,5 μm. **(G)** Quantification of CSC speed from (E-F). Data represent mean values and quartiles. n = 6 seedlings, 414 particles and 12 cells per treatment were analysed per experiment. **(H)** Quantification of CESA particles at the plasma membrane, from experiment showed in (E-F). Data represent mean values (dashes) and quartiles (dots). n = 6 seedlings and 29 cells per treatment were analysed per experiment. The experiments were repeated three times with similar results. Imaging was performed by Christopher Kesten (Sánchez-Rodriguez's Lab, ETH Zurich).

To further investigate the cause of this massive TTL3 relocation, we generated *prc1-1 CESA6* mutant lines expressing TTL3-GFP (Fig. 16A). Our reasoning behind this was that the *prc1*-1 mutant already present a ~50% crystalline cellulose of the WT in control conditions, allowing to investigate if the re-localization of TTL3-GFP to the plasma membrane is triggered by a reduction in the cellulose content. Indeed, we could observe a re-localization of TTL3-GFP to clusters at the plasma membrane and a strong increase of TTL3-GFP histogram skewness (Fig. 16B) in the *prc1-1* background. Altogether, these data suggest the crucial role of TTL proteins in maintaining the integrity of the CSC during conditions that produce a decrease in the crystalline cellulose content.

Mutation within the cytosolic domain in *CESA3* confers resistance to the herbicide isoxaben (Scheible et al., 2001), which suggest that isoxaben target is the catalityc domain of the CESA enzymes. Because TTLs interact with the cytosolic domain of CESA1, isoxaben could interfere in the TTL-CSC interaction and TTL3 relocation to plasma membrane under stress. Interestingly, the skewness of the TTL3-GFP signal remained unaffected in presence of 1 nM isoxaben, while some of the tdT-CESA6 was accumulated in Golgi and and/or

other cytoplasmic compartments, although most of the tdT-CESA6 signal was observed as motile CSC particles (Fig. 16 C-E). Thus, isoxaben could block the interacting site of TTL3 with the CSC, preventing TTL3 accumulation in the plasma membrane during stress and therefore confirming that TTL proteins interact with the catalytic domain of the CSC. Moreover, isoxaben action depletes CSC from the plasma membrane and CSCs are immediately internalized into SmaCCs (Paredez et al., 2006). Another nonexclusive hypothesis is that, TTL3 only is attached to active CSC during adverse conditions, where CSCs needs to be located in the plasma membrane to produce cellulose microfibrils and this could not occur once CSC are internalized into SmaCCs after prolonged isoxaben treatment.

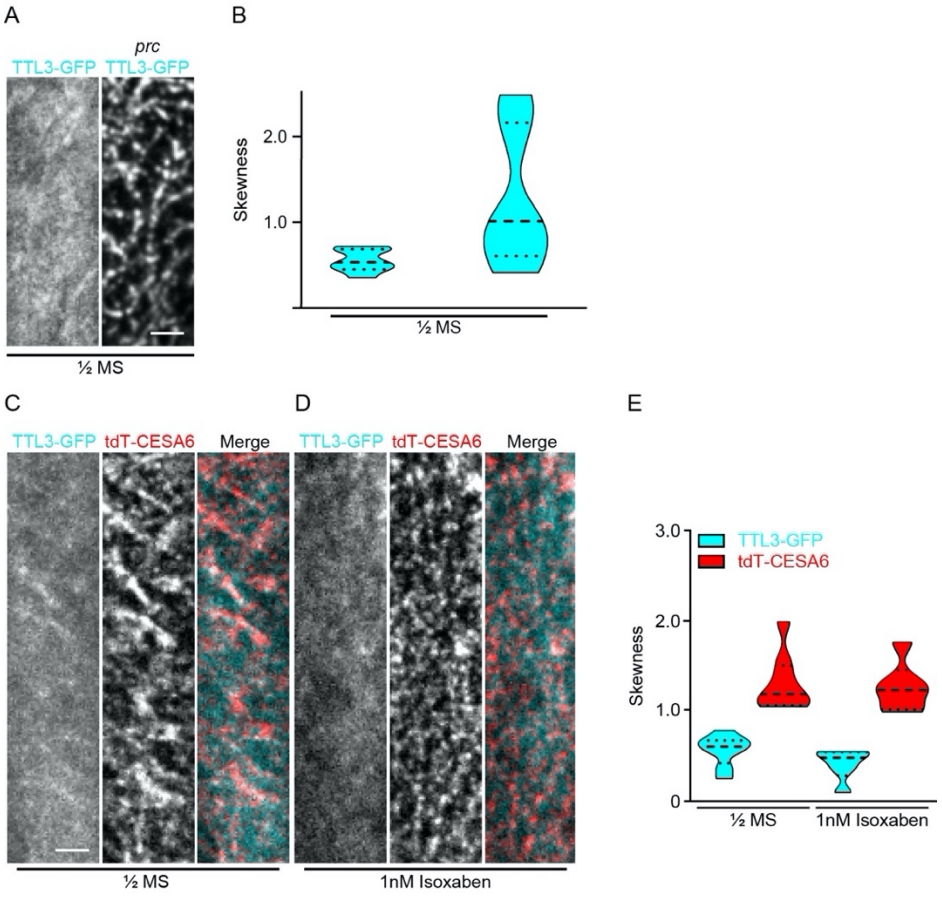

Figure 16. Defects in the cellulose synthase complex, but not in presence of Isoxaben, implies TTL3 massive relocation to plasma membrane. (A) TTL3-GFP shows clear plasma membrane location in the *prc1-1* background. Imaging of *TTL3-GFP 2.4* was performed in 3-day-old etiolated

seedlings in hypocotyl cells using spinning disk microscopy. Bar = 2,5 μm. **(B)** Quantification of the skewness of TTL3-GFP particles from (A). Data represent mean values (dashes) and quartiles (dots), n = 8 seedlings and 13 cells per treatment were analysed per experiment **(C-D)** TTL3-GFP does not relocate to plasma membrane in presence of 1 nM isoxaben. Single frames of 4-day-old etiolated seedlings of TTL3-GFP and tdT-CESA6, germinated in half-strength MS media without (C) and supplemented with 1 nM isoxaben (D) using spinning disk microscopy. Bar = 2,5 μm. **(E)** Quantification of the skewness of TTL3-GFP and tdT-CESA6 particles from (C-D). Data represent mean values (dashes) and quartiles (dots). n = 6 seedlings and 14 cells per treatment were analysed per experiment. The experiments were repeated three times with similar results. Imaging was performed by Christopher Kesten (Sánchez-Rodriguez's Lab, ETH Zurich).

Chapter 2

Identification of cellulose-related components that act together with TTL proteins

Table of contents

1. Introduction

Cortical microtubules have been identified as sensors of environmental stress in plant cells (Nick, 2013). Thus, microtubules disassemble rapidly after exposure to salt as mentioned in the "Introduction" chapter. Under prolonged stress the microtubule array gradually re-emerges, possibly as an array adapted to stress conditions, where CC proteins appear to be a crucial component during this rearrangement under stress conditions (Endler et al., 2015; Kesten et al., 2019).

Mutations in CC1/CC2 proteins lead to a decrease in cellulose content and hypersensitivity to salinity in plants, as *cc1cc2* double mutant shows an isotropic growth in etiolated hypocotyls during salt stress. Using spinning disk microscopy in etiolated hypocotyls, the dual-labelled GFP-CC1 tdT-CESA6 line revealed that CC1 co-migrates with the CSC in normal conditions and Y2H assays revealed direct interaction, thus proving that CCs are an integral part of the CSC. Moreover, CC proteins (together with the CSC) are associated with SmaCCs/MASCs after exposure to stress, such as isoxaben or salt. Interestingly, mutations in *CC1* and *CC2* genes lead to an abnormal response of the cortical microtubule array, where microtubules are not able to repolymerize after prolonged exposure to salt stress. In the same way, CSC array is altered in *cc1*/*cc2* mutants during adverse conditions. Hence, CC function is crucial to safeguard the the cortical microtubule array and CESA activity during salt stress (Endler et al., 2015; Kesten et al., 2019).

The CC proteins are predicted to contain a transmembrane domain with their N-terminal domains facing the cytosol and the C-terminal parts in the apoplast. In addition, the N-terminal domain of CC proteins has been identified

to interact with microtubules in order to stabilize its cortical array, and deletion of this N-terminal domain prevents CC-microtubule interaction. Moreover, the C-terminal domain have a distinct cellular function. Indeed, the C-terminal domain is important for CESA-related functions and indicate that this part of the protein is responsible for the interaction of the CC1 with the CSC (Endler et al., 2015; Kesten et al., 2019).

Altogether, authors propose a model where CC proteins promote microtubule polymerization during salt stress conditions. Thereby, CSCs are able to synthetize cellulose in the plasma membrane, once microtubules are repolymerized (Endler et al., 2015; Kesten et al., 2019) (Fig. 1).

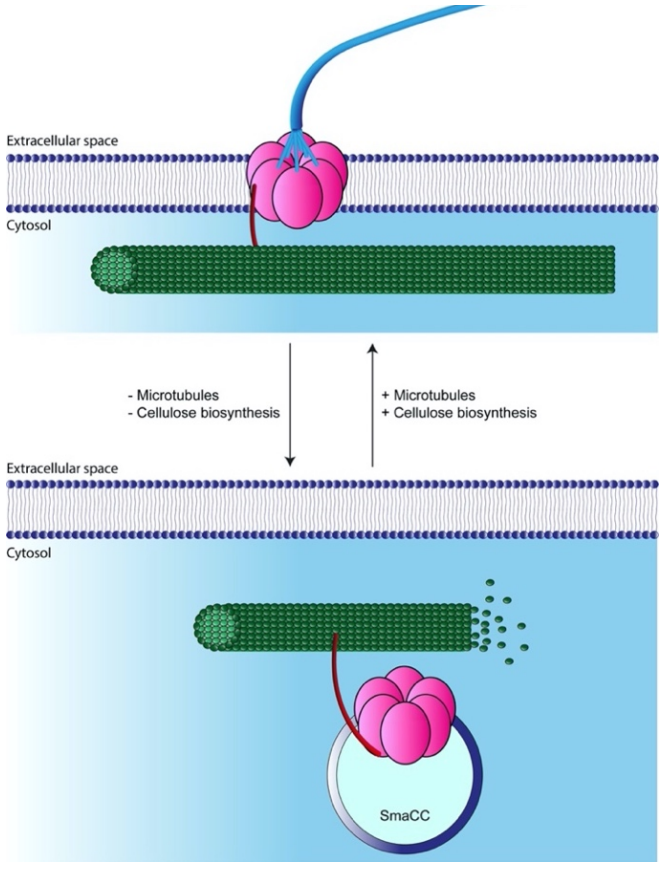

Figure 1. Impact of salt stress on cellulose biosynthesis. Under normal conditions, cellulose synthesis occurs at the plasma membrane and is guided by cortical microtubules. Under salt stress conditions, microtubules rapidly depolymerize and CSCs are removed from the plasma membrane. CC1/CC2 proteins (coloured in red) co-localize with CESAs and can interact with

microtubules to promote microtubule dynamics. CC protein activity promotes the reformation of cortical microtubules, remobilization of CSCs to the plasma membrane, and the sustained recovery of cellulose synthesis under salt stress conditions (Endler et al., 2015).

Similar to yeast, plant cells modulate changes in plant cell wall integrity and transduce a signal back to regulate cell wall synthesis, including cellulose synthesis. Receptor-like kinases (RLKs) from several distinct clades have been proposed to be involved in cell wall sensing. FEI1 and FEI2 are leucine-rich repeat (LRR) RLKs that regulate cell wall synthesis in various contexts and have been implicated in cell wall-related signalling. Double *fei1fei2* mutants display isotropic root growth that is clearly associated with reduced cellulose biosynthesis as determined by assays measuring incorporation of ^{14}C glucose into cellulose in roots (Xu et al., 2008).

Root swelling in *fei1fei2* mutants is suppressed by inhibitors of the ethylene precursor 1-aminocyclopropane-1-carboxylic acid (ACC), but not by inhibitors of ethylene signalling or by genetic disruption of ethylene perception (Xu et al., 2008). In fact, FEI1-FEI2 proteins act as scaffold to localize ACC synthase (ACS) or may complex ACS with other proteins. The *fei1fei2* phenotype is also reverted by mutations in auxin biosynthesis genes, which are also able to partially suppress other cellulose-deficient mutants such as *prc1-1*, *cob*, and *sos5*, providing a link between auxin signalling and cell wall function (Steinwand et al., 2014).

SOS5 is localized primarily to the plasma membrane in *Arabidopsis* roots and is retained in the apoplast following plasmolysis (Xue et al., 2017). Genetic analyses indicate that the *FEIs* act in a linear pathway with *SOS5* in roots (Xu et al., 2008; Basu et al., 2016) (Fig. 2), although the interaction might be more complex during cellulose synthesis in seed coat mucilage that previously

described (Griffiths et al., 2015). Moreover, analysis of mutations in the AGP-specific galactosyltransferases GALT2 and GALT5 shows that they also act in the SOS-FEI5 pathway and thus suggests that glycosylation of SOS5 contributes to its function. The *galt2*, *galt5* and *galt2galt5* mutants phenocopy *sos5* and *fei1fei2* and display reduced levels of cellulose (Basu et al., 2016)

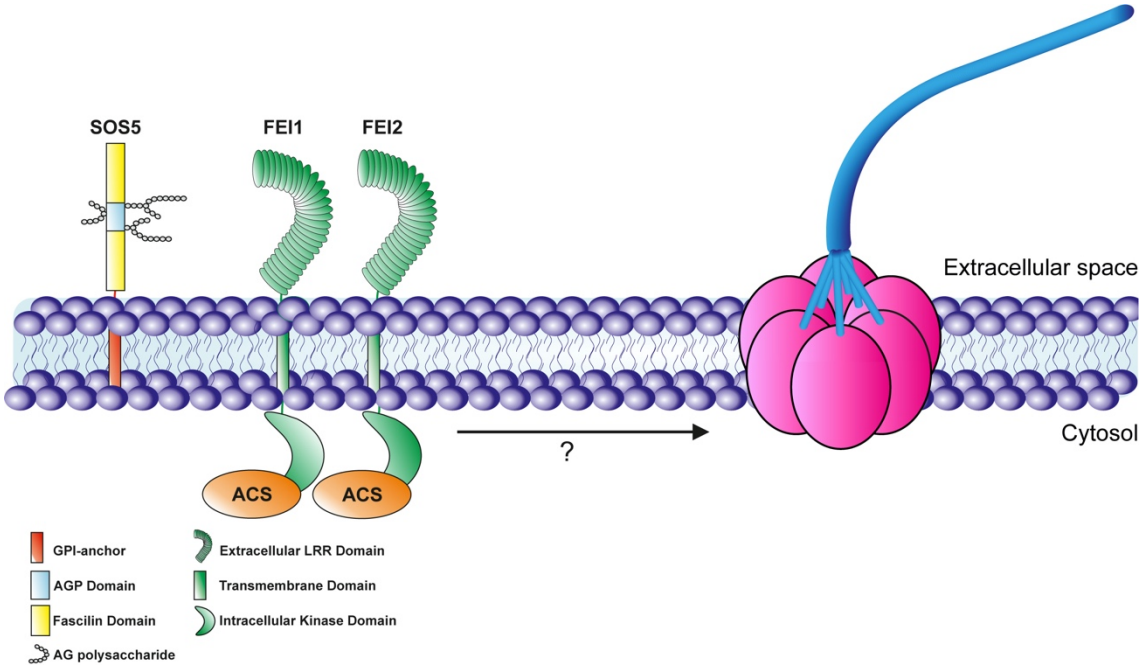

Figure 2. The SOS5/FEI1-FEI2 pathway promotes cellulose biosynthesis. FEI LRR-RLKs play a role in regulating cell wall architecture, possibly mediating interactions between the cell wall and intracellular signalling pathways. The extracellular SOS5 protein also is involved in this pathway, where the FEI RLKs may act as a scaffold to localize ACS or may complex ACS with other proteins.

2. Results

In order to elucidate the possible link between TTLs and different cellulose-related components, we used biochemical and molecular approaches to investigate the connection between TTLs and other regulators that promote cellulose biosynthesis, such as SOS5, FEI1/FEI2 and CC1/CC2 proteins.

2.1 TTLs acts independently to FEI proteins in cellulose biosynthesis

It has been previously reported that TTL proteins are associated with several RLKs such as BRL2 to influence leaf venation and BRI1 in the BR signalling pathway (Ceserani et al., 2009; Amorim-Silva et al., 2019). Furthermore, TTLs have a positive role in cellulose biosynthesis as showed in "Chapter 1". Thus, it is possible that TTL function could function downstream of an RLKs, which could sense perturbations in the extracellular space and subsequently transduce a signal to downstream cytosolic components. Several RLKs have been identified as positive regulators of the cellulose biosynthesis machinery as mentioned in "Introduction", such as the FEI1 and FEI2 LRR-RLKs. Thus, TTLs can associate with FEI1/FEI2 in order to promote cellulose biosynthesis during adverse conditions.

Mutations in *fei1fei2* double mutant cause radially swelling in the root tip during sucrose stress (Xu et al., 2008), which phenocopy *ttl* mutants as showed in "Chapter 1" (Fig. 3A). Furthermore, the typical root swelling in *fei1fei2* mutants could be suppressed by inhibitors of the ethylene biosynthesis, 1-aminocyclopropane-1-carboxylic acid (ACC) or 2-aminoisobutyric acid (AIB), but not by inhibitors of ethylene signalling or by disruption of ethylene perception (Silver thiosulfate). Thus, we tested if *ttl13* mutant phenocopy *fei1fei2* mutant in presence of those chemical agents.

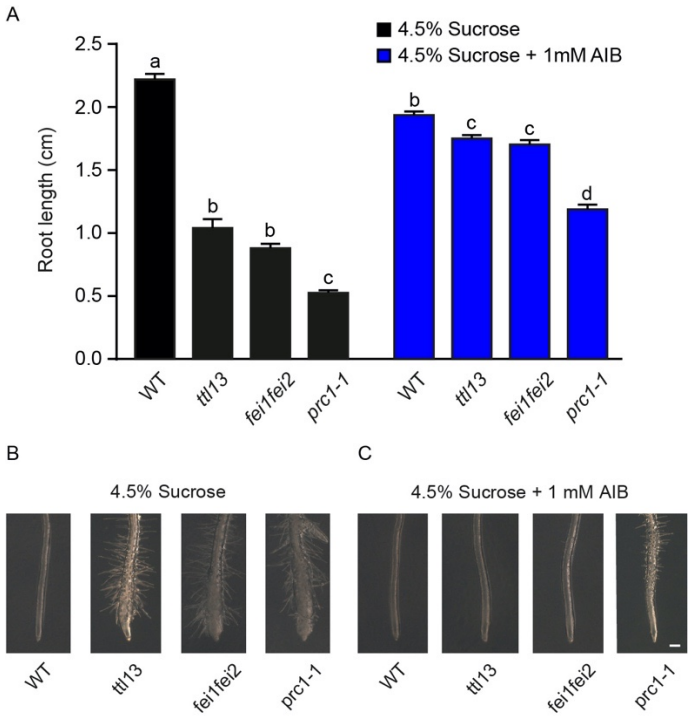

Figure 3. Root swelling in *ttl* mutant seedlings grown in the presence of high sucrose was prevented by AIB. (A) Phenotypes of seedlings grown on agar-solidified MS medium containing 0% sucrose for 3 days and then transferred to MS medium containing 4.5% sucrose or 4.5% sucrose plus AIB (1 mM) as indicated and grown for additional 4 days. **(B-C)** Close-ups of root tips from seedlings represented in (A). Error bars show SE ($n > 15$). Data were analysed with two-way ANOVA. $P < 0.05$. Bar = 1 μm. The experiment was repeated three times with similar results.

As mentioned before, *ttl13* mutant showed a decrease of growth anisotropy and an exacerbated isotropic growth similarly to *fei1fei2* mutants in presence of 4.5% sucrose (Fig. 3A, B). This isotropic *fei1fei2* phenotype could be rescued in presence of AIB, that is a competitive inhibitor of ACC conversion to ethylene, process catalysed by the ACC oxidase enzyme (Xu et al., 2008) (Fig. 3A, C). Four days after transfer the seedlings to MS media supplemented with 4.5% Sucrose plus 1 mM AIB we observed that both, *ttl1ttl3* and *fei1fei2* presented roots significatively longer in presence of AIB than when gowning with high sucrose without AIB supplementation (Fig. 3A). Furthermore, root anisotropy was comparable to wild-type seedlings in AIB treatment but not in high sucrose (Fig.

3A, C). Thus, *ttl* mutants also phenocopy the suppression of the *fei1fei2* root swelling phenotype by the ethylene biosynthesis inhibitor AIB.

Silver thiosulfate inhibits ethylene perception (Burg and Burg, 1967; Xu et al., 2008) and interestingly, while inhibitors of the ethylene biosynthesis suppressed *fei* mutant phenotypes, disruption of ethylene perception did not (Xu et al., 2008). Hence, in order to elucidate how TTLs respond in presence of silver thiosulfate, we transferred 3-day-old seedlings to agar-solidified MS medium supplemented with 4.5% Sucrose plus silver thiosulfate. The typical *ttl13* and *fei1fei2* root isotropic phenotype could be appreciated 4 days after seedlings have been transferred to MS medium supplemented with 4.5% sucrose (Fig. 3A, B). Surprisingly, 2 days after transferring seedlings to MS medium supplemented with 4.5% sucrose plus in presence of silver thiosulfate, we observed an exacerbated isotropic phenotype in *ttl13* and *fei1fei2* roots (Fig. 4A-B).

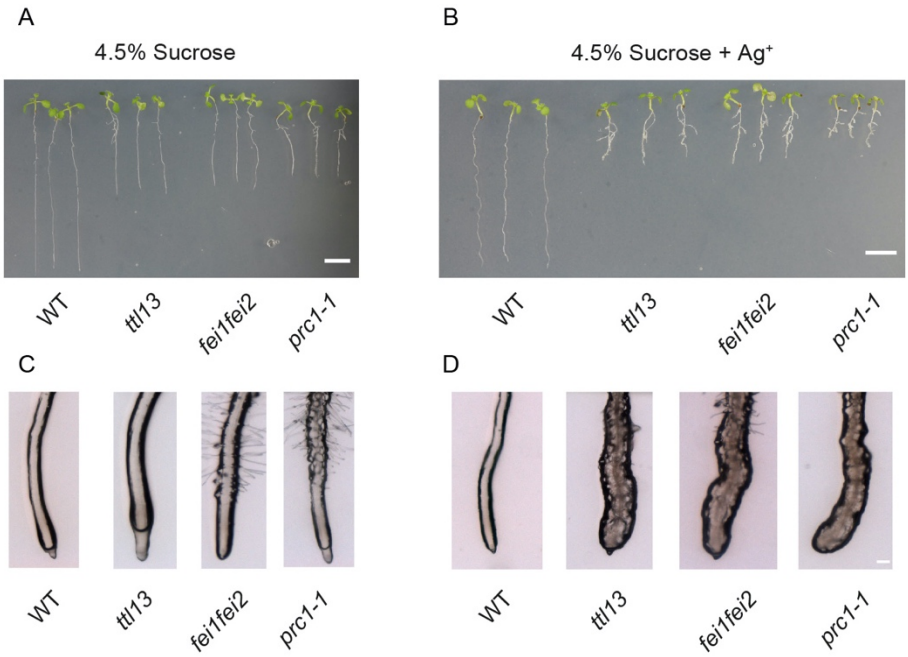

Figure 4. Ethylene perception inhibition did not restore the anisotropic root growth in *ttl13* mutant in presence of 4.5% sucrose. (A-B) Phenotypes of seedlings grown on agar-solidified MS medium containing 0% sucrose for 4 d and then transferred to MS medium containing 4.5% sucrose (A) or 4.5% sucrose plus silver thiosulfate (B) as indicated and gown for additional 2 days

Bar = 5 mm. **(C-D)** Close-ups of root tips from (A-B). Bar = 1 μm. Ag^+ is the abbreviate form of silver thiosulfate. The experiment was repeated three times with similar results.

The phenotypes observed in *ttl13* and *fei1fei2* mutants in presence of AIB and silver thiosulfate could be a general effect in cellulose defective mutants. Thus, next we investigated the effects of ethylene biosynthesis and perception inhibition in the *prc1-1* mutant. Interestingly, in presence of 4.5% sucrose plus either AIB or silver thiosulfate, *prc1-1* mutants behave similarly to *ttl13* and *fei1fei2* double mutants (Fig. 3 and 4). Hence, these data suggest that inhibition of ethylene biosynthesis by AIB, but not blocking of ethylene perception by silver thiosulfate, could increase growth anisotropy in cellulose-defective mutants.

Because *ttl* mutants phenocopy *fei* mutants in multiple experiments, we investigated the possible interaction *in vivo* by performing co-immunoprecipitation (Co-IP) assays after transient expression of tagged full-length TTL3 and FEI1 in *N. benthamiana*. After immunoprecipitation of FEI1-GFP using GFP-Trap beads, we detected a strong interaction between TTL3-HA and FEI1-GFP (Fig. 5A). Then, the interaction between FEI1 and TTL3 was also investigated using bimolecular fluorescence complementation (BiFC) assays in *N. benthamiana* leaves, which provide additional information about the subcellular localization of the interaction (Fig. 5B). Coexpression of the TTL3-N-terminal half of YFP (nYFP) with the FEI1-C-terminal half of YFP (cYFP) reconstituted functional YFP proteins at the plasma membrane, confirming the interaction and consistent with the plasma membrane localization of FEI1. BAK1, also known as SERK3, is transmembrane kinase that function as BR coreceptor (Ma et al., 2016), and it was used here as negative control for the BiFC experiments. The confocal microscopy analyses revealed that, despite the expression of the BAK1-nYFP with FEI1-cYFP and also TTL3-nYFP with BAK1-

cYFP did reconstitute functional YFP proteins, only a weak signal is observed when compared to the coexpression of TTL3-nYFP with FEI1-cYFP.

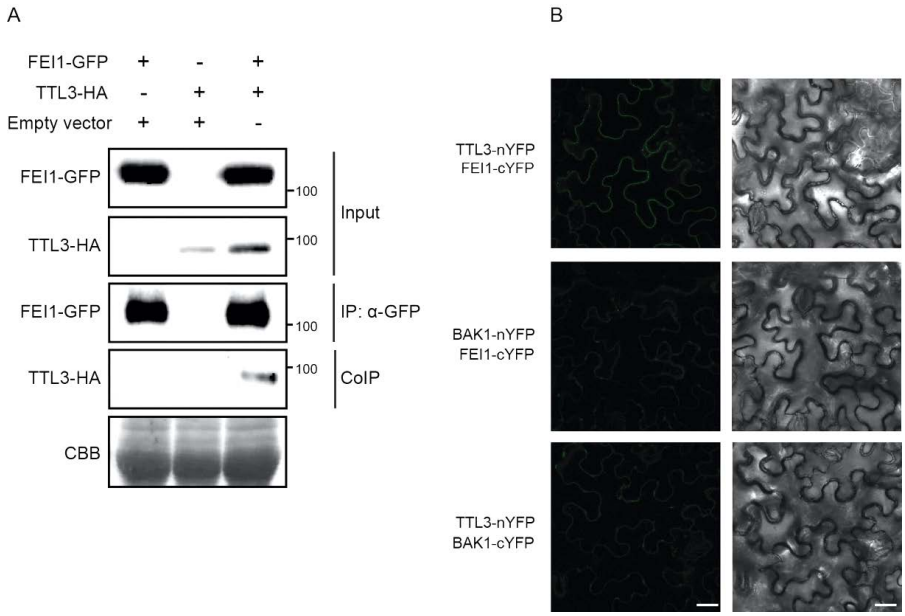

Figure 5. TTL3 associates with FEI1 kinase. (A) TTL3 co-immunoprecipitates with FEI1. FEI1-GFP and TTL3-HA were transiently expressed in *N. benthamiana*. GFP tagged protein was immunoprecipitated using anti-GFP-Trap beads. Total (input), IP, and CoIP proteins were analyzed by immunoblotting. **(B)** BiFC shows close proximity of TTL3 with FEI1. *N.benthamiana* leaves were co-agroinfiltrated with the Agrobacterium strains harboring aconstruct to express the TTL3 protein fused to the N-terminal half of YFP and the FEI1 protein fused to the C-terminal half of YFP and observed under laser scanning confocal microscope. BAK1 fused to the N-terminal half of YFP and to the C-terminal half of YFP was used as negative control. From left to right columns, images show BiFC YFP fluorescence in green and bright-field. Bar = 25 μm. The experiment was repeated two times with similar results.

As shown in "Chapter 1", a massive TTL3-GFP relocation to the plasma membrane from the cytosol occurs in order to safeguard CSC and cortical microtubule arrays during stress conditions. Thus, if FEI proteins act upstream TTLs, preventing the disruption of the CSC complex after stress, we expect that lost-of-function mutations in *FEI* genes will negatively affect to the massive TTL3 relocation to plasma membrane. To test this hypothesis, we generated a stable TTL3-GFP *Arabidopsis* line, driven by its native promoter, in the *fei1fei2* mutant

background. Using spinning-disk microscopy, we observed clear relocation of TTL3 protein after 2,5 h exposure to 4.5% sucrose compared with control conditions (Fig. 6A). This data suggests that TTL3 mode of action is independent of FEI proteins and could act in different pathways promoting cellulose biosynthesis. Absence of *FEI* genes also produce defects in mucilage production, disenabling typical seed separation when this thick, gluey substance is not produced (Xu et al., 2008) (Fig. 6B). However, we did not observe these defects in mucilage production in *ttl13* seeds that was similar to wild-type seeds, whereas *fei1fei2* displayed an impairment in mucilage production (Fig. 6B). Thus, supporting the hypothesis that TTL3 function is independent of FEI proteins, and could act in different pathways. This hypothesis is also supported by the fact that TTLs operate independently of the FEI1/FEI2-SOS5 pathway based on the genetic interaction analysis of TTL1 and TTL3 with SOS5, described in Chapter 1.

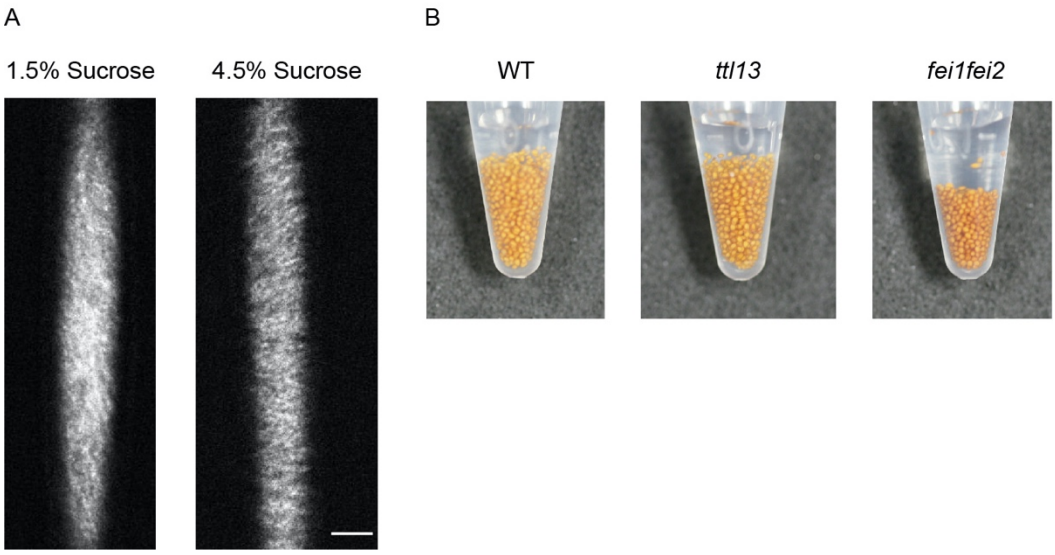

Figure 6. TTLs mode of action may be independent of FEI protein activity. (A) GFP fluorescent foci in *fei1fei2 TTL3p::TTL3-GFP* display a massive relocation to the plasma membrane when treated with 4.5% sucrose. Imaging of *fei1fei2* TTL3-GFP was performed in hypocotyl cells of 3-day-old etiolated seedlings. Etiolated seedlings were transferred to control (1.5% Sucrose) and stress conditions (4.5% Sucrose) in MS liquid media and imaged after 2,5 h. Bar = 5 μm **(B)** *ttl13* mutant is not affected in mucilage production. Seed volumes of 10 mg of seeds were suspended in 100 μL water.

2.2 TTL3 is closely located to CC proteins in *N. benthamiana*

The importance of cortical microtubules in cellulose biosynthesis have been well established (Wang et al., 2007; Fujita et al., 2013; Endler et al., 2015; Kesten et al., 2019). In fact, CC proteins are essential for maintaining the cortical microtubule array during adverse conditions, facilitating microtubule polymerization and consequently promoting catalysis of cellulose microfibrils. Because *ttl* mutants showed an impaired microtubule repolymerization response after exposure to salt stress, is possible that TTLs act together with CC proteins in order to safeguard the microtubule cortical array.

Therefore, we investigated the possible TTL-CC *in vivo* association by performing BiFC assays in *N. benthamiana*. Coexpression of the TTL3-N-terminal half of YFP (nYFP) with the CC1-C-terminal half of YFP (cYFP) showed a strong signal, confirming that TTL3 could interact with CC1. On other hand no BiFC signal was observed for the also reported TTL3-BAK1 negative control, which validate the present experiment (Amorim-Silva et al., 2019) (Fig. 7A). Hence, we further investigated this possible interaction by performing Co-IP in *N. benthamiana*. However, we did not observe association between TTL3-HA and either GFP-CC1 or GFP-CC2 proteins, as TTL3 did not co-immunoprecipitated with either CC1 or CC2 (Fig. 7B). Thus, suggesting that an association between TTL and CC proteins may not occur, at least in the tested conditions, although further studies are required to confirm this hypothesis.

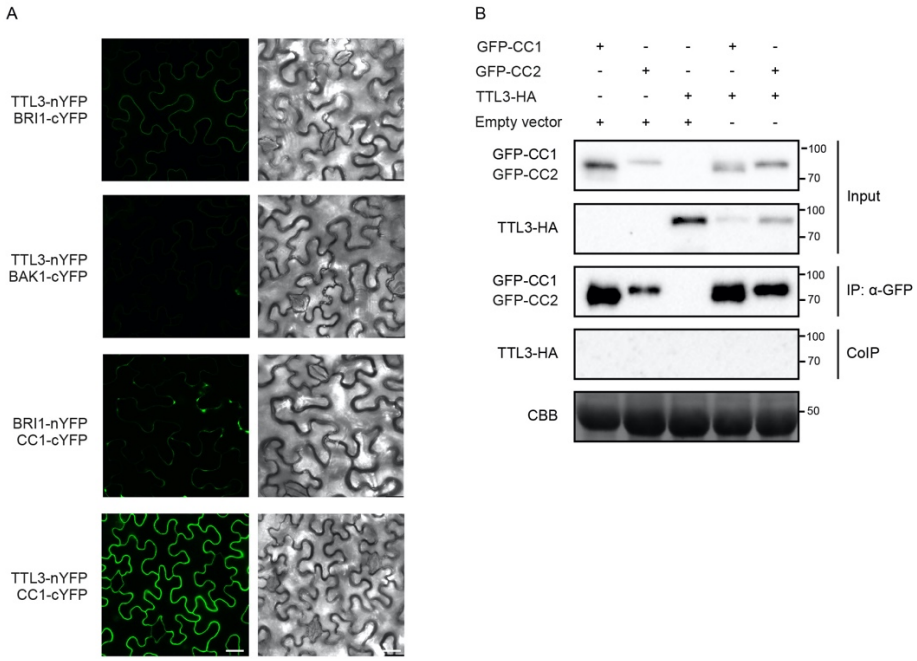

Figure 7. TTL3 do not associate with CC1 protein, but BiFC reveals TTL3-CC1 proteins proximity. (A) BiFC shows close proximity of TTL3 with CC1. *N.benthamiana* leaves were co-agroinfiltrated with the Agrobacterium strains harboring a construct to express the TTL3 protein fused to the N-terminal half of YFP and the CC1 protein fused to the C-terminal half of YFP and observed under laser scanning confocal microscope. From left to right columns, images show BiFC YFP fluorescence in green and bright-field. Bar = 25 μm. The experiment was repeated two times with similar results. BAK1 fused to the N-terminal half of YFP and to the C-terminal half of YFP was used as negative control. **(B)** TTL3 do not co-immunoprecipitates with CC proteins. GFP-CC1, GFP-CC2 and TTL3-HA were transiently expressed in N. benthamiana. GFP tagged protein was immunoprecipitated using anti-GFP-Trap beads. Total (input), IP, and CoIP proteins were analyzed by immunoblotting.

General Discussion

Abiotic and biotic stresses have a significant impact on plant development and growth. Therefore, improving plant performance during adverse conditions becomes essential for human beings. In this thesis, we describe a novel mechanism for how the major plant biomass producing enzyme complex, the CSC, can be sustained in its plasma membrane localization and is regulated during stress through the action of TTL proteins.

In *Arabidopsis*, several stresses have been identified as inhibitors of CSC function, leading to a decrease in the production of cellulose microfibrils. Among them, high levels of exogenous sucrose have a negative impact in cellulose biosynthesis (Fagard et al., 2000; Xu et al., 2008; Polko et al., 2018). In this work, we observed that in presence of 4.5% sucrose, only mutations in *TTL1* and *TTL3* lead to growth defects. Mutations in *TTL4*, another *TTL* family member, previously reported for its role in osmotic stress tolerance and BR signalling pathways, did not seemed to play a role in growth under high sucrose (Lakhssassi et al., 2012; Amorim-Silva et al., 2019). Mutations that affect cell wall and cellulose synthesis have an impact on plant salt tolerance (Shi et al., 2003; Chen et al., 2005; Jae et al., 2008; Zhu et al., 2010). In fact, this cellulose-related phenotype of the *ttl13* double mutant in sucrose stress, was further confirmed when exposed to salt stress conditions as previously reported (Lakhssassi et al., 2012). Surprisingly, the growth defects in *ttl13* etiolated seedlings grown in high sucrose did not correlate with a decrease in the cellulose content respect to wild-type plants, which could denote an impaired arrangement of the spatial organization of cellulose microfibrils. This behaviour was also observed in other cellulose-related mutants (Polko et al. 2018; Chaudhary et al. 2020). However, in *ttl13* roots we did observe a significant decrease of the cellulose content when compared with wild-type roots, but this decrease is related with the decrease in the total glucose content of *ttl13* roots, as glucose is the source for cellulose microfibrils. Taken together, this data clearly indicates that *TTL1* and *TTL3* play

important roles in maintaining proper root and hypocotyl growth under adverse conditions that impact on cellulose biosynthesis.

The introduction of loss-of-function mutations of *TTL* genes in the cellulose defective *sos5-2* mutant cause an additive phenotype when compared with *ttl13* and *sos5* mutants. This additive effect is observed even in control conditions, which indicates that pathways where *TTLs* and *SOS5* participate in plant growth and development under normal conditions. In fact, this is a common feature, since genes that could regulate cellulose biosynthesis have a non-redundantly effects as previously reported. (Xu et al., 2008; Endler et al., 2016; Ben-Tov et al., 2018). Genetic disruption of cellulose biosynthesis, caused by the knock-out of *CESA6* gene (*prc1-1* mutant allele) in the *ttl13* mutant, again produce an additive phenotype in both control and stress conditions, which accentuate the important function of *TTL1* and *TTL3* genes in cellulose biosynthesis.

Several regulators have been identified as integral components of the CSC, such as CSI1, CC, KOR (Li et al., 2012; Vain et al., 2014; Endler et al., 2015; Kesten et al., 2019) . In this work, we show that TTL proteins are new members of the active CSC at the plasma membrane. Despite the mainly cytoplasmic localization of TTL3, TTL3 tracks together with the CSC at the plasma membrane in control conditions. In fact, TTL3 directly interact with the catalytic loop of CESA1 through its IDR. The CESA1 catalytic loop is also important for the interaction with other cellulose synthesis regulators, such as SHOU4 proteins (Polko et al. 2018). Interestingly, we observe that TTL3 IDR is essential to complement the isotropic phenotype showed in the *ttl13* during adverse conditions, suggesting that deletion of TTL3 IDR prevents the TTL-CSC interaction.

It was previously described that mutations in *TTL* genes had an impact in plant salt tolerance, however, the underlying mechanisms were unresolved (Lakhssassi et al., 2012). It has also been reported that mutations in genes involved in cellulose biosynthesis also lead to salt stress hypersensitivity (Shi et al., 2002; Xu et al., 2008; Endler et al., 2015; Zhang et al., 2016). In this thesis we confirmed that cellulose biosynthesis in negatively affected in *ttl13* mutant and revealed that TTL proteins maintain the cell wall integrity via safeguarding the CSC during adverse conditions. In fact, during salt stress exposure, CSC was completely depleted from the plasma membrane in *ttl13* during the course of the experiment, very rapidly compared with disruption of other cellulose biosynthesis regulators, such as CC proteins (Endler et al., 2015; Kesten et al., 2019). Interestingly, TTL3 relocates to plasma membrane after 28h of salt stress exposure, interacting with the CSC, with an almost complete depletion of its typical cytosolic localization. In addition to the role of TTLs in CSC stability after 28h they also function in the short-term dynamics of the CSC upon stress, based on the fast CSC depletion just after 30 minutes of salt stress.

TTL genes also have an impact in the microtubule cortical array during salt stress. While in WT plants microtubules are completely abolished after 2h of saline exposure and re-assembled within 8h (Wang et al., 2007; Fujita et al., 2013; Endler et al., 2015; Kesten et al., 2019), in *ttl13* mutant microtubules were not completely depolymerized at 2h, suffered a brief re-polymerization phase within 8 h and collapsed within 28 h of NaCl treatment. This altered response could be explained by the extendedly described crosstalk between the CSC and microtubules. Several studies propose that CSC stability is crucial for maintaining an appropriate microtubule cortical array, rather than the importance of microtubules for the CSC. In fact, microtubule depolymerization could be produced by either mutations in the CSC complex (Fisher and Cyr, 1998; Chu et al., 2007; Paredez et al., 2008) or drugs that inhibit cellulose synthesis, such

as isoxaben (Paredez et al., 2008). Furthermore, at 2 h of salt stress exposure, microtubules were not depolymerized, while CSCs were completely depleted from plasma membrane, thus indicating that TTL function is more important for the CSC rather than microtubules. However, in *ttl13* microtubules were completely abolished within 28h and not before, that coincides with the timing of TTL3 relocation and maximum difference in CSC density between the *ttl13* and WT backgrounds and this could be explained by the role of CC proteins (Endler et al., 2015; Kesten et al., 2019). We propose that because there are no CESAs going back to the plasma membrane from 6-8 h in the *ttl13* mutant under stress, there are no CC proteins in plasma membrane, as they are integral components of the CSC, and the absence of plasma membrane CC proteins prevent the reassembling of the microtubule cortical array and microtubules get fully depolymerized.

The TTL3-GFP relocation to plasma membrane is not specifically triggered by salt stress since TTL3-GFP also relocalised to the plasma membrane in the presence of high levels of exogenous sucrose. No differences on CSC density were observed in *ttl13* compared with WT during sucrose stress, however, CSC speed decreased in the WT background while remained unaffected in the *ttl13* mutant. Thus, these data provide important information about the role of TTLs in CSC activity, as CSC movement depends on its catalytic activity (Morgan et al., 2013). Therefore, an increase of CSC speed in the *ttl13* background suggests an increase of CSC activity, probably producing cellulose microfibrils with a lower quality, likely with a reduced length or increased fragility of the microfibrils (Wasteneys, 2004).

Reduction of the cellulose content by introducing the *prc1-1* mutation into the complementing line also caused a massive relocation of TTL3-GFP to the plasma membrane. Surprisingly, treatment with the cellulose inhibitor isoxaben

did not produce the typical TTL3 relocation although *ttl13* presented an enhanced sensitivity to isoxaben when compared to WT. Isoxaben promotes active CSC internalization in SmaCCs. Therefore, if TTL3 only is attached to active CSCs during adverse conditions, CSCs needs to be located in the plasma membrane allowing TTL3 binding and this could not occur once CSC are internalized into SmaCCs after prolonged isoxaben treatment. Isoxaben acts in the catalytic loop of the CSC (Scheible et al. 2001), therefore, another possibility is that isoxaben could block the CESA1-TTL3 interaction reported by Y2H assays, thereby preventing the TTL3 relocation to plasma membrane that could depend on its interaction with the CSC.

The *ttl13* mutant phenocopy most of the cellulose-related phenotypes of *fei1fei2*. However, TTL3-GFP relocates to plasma membrane in absence of *FEI* genes during sucrose stress, therefore TTL3 relocalization seems to be independent of the SOS5/FEI1-FEI2 pathway. Furthermore, we observed that *TTL1* and *TTL3* mutations in the *sos5-2* mutants cause an additive phenotype and *ttl13* mutant was unaffected in mucilage production, contrary to *fei1fei2* mutants. Thereby, these data suggest that TTLs could be stabilizing the CSC at the plasma membrane, independently of *SOS5*, *FEI1* and *FEI2* function. The association between FEI1 and TTL3 in *N. benthamiana* using Co-IP is very strong, however the meaning of this remains elusive.

The CC proteins function under salt stress could be dependent of TTL function based on the analysis of the microtubule density. We observed that TTL3 proteins were closely located to the CC1 using BiFC as expected, as both proteins are members of the CSC. However, we did not observe association in transient coexpression in *N. benthamiana*. Thus, further studies are necessary to elucidate this hypothesis.

How does TTL function mechanistically in cellulose biosynthesis? Salt stress conditions inhibit cellulose biosynthesis resulting in a decrease in the content of crystalline cellulose. Our data support that this decrease in the cellulose content activates an unknown signalling pathway that promote TTL3 relocation to the plasma membrane and interaction through its IDR with the catalytic loop of the CSC. This interaction would in turn increases the stability of the CSC during stress conditions. TTLs could also safeguard the cortical microtubule array, stabilizing the CSC at the plasma membrane and/or promoting microtubule reassembling during adverse conditions via CC proteins, an integral component of the CSC (Fig.1A, "Discussion" chapter). One possibility is that in absence of *TTL1* and *TTL3* genes, CC proteins could not promote microtubule reassembling during adverse conditions, because CSCs are not stable in the plasma membrane. This would lead to the re-establishment of cellulose biosynthesis and the described phenotypic outcomes of *ttl* mutants (Fig.1B, "Discussion" chapter).

Several regulators have been identified as members of the CSC complex in order to safeguard the CSC activity during salt stress conditions, such as the mentioned CC proteins (Endler et al., 2015; Kesten et al., 2019). In addition, CSI1 protein is also essential for cellulose biosynthesis in saline conditions, as *csi1* mutants showed hypersensitivity to salt (Zhang et al., 2016). Both proteins have in common that are constitutive members of the CSC and their location do not depend of environmental changes. In this work, we discover a novel mechanism where TTL3 and must likely TTL1, change its predominant cytosolic location to the plasma membrane, in order to safeguard the CSC integrity, during stress episodes. Thus, our findings outline a mechanism in which cytosolic proteins could protect the CSC during adverse conditions, uncovering a new mode of action not previously described. Hence, the stress-dependent response is not confined to the CSC members in the plasma membrane as previously described,

but it also depends on other cytosolic components which response is dependent to the environmental conditions.

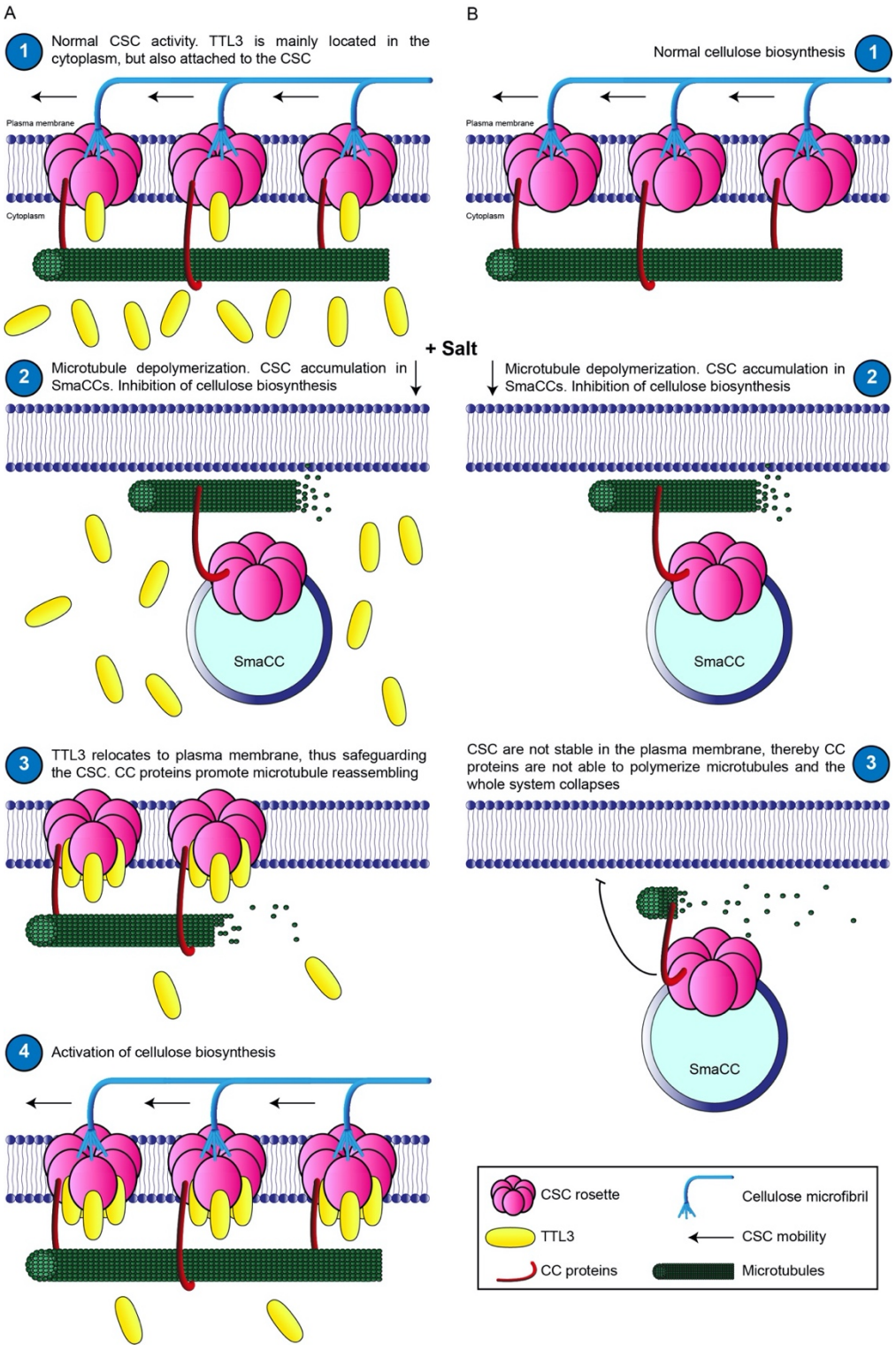

Figure 1. TTL3 safeguard cellulose biosynthesis machinery in response to salt stress tolerance. **(A)** TTL3 protects the CSC during adverse conditions. (1) In normal conditions, where normal

CSC activity is occurring, TTL3 is mainly located in the cytoplasm but it is also attached to the CSC in the plasma membrane, in a minor proportion. (2) During saline conditions, an internalization of CSCs to SmaCCs is produced in response to stress, where CC proteins still attached to the CSC and the unstable microtubules. (3) Within 28h, TTL3 massively relocates to the plasma membrane in response to a decrease of the cellulose content, that could be sensed by extracellular components that transduce a signal to TTL3, such as RLKs. Thus, CSCs are delivered to the plasma membrane, where TTL3 stabilize them and subsequently the CC function, that promotes microtubule reassembling. (4) Since TTL3 stabilize the cellulose biosynthesis machinery, an activation of cellulose biosynthesis is produced. **(B)** Cellulose biosynthesis is negatively compromised by the absence of TTL function. (1) In absence of TTL1 and TTL3 proteins, normal cellulose biosynthesis is produced. (2) During saline conditions, an internalization of CSCs to SmaCCs is occur in response to stress, where CC proteins still attached to the CSC and the unstable microtubules. (3) Due to the absence of TTL proteins, the CSC complex is not stable in the plasma membrane, thereby CC proteins are not able to promote the reassembling of the microtubule cortical array. Thus, microtubules are abolished within 28h and a complete inhibition of cellulose biosynthesis is produced, producing the collapse of the whole system.

Conclusions

1. Mutation in *TTL* genes cause altered growth in presence of cellulose biosynthesis inhibitors, such as isoxaben, salt and sucrose stress.

2. *TTL* family is composed by four members, where only *TTL1* and *TTL3* play an important role in maintaining a proper root and hypocotyl growth under adverse conditions.

3. Cell wall integrity could be compromised in *ttl* mutants. In fact, spatial organization of cellulose microfibrils could be affected in etiolated *ttl* mutants under sucrose stress, whereas a decrease in the cellulose content was observed in *ttl* roots.

4. Mutation in *TTL* genes lead to additive effects in cellulose defective mutants, most likely by decrease of the cellulose content in the plant cell wall.

5. *TTL* genes act non-redundantly with other pathways that promote cellulose biosynthesis, such as the *SOS5*/*FEI1-FEI2* pathway.

6. In the complementing *TTL3-GFP 2.4* line, *TTL3* expression complement the isotropic phenotype of the *ttl13* mutant during adverse conditions indicating a similar function for TTL1 and TTL3 proteins.

7. TTL3 and likely TTL1 are a new members of the Cellulose Synthase Complex, both interacting with the catalytic loop of CESA1 through its Intrinsic Disorder Region (IDR).

8. The IDR of TTL3 is essential to complement the isotropic phenotype displayed by the *ttl13* mutant upon adverse conditions.

9. TTL3 relocates to plasma membrane to safeguard the CSC under adverse conditions, probably by transmitting a signal, caused by the decrease of the cellulose content in the plant cell wall.

10. TTL proteins likely prevent microtubule instability through promoting CC function at the plasma membrane.

Resumen

Los cambios en las condiciones ambientales tienen un impacto tanto en la producción de biomasa vegetal como en el patrón de crecimiento de las plantas (Qin et al., 2011). Se estima que los estreses abióticos, incluidos la sequía, el calor, el frío y la salinidad, son el factor causante de hasta el 50% de la pérdida de rendimiento en cosechas (Boyer, 1982). Sin embargo, los mecanismos que vinculan el estrés salino y la producción de biomasa en plantas siguen se conocen muy poco.

La biomasa vegetal se compone en gran parte de las paredes celulares de plantas, que proporcionan el principal recurso sostenible para muchos productos humanos, incluidos alimentos y combustible (Somerville et al., 2010; McFarlane et al., 2014). La celulosa contribuye a la mayor parte de las paredes celulares de las plantas y es el biopolímero más abundante en la Tierra. La celulosa es una estructura paracristalina de cadenas de β- (1 → 4) -D-glucano, que se sintetizan individualmente mediante complejos (CSCs) de celulosa sintasas (CESA), que generalmente se disponen como rosetas hexaméricas (Mueller y Brown, 1980) y pueden cristalizar en microfibrillas de celulosa conectadas por enlaces de hidrógeno intra e intermoleculares (McFarlane et al., 2014). Estas microfibrillas que proporcionan la resistencia a la tracción de la pared celular principal son esenciales para el desarrollo de la planta (Hofte y Voxeur, 2017). Debido a que la celulosa es el principal polímero de la pared celular, la longitud, el ángulo y la cristalinidad de las microfibrillas de celulosa son determinantes importantes de las propiedades físicas de dicha pared celular (Nishiyama, 2009).

Las paredes celulares de las plantas contienen dos tipos diferentes de paredes celulares; una pared primaria que rodea a todas las células en crecimiento y una pared secundaria que proporciona soporte a células especializadas, ubicadas entre el protoplasma y la pared celular primaria (McFarlane et al., 2014; Meents et al., 2018). Los CSC se caracterizan por contener

tres subunidades CESA distintas que forman el complejo funcional (McFarlane et al., 2014; Polko y Kieber, 2019). Por lo tanto, los CSC de pared primaria en Arabidopsis requieren que los genes CESA1, CESA3 y CESA6 sean funcionales (Persson et al., 2007; Desprez et al., 2007; Polko y Kieber, 2019). Presumiblemente, los CSC se ensamblan en el retículo endoplásmico (ER) o Golgi y se transportan a la superficie celular, donde se insertan en la membrana plasmática adyacente a los microtúbulos corticales (Gutiérrez et al., 2009). Las CESAs también se pueden encontrar en pequeños compartimentos relacionados con Golgi denominados pequeños compartimentos de CESA (smaCCs) (Gutiérrez et al., 2009), o compartimentos de CesA asociados a microtúbulos (MASC) (Crowell et al., 2009), involucrados en exocitosis o endocitosis de los CSC (Gutiérrez et al., 2009; Crowell et al., 2009).

Según el modelo actual, la biosíntesis de celulosa se correlaciona directamente con el movimiento de las CSC en la membrana plasmática (es decir, dirección y velocidad) esenciales para el depósito de microfibrillas de celulosa nacientes (Gutiérrez et al., 2009). El patrón de movimiento de las CESAs coincide con los microtúbulos corticales subyacentes (MT), lo que respalda que estas fibrillas del citoesqueleto guíen los CSC mientras producen celulosa (Gutiérrez et al., 2009; Kesten et al., 2019).

Es ampliamente conocido que el estrés salino tiene serias consecuencias para el crecimiento de las plantas y la producción de cultivos, donde los mutantes defectuosos de celulosa son especialmente sensibles a las condiciones salinas. De hecho, la mayoría de estos fenotipos defectuosos están causados por un deterioro de la matriz cortical de microtúbulos (Endler et al., 2015). De hecho, los microtúbulos se despolimerizan rápidamente después de la exposición a la sal y otros estreses osmóticos (Komis et al., 2002) y se requiere una repolimerización posterior para la adaptación de las células vegetales a los episodios de estrés

(Wang, 2007). En Arabidopsis, varios genes CESA han sido implicados en las respuestas al estrés salino mediante análisis in silico (13). De hecho, el tratamiento con sal afecta negativamente las trayectorias de CesA en la membrana plasmática y, por lo tanto, la deposición de celulosa (Paredez, 2006). Además, mutaciones en las proteínas CC producen una disminución de la densidad de CSC en la membrana plasmática durante los episodios de estrés salino (Endler, 2015; Kesten, 2019). Según eso, los autores subrayan un mecanismo sobre cómo los componentes integrales de CSC para sostener la biosíntesis de celulosa durante condiciones adversas.

El crecimiento vegetal se logra principalmente mediante la expansión celular más que con la división celular. Para lograr el crecimiento direccional, las células vegetales experimentan una expansión anisotrópica, y las microfibrillas de celulosa se depositan perpendiculares al eje de crecimiento (McFarlane et al., 2014). El estrés salino produce una inhibición de la biosíntesis de celulosa, lo que conduce a una disminución de la anisotropía del crecimiento en mutantes con defectos en biosíntesis de celulosa (Polko y Kieber, 2019; Kesten et al., 2019).

En Arabidopsis, la familia de genes TETRATRICOPEPTIDE THIOREDOXIN-LIKE (TTL) está compuesta por cuatro miembros (TTL1 a TTL4). Curiosamente, las proteínas TTL se identificaron originalmente para tener un papel en la tolerancia a la sal. De hecho, las mutaciones en TTL1, TTL3 y TTL4 causan un crecimiento reducido bajo tensiones abióticas, como la salinidad y la sequía, que se caracteriza por un elongamiento reducido de la raíz y deterioradas respuestas osmóticas durante el desarrollo de las plántulas. (Rosado et al., 2006; Ceserani et al., 2009; Lakhssassi et al., 2012). Sin embargo, el mecanismo que describe la respuesta adaptativa al estrés salino en las proteínas TTL sigue siendo desconocido. Debido a que el estrés salino afecta negativamente la integridad de la pared celular de la planta, causando un crecimiento isotrópico en mutantes *ttl*,

en este trabajo estudiamos el papel de las proteínas TTL en la producción de celulosa, el principal componente de las pared celular en plantas.

Porque los genes TTL pertenecen a una familia de cuatro miembros en Arabidopsis (TTL1 a TTL4) (Rosado, 2006; Lakhssassi, 2012), determinamos si los mutantes individuales *ttl* fenocopian mutantes descritos que son defectuosos en la biosíntesis de celulosa. Comenzamos analizando la respuesta de mutantes *ttl* en condiciones de alta sacarosa (4,5%), suplementada en medio MS que se conoce que exacerba la expansión celular isotrópica característica de los mutantes defectuosos de celulosa (Xu, 2008; Fagard, 2000). En estas condiciones, tanto *ttl1* como *ttl3* mostraron raíces más cortas y exhibieron una fuerte expansión radial de la punta de las raíz en comparación con las plántulas WT, mientras que las raíces de *ttl2* y *ttl4* fueron similares al WT. Luego investigamos la redundancia de *TTL1*, *TTL3* y *TTL4* en las respuestas a alta sacarosa analizando el crecimiento del mutante doble *ttl1 ttl3* (*ttl13*) y el mutante triple *ttl1 ttl3 ttl4* (*ttl134*). No se encontraron diferencias obvias entre el isotropismo de la raíz de *ttl13* y *ttl134*, pero ambas mostraron un crecimiento isotrópico aditivo respecto a los mutantes individuales *ttl1* o *ttl3*. Además de los defectos de crecimiento de la raíz, los componentes involucrados en la biosíntesis de celulosa generalmente muestran un crecimiento defectuoso de hipocotilo (Yeats et al., 2016; Ivakov et al., 2017; Kesten et al., 2019). Encontramos que *ttl13* y *ttl134* muestran una reducción similar en la longitud del hipocotilo en relación con el WT bajo condiciones de 4.5% de sacarosa.

De hecho, esta alteración del crecimiento en el mutante *ttl13* en estrés por sacarosa, se volvió a confirmar cuando se expuso a condiciones de estrés salino tal y cómo se publicó anteriormente (naoufal). Sorprendentemente, los defectos de crecimiento en plántulas etioladas *ttl13* bajo estrés por sacarosa no se correlacionaron con una disminución en el contenido de celulosa con respecto a

las plantas de tipo silvestre, lo que podría denotar una disposición espacial defectuosa de las microfibrillas de celulosa. Este comportamiento también se observó en otros mutantes relacionados con defectos en biosíntesis de celulosa (Polko et al., 2018; Chaudhary et al., 2020). Sin embargo, en raíces *ttl13* observamos una disminución significativa del contenido de celulosa en comparación con las raíces de tipo silvestre, pero esta disminución está directamente relacionada con la disminución en el contenido total de glucosa de las raíces *ttl13*. En definitiva, estos datos indican que *TTL1* y *TTL3* juegan un papel importante en el mantenimiento adecuado del crecimiento de raíces e hipocótilos durante episodios de estrés.

Se han identificado varios reguladores que salvaguardan la biosíntesis de celulosa durante condiciones adversas. Las proteínas ancladas a membrana plasmática mediante un glucosil-fosfatidilinositol (GPI), como el gen Salt-Overly Sensitive 5 (SOS5), codifica dominios similares a AGP y fascilina y mutaciones en este gen (mutante *sos5-2*) provoca la alteración del crecimiento celular y la inhibición del crecimiento raíz bajo 100 mM NaCl (Shi, 2002). Para realizar un análisis genético entre *TTL* y el gen *SOS5*, generamos un triple mutante homocigoto *ttl13 sos5-2* cruzando el mutante *ttl13* con *sos5-2*. Los mutantes individuales *ttl13* y *sos5-2* etiolados de 5 días de edad no se distinguieron del fenotipo silvestre en condiciones de control, pero sorprendentemente, el mutante doble *ttl13 sos5-2* ya presentaba una reducción en la longitud del hipocotilo y un ligero crecimiento isotrópico, en comparación con las líneas parentales. Este crecimiento reducido de *ttl13 sos5*-2 también se observó en la roseta de plantas crecidas en día corto y sugiere que, si bien ambas proteínas tienen un papel en la biosíntesis de celulosa durante el crecimiento normal, una compensa la pérdida de la otra. Tras el tratamiento con 100 mM NaCl, *ttl13* y *sos5*-2 mostraron un crecimiento reducido respecto a las plántulas WT, mientras que el doble mutante *ttl13 sos5-2* presentó una reducción extrema de la longitud del hipocótilo y un

engrosamiento de éste, que resultó en un fenotipo enano. En general, nuestros datos indican que las mutaciones *ttl* y *sos5* tienen un efecto aditivo que sugiere que actúan de manera no lineal.

La respuesta de la planta al estrés salino también depende de la actividad apropiada del CSC, como una mutación en el gen CESA6 (mutante *prc1-1*), que provoca una alteración del crecimiento de la raíz en plántulas de Arabidopsis bajo estrés salino (Zhang, 2016). Para investigar más a fondo si los fenotipos extremos de *ttl13 sos5-2* bajo estrés son la consecuencia de la interrupción de vías independientes que regulan la biosíntesis de celulosa, disminuimos el contenido de celulosa de *ttl13* utilizando una estrategia genética. Introdujimos en *ttl13* un alelo de pérdida de función de CESA6, *prc1-1* que se conoce que disminuye alrededor del 50% del contenido de celulosa (Fagard, 2000). Las plántulas etioladas de *prc1-1* de 5 días de edad mostraron una mayor expansión radial de los hipocotilos que *ttl13* y *prc1-1* en condiciones de control y 100 mM NaCl, aunque no se encontraron diferencias en la longitud. El efecto aditivo de la mutación *ttl13* en las plantas *prc1-1* fue evidente en plantas crecidas en día corto, que mostraron un fenotipo enano. En general, el fenotipo aditivo que se muestra en el mutante *ttl13 prc1-1* en relación con *ttl13* y *prc1-1* respalda el papel crucial de los genes *TTL1* y *TTL3* en la biosíntesis de celulosa.

Anteriormente hemos demostrado que las respuestas defectuosas en brasinoesteroides del mutante *ttl134* pueden complementarse con el gen nativo TTL3, fusionado a GFP en el extremo carboxilo de la proteína (Amorim-Silva, 2019). Por lo tanto, investigamos si TTL3-GFP también podría complementar los defectos de crecimiento mostrados por los mutantes *ttl* en condiciones adversas. De hecho, esta línea complementaba el crecimiento isotrópico de mutantes *ttl* a niveles de WT en respuesta a un alto nivel de sacarosa y estrés salino. Indica además, que la única acción de TTL3 complementa la función de TTL1 y TTL3.

Para investigar la localización subcelular de TTL3, tomamos imágenes de la línea TTL3-GFP en células interfásicas de hipocótilos etiolados. La señal de GFP mostró una localización importante de la proteína en el citosol. Además, también pudimos discernir señales débiles de focos móviles en la membrana plasmática que estaban ocultados por el alto fondo citosólico. Por lo tanto, desarrollamos una mejora de la imagen que nos permitió eliminar casi por completo el fondo citosólico y aislar estas partículas móviles localizadas en la membrana plasmática. La localización y el comportamiento de estas partículas fue similar a lo que se informó anteriormente para el CSC (Paredez et al. 2006), lo que indica que TTL3 podría moverse junto con el CSC. Por lo tanto, generamos una línea TTL3-GFP y tdTomato (tdT) -CESA6 (Sampathkumar et al. 2013) en el fondo doble mutante *ttl13* y observamos que ambas proteínas migraban juntas en la membrana plasmática. Para corroborar la colocalización TTL3-CESA, confirmamos que TTL3-GFP se mueve bidireccionalmente con una velocidad promedio de 271 ± 86 nm / min, similar a tdT-CESA6.

Dado que TTL3-GFP colocaliza con el complejo CSC, investigamos si TTL3 puede interactuar directamente con las proteínas CESA1, CESA3 y CESA6 utilizando ensayos de dos híbridos de levadura (Y2H). Anteriormente hemos demostrado que la secuencia proteica completa de TTL3 no es estable en levadura (Amorim-Silva et al., 2019). Por lo tanto, utilizamos como presas (AD) la región N-terminal de TTL3 que contenía la región intrínsecamente desordenada (IDR) y los dos primeros TPR (TTL3-N) y la región C-terminal TTL3 que contenía los seis TPR y el motivo TRLX (TTL3-C). Como cebos (BD), utilizamos el dominio citosólico N-terminal (dominio N) y el dominio de interacción citosólica (dominio I) de CESA1, CESA3 y CESA6 (McFarlane et al., 2014; Polko et al., 2018). Nuestro análisis Y2H indicó que TTL3-N interactuaba específicamente con CESA1-I y débilmente con CESA1-N pero no con ninguno de los otros dominios de CESA3 o CESA6. La construcción TTL3-C comparte los

dos primeros TPR con TTL3-N y no interactúa con ninguno de las CESA analizadas, lo que sugiere que el dominio TTL3 IDR encontrado en TTL3-N es necesario para la interacción. No se encontraron interacciones entre TTL3-N y TTL3-C con ninguno de los dominios CESA3 o CESA6, lo que indica que la interacción entre TTL3 y el complejo CSC fue específica para CESA1. Además de TTL3, el gen TTL1 también tiene un papel importante en la biosíntesis de celulosa. Por lo tanto, generamos una construcción de presa (AD) que contenía la región N-terminal de TTL1 equivalente a la generada para TTL3-N, es decir, la región intrínsecamente desordenada (IDR) y los dos primeros dominios TPR (TTL1-N). Así, TTL1-N también interactuó con el dominio CESA1-N y CESA1-I, que también se correlaciona con la identidad similar de la predicción de los segmentos IDR de las TTLs.

La interacción del dominio N-terminal de TTL3 y TTL1 con CESA1 sugiere un papel importante del IDR para la función TTL. Para investigar la función de la IDR in vivo, se generó una construcción genómica TTL3-GFP que carece de la IDR bajo la expresión del promotor de TTL3 (*TTL3: TTL3$^{\Delta IDR}$-GFP*). Después de la transformación de esta construcción en el doble mutante *ttl13* por inmersión floral, seleccionamos un total de 38 líneas resistentes a higromicina. La expresión de la proteína TTL3$^{\Delta IDR}$-GFP en líneas de segregación T2 se comparó con la de TTL3-GFP usando análisis de inmunotransferencia con anticuerpos GFP. En base a los niveles de expresión y la presencia de una única inserción, seleccionamos las líneas *TTL3$^{\Delta IDR}$-GFP 11.1* y *TTL3$^{\Delta IDR}$-GFP 35.1* para un análisis posterior. Luego investigamos los fenotipos raíz de las líneas *TTL3$^{\Delta IDR}$-GFP 11.1* y *TTL3$^{\Delta IDR}$-GFP 35.1* junto con la línea de complementación *TTL3-GFP 2.4* en presencia de NaCl. Si bien todos los genotipos presentaron un crecimiento de la raíz WT en condiciones de control, *TTL3$^{\Delta IDR}$-GFP 11.1* y *TTL3ΔIDR-GFP 35.1* no complementaron el fenotipo isotrópico de la raíz de *ttl13* (Fig.11F-G), lo que

respalda que el IDR de TTL3 (y probablemente TTL1) es importante para su función, muy probablemente a través del CESA1.

Dado que TTL3 interactúa directamente con las proteínas CESA en levadura, las líneas TTL3-GFP que carecen de IDR no complementaron las mutaciones *ttl13* y TTL3 se mueve junto con el CSC en la membrana plasmática, consideramos a TTL3 como un nuevo miembro del CSC.

Para comprender cómo las proteínas TTL afectan la maquinaria de la biosíntesis de celulosa tras el estrés salino, generamos una línea doblemente marcada YFP-CESA6 mCh-TUA5 en fondo mutante *ttl13*. Se tomaron imágenes de hipocótilos etiolados de 3 días después de 30 min y 1 a 32 h de tratamiento con 200 mM NaCl. Como se mostró anteriormente (Wang et al. 2007; Fujita et al. 2013; Endler et al. 2015; Kesten et al. 2019), la matriz de microtúbulos en plantas WT se despolimeriza después de 2 h y se vuelve a ensamblar dentro de las 8 h del tratamiento con sal, donde a su vez se produce una disminución de la densidad de CESA en la membrana plasmática después de 2 h, volviéndose a recuperar a las 28 h. Por el contrario, observamos una rápida disminución de la densidad de CESA en la membrana plasmática despúes de 30 minutos de tratamiento con NaCl en mutantes *ttl13* y los CESA nunca volvieron a membrana plasmática en el transcurso del experimento, lo que indica que las proteínas TTL pueden estar involucradas en la estabilización del CSC en membrana plasmática. La matriz de microtúbulos corticales en plántulas mutantes *ttl13*, por otro lado, no se despolimerizó completamente en 2 h como en plántulas WT y, después de una breve fase de repolimerización en 8 h, colapsó a las 28 h del tratamiento con NaCl. Por lo tanto, estos datos indican una función prominente de las proteínas TTL en la estabilidad del CSC y la matriz de microtúbulos corticales bajo estrés salino.

Dado que las proteínas TTL podrían funcionar para salvaguardar el CSC durante los episodios de estrés salino, decidimos analizar la razón molecular detrás de esta observación. Tratamos hipocotilos de plántulas etioladas de 3 días de edad de la línea *ttl13* TTL3-GFP y tdT-CESA6 con 200 mM NaCl. Una relocalización de la señal de TTL3-GFP a la membrana plasmática en hipocótilos etiolados fue claramente visible, eliminándose casi completamente la señal citosólica de fondo. Esta observación señaló claramente que TTL3 es una proteína citosólica que se relocalizó selectivamente en el CSC tras el estrés. La oblicuidad es una medida de la asimetría de un histograma de la imagen. Dado que la señal citosólica de TTL3-GFP está distribuida de manera bastante uniforme, dio como resultado una asimetría bastante baja del histograma. Por eso, razonamos que la acumulación de TTL3-GFP en la membrana plasmática tras la exposición al estrés, podría resultar en una mayor asimetría debido a la formación de grupos, (Higaki et al. 2010). De hecho, la relocalización de TTL3-GFP del citosol a la membrana plasmática tras el estrés dio como resultado una asimetría significativamente incrementada, mientras que la asimetría de la señal tdT-CESA6 no se vio afectada en su mayor parte. De este modo, la asimetría se puede utilizar como una medida de la localización de la membrana plasmática de las proteínas citosólicas si se produce una formación de agrupación de señales en este caso. Para probar si las proteínas TTL son importantes para el suministro de CSC a la membrana plasmática, realizamos experimentos FRAP en la línea *ttl13* YFP-CESA6. Después del foto-blanqueo, observamos dinámicas comparables entre los fondos mutantes WT y ttl13, lo que sugiere que los TTL no están involucrados en el suministro de CSC a la membrana plasmática.

Como se ha comentado anteriormente, altos niveles de sacarosa exógena dieron como resultado un defecto en el crecimiento de *ttl13* en comparación con WT. Por lo tanto, para investigar el mecanismo molecular implicado, tratamos plántulas etioladas de 3 días de edad de la línea *ttl13* TTL3-GFP y tdT-CESA6 en

condiciones de 4,5% de sacarosa. Curiosamente, nuevamente observamos una relocalización de la señal TTL3-GFP a la membrana plasmática después de una alta exposición a sacarosa, donde observamos una mayor asimetría debido a la formación de agrupaciones de señal TTL3-GFP, en contraste con las condiciones de control. Luego cuantificamos la densidad de partículas de TTL3-GFP y tdT-CESA6 en la membrana plasmática bajo condiciones de control y alta sacarosa. La densidad de partículas de ambas proteínas fue idéntica en condiciones control y no cambió con el tratamiento con 4,5& de sacarosa, lo que resalta aún más que el conjunto de proteínas TTL3 no cambia durante el tratamiento de alta sacarosa y la acumulación de TTL3-GFP en membrana se debe a su reubicación desde el citosol a la membrana plasmática. Para analizar cómo una ausencia de la actividad TTL afectó a la maquinaria de síntesis de celulosa, probamos la línea *ttl13* de doblemente marcada YFP-CESA6 y mCh-TUA5 en 4,5% de sacarosa. En la misma línea que los análisis fenotípicos, la velocidad como la densidad del CSC en condiciones de control no se distinguían entre las plantas WT y *ttl13*. Sin embargo, el tratamiento con 4,5% de sacarosa resultó en una disminución de la velocidad de CSC en la membrana plasmática en plantas WT pero no en mutantes *ttl13*, mientras que la densidad de CSC permaneció en niveles de control en ambos genotipos.

Para corroborar aún más esta relocalización masiva de TTL3, generamos líneas mutantes *prc1-1* que expresan TTL3-GFP. Nuestro razonamiento detrás de esto fue que el mutante prc1-1 en condiciones de control, presenta aprox. 50% menos celulosa cristalina que WT y, por lo tanto, nos permite investigar si la reubicación de TTL3 en la membrana plasmática se desencadena por una reducción en el contenido de celulosa. De hecho, observamos una relocalización de TTL3-GFP en membrana plasmática y un fuerte aumento de la asimetría del histograma TTL3-GFP en el fondo *prc1-1*. En conjunto, estos datos sugieren el papel crucial de las proteínas TTL para mantener la integridad del CSC durante

condiciones adversas que producen una disminución en el contenido de celulosa cristalina.

La mutación dentro del dominio citosólico en CESA3 confiere resistencia al herbicida isoxaben (Scheible et al. 2001), lo que sugiere que el objetivo del isoxaben es el dominio catalítico de las enzimas CESA. Debido a que los TTL interactúan con el dominio citosólico de CESA1, el isoxaben podría interferir en la interacción TTL-CSC y la relocalización de TTL3 a la membrana plasmática bajo estrés. Curiosamente, la asimetría de la señal TTL3-GFP no se vio afectada en presencia de isoxaben 1 μM, mientras que la mayor parte de tdT-CESA6 se acumuló en Golgi y/u otros compartimentos citoplasmáticos. Por lo tanto, isoxaben podría bloquear el sitio de interacción de TTL3 con el CSC, evitando la acumulación de TTL3 en la membrana plasmática durante el estrés y, por lo tanto, confirmando que las proteínas TTL interactúan con el dominio catalítico del CSC. Sin embargo, otra hipótesis no excluyente, es que la proteína TTL3 se una a CSCs que se encuentren catalíticamente activos, esto es en membrana plasmática. El isoxaben provoca la acumulación de CSCs en vesículas, retirándolas de membrana plasmática, por ello puede ser que TTL3 no se una a estos complejos cuando se encuentran en otros compartimentos y el complejo se encuentre inactivo.

Para dilucidar el posible vínculo entre TTL y diferentes componentes relacionados con la celulosa, utilizamos enfoques bioquímicos y moleculares para investigar la conexión entre TTL y otros reguladores que promueven la biosíntesis de celulosa, como las proteínas SOS5, FEI1/FEI2 y CC1/CC2.

Es ampliamente conocido que las proteínas TTL están claramente asociadas con varias RLK como BRL2 que influyen en la nervadura de la hoja y BRI1 en la vía de señalización de BR (Ceserani et al., 2009; Amorim-Silva, 2019).

Además, las proteínas TTL tienen un papel positivo en la biosíntesis de celulosa. Por lo tanto, es plausible que la función TTL pueda funcionar corriente abajo de una RLK, lo que podría detectar perturbaciones en el espacio extracelular y posteriormente transducir una señal a los componentes citosólicos. Se han identificado varias RLK como reguladores positivos de la maquinaria de biosíntesis de celulosa, como las LRR-RLK FEI1 y FEI2. Por lo tanto, es posible que las TTL puedan asociarse con FEI1/FEI2 para promover la biosíntesis de celulosa durante condiciones adversas.

Las mutaciones en el doble mutante *fei1fei2* causan una expansión radial de la punta de la raíz durante el estrés por sacarosa (Xu, et al 2008), de manera similar a los mutantes *ttl*. Por lo tanto, una posible conexión FEI-TTL podría ser hipotetizada. Además, la expansión radial típica de la raíz en los mutantes *fei1fei2* puede ser suprimida por inhibidores de la biosíntesis de etileno: ácido 1-aminociclopropano-1-carboxílico (ACC) o ácido 2-aminoisobutírico (AIB), pero no por inhibidores de la señalización de etileno o por la interrupción de percepción de etileno (tiosulfato de plata). Por lo tanto, probamos si *ttl13* fenocopia a *fei1fei2* en presencia de esos agentes químicos.

El fenotipo isotrópico en 4,5% de sacarosa podría rescatarse en presencia de AIB, que es un inhibidor competitivo de la conversión de ACC a etileno, proceso catalizado por la enzima ACC oxidasa (Xu et al., 2008). De hecho, cuatro días después de transferir las plántulas a medios MS suplementados con sacarosa al 4,5% más AIB 1 mM, observamos que tanto *ttl13* como *fei1fei2* presentaron raíces significativamente más largas en presencia de AIB que sin suplementación con AIB. Es conocido que el tiosulfato de plata inhibe la percepción de etileno (Burg y Burg, 1967; Xu et al., 2008) y, curiosamente, el fenotipo mutante *fei* es suprimido por inhibidores de la biosíntesis de etileno, pero no por la interrupción de la percepción de etileno (Xu et al.., 2008). Sorprendentemente, solo 2 días

después de transferir las plántulas al medio MS suplementado con sacarosa al 4.5% más en presencia de tiosulfato de plata, observamos un fenotipo isotrópico exacerbado en las raíces *ttl13* y *fei1fei2*. Nuevamente, el mutante *ttl13* fenocopia a *fei1fei2* cuando la percepción de etileno es inhibida por la presencia de tiosulfato de plata, al igual que al ocurría con AIB.

Debido a que los mutantes *ttl* fenocopian a los mutantes *fei* en múltiples experimentos, investigamos la posible interacción in vivo realizando ensayos de coinmunoprecipitación (Co-IP) mediante expresión transitoria de la secuencia completa de TTL3 y FEI1 en *N. benthamiana*. Después de la inmunoprecipitación de FEI1-GFP utilizando resina anti-GFP, detectamos una fuerte interacción entre TTL3-HA y FEI1-GFP. Además, la interacción entre FEI1 y TTL3 también se investigó utilizando ensayos de complementación de fluorescencia bimolecular (BiFC) en hojas de *N. benthamiana*, que proporcionan información adicional sobre la localización subcelular de la interacción. La coexpresión de la mitad N-terminal de YFP unida a TTL3 junto a la mitad C-terminal de YFP unida a FEI1 de YFP (cYFP) reconstituyó proteínas YFP funcionales en la membrana plasmática, confirmando la interacción y siendo consistente con la localización de la membrana plasmática de FEI1.

Como se mencionó anteriormente, se produce una relocalización masiva de TTL3 a la membrana plasmática desde el citoplasma, para salvaguardar al CSC y a la red de microtúbulos corticales durante condiciones de estrés. Por lo tanto, si las proteínas FEI actúan corriente arriba de TTL, protegiendo al CSC después de la exposición a estrés, esperamos que las mutaciones de pérdida de función en los genes FEI afecten negativamente a la reubicación masiva de TTL3 en la membrana plasmática. Para probar esta hipótesis, generamos una línea de *Arabidopsis* TTL3-GFP estable, bajo el control de su promotor nativo, en el fondo mutante *fei1fei2*. Utilizando microscopía de disco giratorio, observamos una clara

relocalización de la proteína TTL3 después de 2,5 h de exposición al 4,5% de sacarosa en comparación con las condiciones de control. Estos datos sugieren que el modo de acción de TTL3 es independiente al de las proteínas FEI y podría actuar en diferentes vías que promueven la biosíntesis de celulosa. Esta hipótesis también está respaldada por el hecho de que los TTL funcionan independientemente de la vía SOS5/FEI1-FEI2, gracias al análisis de interacción genética de TTL1 y TTL3 con SOS5, descrito anteriormente.

La importancia de los microtúbulos corticales en la biosíntesis de celulosa se ha demostrado ampliamente (Endler et al., 2015, Wang et al., X; Kesten et al., 2019). De hecho, las proteínas CC son esenciales para mantener la matriz de microtúbulos corticales durante condiciones adversas, facilitando la polimerización de los microtúbulos y, en consecuencia, promoviendo la catálisis de las microfibrillas de celulosa. Debido a que los mutantes *ttl* mostraron una respuesta de repolimerización de microtúbulos distinta al WT después de la exposición al estrés salino, es posible que los TTL actúen junto con las proteínas CC para salvaguardar la matriz cortical de microtúbulos.

Por lo tanto, investigamos la posible asociación *in vivo* de TTL-CC realizando ensayos de BiFC en *N. benthamiana*. La coexpresión de la mitad N-terminal de YFP unida a TTL3 junto a la mitad C-terminal de YFP unida a CC1 de YFP (cYFP) mostró una señal intensa, confirmando que TTL3 podría interactuar con CC1. Por lo tanto, investigamos más esta posible interacción mediante la realización de Co-IP en *N. benthamiana*. Sin embargo, no observamos asociación entre TTL3-HA y las proteínas GFP-CC1 o GFP-CC2, ya que TTL3 no co-inmunoprecipitó con CC1 o CC2. Por lo tanto, lo que sugiere que una asociación entre las proteínas TTL y CC puede no ocurrir, al menos en las condiciones probadas (sin estrés), aunque se requieren más estudios para confirmar esta hipótesis.

Entonces, ¿cómo funciona las proteínas TTL mecánicamente en la biosíntesis de celulosa? Durante condiciones de estrés salino se produce una inhibición de la biosíntesis de celulosa, seguida de una disminución en el contenido de celulosa cristalina. De alguna manera, esta disminución en el contenido de celulosa activa una vía de señalización desconocida que promueve la relocalización de TTL3 a la membrana plasmática. De este modo, el IDR de TTL3 interactúa con el dominio catalítico del CSC (concretamente con CESA1), evitando así la inestabilidad del CSC durante condiciones de estrés. Además, las TTLs podrían salvaguardar indirectamente la matriz de microtúbulos corticales, estabilizando el CSC en la membrana plasmática, promoviendo el reensamblado de microtúbulos durante condiciones adversas a través de proteínas CC, un componente integral del CSC. Además, en ausencia de genes TTL, las proteínas CC no podrían promover el reensamblado de microtúbulos durante condiciones adversas, porque las CSC no son estables en la membrana plasmática. Por lo tanto, la biosíntesis de celulosa no se restablece, lo que lleva al colapso de todo el sistema.

Se han identificado varios reguladores como miembros del complejo CSC, con el fin de salvaguardar la actividad CSC durante las condiciones de estrés salino, como las mencionadas proteínas CC (Endler et al. 2015; Kesten et al. 2019). Además, la proteína CSI1 también es esencial para la biosíntesis de celulosa en condiciones salinas, ya que los mutantes *csi1* muestran hipersensibilidad a condiciones salinas (Zhang, 2016). Lo que tienen en común ambas proteínas es que son miembros constitutivos del CSC y su ubicación no depende de los cambios ambientales. En este trabajo, descubrimos un mecanismo novedoso en el que las proteínas TTL cambian su predominante localización citosólica a membrana plasmática, para salvaguardar la integridad del CSC, durante los episodios de estrés.

Por lo tanto, nuestros hallazgos describen un mecanismo en el cual las proteínas citosólicas podrían proteger el CSC durante condiciones adversas, descubriendo un nuevo modo de acción no descrito previamente. Por ello, la respuesta dependiente de estrés no se limitaría solamente a los miembros de CSC que se encuentran en membrana plasmática como se describió anteriormente, sino que también depende de otros componentes citosólicos cuya respuesta depende de las condiciones ambientales.

Annex

The Plant Cell, Vol. 31: 1807–1828, August 2019, www.plantcell.org © 2019 ASPB.

TTL Proteins Scaffold Brassinosteroid Signaling Components at the Plasma Membrane to Optimize Signal Transduction in Arabidopsis

Vítor Amorim-Silva,[a] Álvaro García-Moreno,[a] Araceli G. Castillo,[b] Naoufal Lakhssassi,[c] Alicia Esteban del Valle,[a] Jessica Pérez-Sancho,[a] Yansha Li,[d] David Posé,[a] Josefa Pérez-Rodriguez,[a] Jinxing Lin,[e] Victoriano Valpuesta,[a] Omar Borsani,[f] Cyril Zipfel,[g,h] Alberto P. Macho,[d,g] and Miguel A. Botella[a,1]

[a] Departamento de Biología Molecular y Bioquímica, Instituto de Hortofruticultura Subtropical y Mediterránea "La Mayora," Universidad de Málaga-Consejo Superior de Investigaciones Científicas (IHSM-UMA-CSIC), Universidad de Málaga, Campus Teatinos, 29071 Málaga, Spain

[b] Departamento de Biología Celular, Genética y Fisiología, Instituto de Hortofruticultura Subtropical y Mediterránea "La Mayora," Universidad de Málaga-Consejo Superior de Investigaciones Científicas (IHSM-UMA-CSIC), Universidad de Málaga, Campus Teatinos, 29071 Málaga, Spain

[c] Department of Plant, Soil and Agricultural Systems, Southern Illinois University, Carbondale, Illinois 62901

[d] Shanghai Center for Plant Stress Biology, CAS Center for Excellence in Molecular Plant Sciences, Shanghai Institutes of Biologic Sciences, Chinese Academy of Sciences (CAS), Shanghai, China

[e] College of Biological Sciences and Technology, Beijing Forestry University, Beijing 100083, China

[f] Departamento de Biología Vegetal, Laboratorio de Bioquímica, Facultad de Agronomía Universidad de la República, Montevidec Uruguay

[g] The Sainsbury Laboratory, University of East Anglia, Norwich Research Park, Norwich, NR4 7UH, United Kingdom

[h] Institute of Plant and Microbial Biology and Zurich-Basel Plant Science Center, University of Zurich, CH-8008 Zurich, Switzerlar

ORCID IDs: 0000-0002-3978-7205 (V.A.-S.); 0000-0001-7007-998X (Á.G.-M.); 0000-0003-3990-5475 (A.G.C.); 0000-0002-8255-94 (N.L.); 0000-0003-3039-1172 (A.E.d.V.); 0000-0002-6201-3240 (J.P.-S.); 0000-0002-4864-9461 (Y.L.); 0000-0003-3332-4661 (D.P 0000-0003-1676-2053 (J.P.-R.); 0000-0001-9338-1356 (J.L.); 0000-0003-0922-6615 (V.V.); 0000-0002-9111-5801 (O.B.); 0000-000 4935-8583 (C.Z.); 0000-0001-9935-8026 (A.P.M.); 0000-0002-8867-1831 (M.A.B.)

Brassinosteroids (BRs) form a group of steroidal hormones essential for plant growth, development, and stress response BRs are perceived extracellularly by plasma membrane receptor-like kinases that activate an interconnected signal transductio cascade, leading to the transcriptional regulation of BR-responsive genes. *TETRATRICOPEPTIDE THIOREDOXIN-LIKE* (*TT* genes are specific for land plants, and their encoded proteins are defined by the presence of protein–protein interaction motive that is, an intrinsic disordered region at the N terminus, six tetratricopeptide repeat domains, and a C terminus with homolog to thioredoxins. TTL proteins thus likely mediate the assembly of multiprotein complexes. Phenotypic, molecular, and genet analyses show that TTL proteins are positive regulators of BR signaling in Arabidopsis (*Arabidopsis thaliana*). TTL3 direct interacts with a constitutively active BRASSINOSTEROID INSENSITIVE1 (BRI1) receptor kinase, BRI1-SUPPRESSOR phosphatase, and the BRASSINAZOLE RESISTANT1 transcription factor and associates with BR-SIGNALING KINASE BRASSINOSTEROID INSENSITIVE2 kinases, but not with BRI1-ASSOCIATED KINASE1. A functional TTL3-green fluoresce protein (GFP) shows dual cytoplasmic plasma membrane localization. Depleting the endogenous BR content reduces plasn membrane localization of TTL3-GFP, while increasing BR content causes its plasma membrane relocalization, where strengthens the association of BR signaling components. Our results reveal that TTL proteins promote BR responses ar suggest that TTL proteins may function as scaffold proteins by bringing together cytoplasmic and plasma membrane B signaling components.

INTRODUCTION

Brassinosteroids (BRs) are a family of growth-promoting hormones with essential roles in a wide range of developmental and physiological processes (Belkhadir and Jaillais, 2015; Chaiwanc et al., 2016; Jaillais and Vert, 2016). However, in addition to th well-established function in growth, essential roles in the trade-c between growth and tolerance to biotic and abiotic stress ep sodes are now being unveiled (Lozano-Durán and Zipfel, 201 Zhang et al., 2016; Nolan et al., 2017; Tian et al., 2018). BRs a perceived at the plasma membrane by ligand-induced heter dimers of the receptor kinases BRASSINOSTEROID INSENSITIVI (BRI1) and SOMATIC EMBBRYOGENESIS RECEPTOR KINAS (SERK) protein family members, which activates an interco nected signal transduction cascade, leading to the transcriptior

[1] Address correspondence to: mabotella@uma.es.
The author responsible for distribution of materials integral to the findings presented in this article in accordance with the policy described in the Instructions for Authors (www.plantcell.org) is: Miguel A. Botella (mabotella@uma.es).
www.plantcell.org/cgi/doi/10.1105/tpc.19.00150

References

Alonso, José M. et al. 2003. "Genome-Wide Insertional Mutagenesis of Arabidopsis Thaliana." *Science* 301(5633): 653–57.

Amorim-Silva, Vítor et al. 2019. "TTL Proteins Scaffold Brassinosteroid Signaling Components at the Plasma Membrane to Optimize Signal Transduction in Arabidopsis." *The Plant Cell* 31(8): 1807–28.

Anderson, Charles T., and Joseph J. Kieber. 2020. "Dynamic Construction, Perception, and Remodeling of Plant Cell Walls." *Annual Review of Plant Biology* 71(1): 39–69.

Athar, H. R., and M. Ashraf. 2009. "Strategies for Crop Improvement Against Salinity and Drought Stress: An Overview." In *Salinity and Water Stress. Tasks for Vegetation Sciences*, , 1–16. http://link.springer.com/10.1007/978-1-4020-9065-3_1.

Atmodjo, Melani A., Zhangying Hao, and Debra Mohnen. 2013. "Evolving Views of Pectin Biosynthesis." *Annual Review of Plant Biology* 64(1): 747–79.

Bacete, Laura, and Thorsten Hamann. 2020. "The Role of Mechanoperception in Plant Cell Wall Integrity Maintenance." *Plants* 9(5).

Barratt, D. H.Paul et al. 2009. "Normal Growth of Arabidopsis Requires Cytosolic Invertase but Not Sucrose Synthase." *Proceedings of the National Academy of Sciences of the United States of America*.

Baskin, T. I. 2001. "On the Alignment of Cellulose Microfibrils by Cortical Microtubules: A Review and a Model." *Protoplasma* 215(1–4): 150–71.

Baskin, Tobias I. 2005. "Anisotropic Expansion of the Plant Cell Wall." *Annual Review of Cell and Developmental Biology* 21(1): 203–22. http://www.annualreviews.org/doi/10.1146/annurev.cellbio.20.082503.103053.

Basu, Debarati et al. 2016. "Glycosylation of a Fasciclin-Like Arabinogalactan-Protein (SOS5) Mediates Root Growth and Seed Mucilage Adherence via a Cell Wall Receptor-like Kinase (FEI1/ FEI2) Pathway in Arabidopsis." *PLoS ONE* 11(1): 1–27.

Belkhadir, Youssef, and Yvon Jaillais. 2015. "The Molecular Circuitry of Brassinosteroid Signaling." *New Phytologist* 206(2): 522–40.

Ben-Tov, Daniela et al. 2018. "The Role of COBRA-LIKE 2 Function, as Part of the Complex Network of Interacting Pathways Regulating Arabidopsis Seed Mucilage Polysaccharide Matrix Organization." *Plant Journal* 94(3): 497–512.

Blatch, Gregory L., and Michael Lässle. 1999. "The Tetratricopeptide Repeat: A Structural Motif Mediating Protein-Protein Interactions." *BioEssays*.

Boyer, J. S. 1982. "Plant Productivity and Environment." *Science*.

Brett, Christopher T. 2000. "Cellulose Mlicrofibrils in Plants: Biosynthesis, Deposition, and Integration into the Cell Wall." *International Review of Cytology*.

Brown, R. M. 1985. "Cellulose Microfibril Assembly and Orientation: Recent Developments." *Journal of cell science. Supplement*.

Buchanan, B. B. 2015. Biochemistry and molecular biology of plants *Biochemistry and Molecular Biology of Plants*.

Burg, Stanley P., and Ellen A. Burg. 1967. "Molecular Requirements for the Biological Activity of Ethylene."

Plant Physiology.

Ca??o-Delgado, Ana et al. 2003. "Reduced Cellulose Synthesis Invokes Lignification and Defense Responses in Arabidopsis Thaliana." *Plant Journal* 34(3): 351–62.

Campbell, Malcom M, and Ronald R Sederoff. 1996. "Variation in Lignin Content and Composition." *Plant Physiology*.

Ceserani, Teresa, Anna Trofka, Neeru Gandotra, and Timothy Nelson. 2009. "VH1/BRL2 Receptor-like Kinase Interacts with Vascular-Specific Adaptor Proteins VIT and VIK to Influence Leaf Venation." *Plant Journal*.

Chan, Jordi, Enrico Coen, Jordi Chan, and Enrico Coen. 2020. "Interaction between Autonomous and Microtubule Guidance Systems Controls Cellulose Synthase Report Interaction between Autonomous and Microtubule Guidance Systems Controls Cellulose Synthase Trajectories." *Current Biology*: 1–7. https://doi.org/10.1016/j.cub.2019.12.066.

Chaudhary, Ajeet et al. 2020. "The Arabidopsis Receptor Kinase STRUBBELIG Regulates the Response to Cellulose Deficiency." *PLoS genetics* 16(1): e1008433.

Chen, Zhizhong et al. 2005. "Disruption of the Cellulose Synthase Gene, AtCesA8/IRX1, Enhances Drought and Osmotic Stress Tolerance in Arabidopsis." *Plant Journal*.

Chu, Zhaoqing et al. 2007. "Knockout of the AtCESA2 Gene Affects Microtubule Orientation and Causes Abnormal Cell Expansion in Arabidopsis." *Plant Physiology*.

Clough, Steven J., and Andrew F. Bent. 1998. "Floral Dip: A Simplified Method for Agrobacterium-Mediated Transformation of Arabidopsis Thaliana." *Plant Journal* 16(6): 735–43.

Clouse, Steven D. 2002. "Brassinosteroids Plant Counterparts to Animal Steroid Hormones?" *Vitamins and Hormones*.

Crowell, E. F. et al. 2009. "Pausing of Golgi Bodies on Microtubules Regulates Secretion of Cellulose Synthase Complexes in Arabidopsis." *the Plant Cell Online* 21(4): 1141–54. http://www.plantcell.org/cgi/doi/10.1105/tpc.108.065334.

D'Andrea, Luca D., and Lynne Regan. 2003. "TPR Proteins: The Versatile Helix." *Trends in Biochemical Sciences*.

DEMARTY, MAURICE, CLAUDINE MORVAN, and MICHEL THELLIER. 1984. "Calcium and the Cell Wall." *Plant, Cell & Environment* 7(6): 441–48.

Desai, Arshad, and Timothy J. Mitchison. 1997. "Microtubule Polymerization Dynamics." *Annual Review of Cell and Developmental Biology* 13(1): 83–117.

Desnos, T et al. 1996. "Procuste1 Mutants Identify Two Distinct Genetic Pathways Controlling Hypocotyl Cell Elongation, Respectively in Dark- and Light-Grown Arabidopsis Seedlings." *Development (Cambridge, England)* 122(2): 683–93. http://www.ncbi.nlm.nih.gov/pubmed/8625819.

Desprez, T. et al 2002. "Resistance against Herbicide Isoxaben and Cellulose Deficiency Caused by Distinct Mutations in Same Cellulose Synthase Isoform CESA6." *Plant Physiology* 128(2): 482–90. http://www.plantphysiol.org/cgi/doi/10.1104/pp.128.2.482.

Desprez, T. et al. 2007. "Organization of Cellulose Synthase Complexes Involved in Primary Cell Wall

Synthesis in Arabidopsis Thaliana." *Proceedings of the National Academy of Sciences*.

Desprez, T. et al. 2007. "Organization of Cellulose Synthase Complexes Involved in Primary Cell Wall Synthesis in Arabidopsis Thaliana." *Proceedings of the National Academy of Sciences of the United States of America*.

Doblin, Monika S., Isaac Kurek, Deborah Jacob-Wilk, and Deborah P. Delmer. 2002. "Cellulose Biosynthesis in Plants: From Genes to Rosettes." *Plant and Cell Physiology*.

Van der Does, Dieuwertje et al. 2017. "The Arabidopsis Leucine-Rich Repeat Receptor Kinase MIK2/LRR-KISS Connects Cell Wall Integrity Sensing, Root Growth and Response to Abiotic and Biotic Stresses." *PLoS Genetics* 13(6): 1–27.

Ehrhardt, David W., and Sidney L. Shaw. 2006. "Microtubule Dynamics and Organization in the Plant Cortical Array." *Annual Review of Plant Biology* 57(1): 859–75.

Endler, Anne et al. 2015. "A Mechanism for Sustained Cellulose Synthesis during Salt Stress." *Cell* 162(6): 1353–64.

Endler, Anne et al. 2016. "The Cellulose Synthase Companion Proteins Act Non-Redundantly with CELLULOSE SYNTHASE INTERACTING1/POM2 and CELLULOSE SYNTHASE 6." *Plant Signaling and Behavior* 11(4).

Fagard, M. 2000. "PROCUSTE1 Encodes a Cellulose Synthase Required for Normal Cell Elongation Specifically in Roots and Dark-Grown Hypocotyls of Arabidopsis." *the Plant Cell Online* 12(12): 2409–24. http://www.plantcell.org/cgi/doi/10.1105/tpc.12.12.2409.

Fedoroff, N. V. et al. 2010. "Radically Rethinking Agriculture for the 21st Century." *Science* 327(5967): 833–34.

Fisher, Deborah D., and Richard J. Cyr. 1998. "Extending the Microtubule/Microfibril Paradigm: Cellulose Synthesis Is Required for Normal Cortical Microtubule Alignment in Elongating Cells." *Plant Physiology*.

Fujita, Satoshi et al. 2013. "An Atypical Tubulin Kinase Mediates Stress-Induced Microtubule Depolymerization in Arabidopsis." *Current Biology* 23(20): 1969–78. http://dx.doi.org/10.1016/j.cub.2013.08.006.

Gardiner, John C., Neil G. Taylor, and Simon R. Turner. 2003. "Control of Cellulose Synthase Complex Localization in Developing Xylem." *Plant Cell*.

Gardner, K. H., and J. Blackwell. 1974. "The Structure of Native Cellulose." *Biopolymers*.

Gehl, Christian et al. 2009. "New GATEWAY Vectors for High Throughput Analyses of Protein-Protein Interactions by Bimolecular Fluorescence Complementation." *Molecular Plant* 2(5): 1051–58. http://dx.doi.org/10.1093/mp/ssp040.

Geitmann, Anja, and Joseph K.E. Ortega. 2009. "Mechanics and Modeling of Plant Cell Growth." *Trends in Plant Science* 14(9): 467–78.

George, Johnsy, and S. N. Sabapathi. 2015. "Cellulose Nanocrystals: Synthesis, Functional Properties, and Applications." *Nanotechnology, Science and Applications* 8: 45–54.

Gietz, R. D., and R. H. Schiestl. 1995. "Transforming Yeast with DNA." *Methods in Molecular and Cellular*

Biology 5(5): 255–69.

Gorshkova, Tatyana et al. 2018. "Plant 'Muscles': Fibers with a Tertiary Cell Wall." *New Phytologist* 218(1): 66–72.

Griffiths, Jonathan S. et al. 2015. "Unidirectional Movement of Cellulose Synthase Complexes in Arabidopsis Seed Coat Epidermal Cells Deposit Cellulose Involved in Mucilage Extrusion, Adherence, and Ray Formation." *Plant Physiology* 168(2): 502–20.

Gu, Y. et al. 2010. "Identification of a Cellulose Synthase-Associated Protein Required for Cellulose Biosynthesis." *Proceedings of the National Academy of Sciences* 107(29): 12866–71.

Gutierrez, Ryan et al. 2009. "Arabidopsis Cortical Microtubules Position Cellulose Synthase Delivery to the Plasma Membrane and Interact with Cellulose Synthase Trafficking Compartments." *Nature Cell Biology* 11(7): 797–806. http://dx.doi.org/10.1038/ncb1886.

Haigler, Candace H. 2018. "Two Types of Cellulose Synthesis Complex Knit the Plant Cell Wall Together." *Proceedings of the National Academy of Sciences of the United States of America* 115(27): 6882–84.

Harpaz-Saad, Smadar et al. 2011. "Cellulose Synthesis via the FEI2 RLK/SOS5 Pathway and CELLULOSE SYNTHASE 5 Is Required for the Structure of Seed Coat Mucilage in Arabidopsis." *Plant Journal* 68(6): 941–53.

Harpaz-Saad, Smadar, Tamara L. Western, and Joseph J. Kieber. 2012. "The FEI2-SOS5 Pathway and CELLULOSE SYNTHASE 5 Are Required for Cellulose Biosynthesis in the Arabidopsis Seed Coat and Affect Pectin Mucilage Structure." *Plant Signaling and Behavior* 7(2): 285–88. http://www.tandfonline.com/doi/abs/10.4161/psb.18819.

Heim, Dale R., Jean L. Roberts, Philip D. Pike, and Ignacio M. Larrinua. 1990. "A Second Locus, Ixr B1 in Arabidopsis Thaliana, That Confers Resistance to the Herbicide Isoxaben." *Plant Physiology* 92(3): 858–61.

Hématy, Kian et al. 2007. "A Receptor-like Kinase Mediates the Response of Arabidopsis Cells to the Inhibition of Cellulose Synthesis." *Current Biology* 17(11): 922–31.

Heyndrickx, Ken S., and Klaas Vandepoele. 2012. "Systematic Identification of Functional Plant Modules through the Integration of Complementary Data Sources." *Plant Physiology*.

Higaki, Takumi et al. 2010. "Quantification and Cluster Analysis of Actin Cytoskeletal Structures in Plant Cells: Role of Actin Bundling in Stomatal Movement during Diurnal Cycles in Arabidopsis Guard Cells." *Plant Journal* 61(1): 156–65.

Höfte, Herman, and Aline Voxeur. 2017. "Plant Cell Walls." *Current Biology* 27(17): R865–70. http://dx.doi.org/10.1016/j.cub.2017.05.025.

Hu, Honghong, and Lizhong Xiong. 2014. "Genetic Engineering and Breeding of Drought-Resistant Crops." *Annual Review of Plant Biology* 65(1): 715–41.

Jae, Sook Kang et al. 2008. "Salt Tolerance of Arabidopsis Thaliana Requires Maturation of N-Glycosylated Proteins in the Golgi Apparatus." *Proceedings of the National Academy of Sciences of the United States of America*.

K.Edwards, C.Johnstone and C.Thompson. 1991. "A Simple and Rapid Method for the Preparation of Plant

Genomic." *American Society of Agricultural and Biological Engineers Annual International Meeting 2014, ASABE 2014* 19(6): 1349.

Kadota, Yasuhiro, Alberto P. Macho, and Cyril Zipfel. 2016. "Immunoprecipitation of Plasma Membrane Receptor-Like Kinases for Identification of Phosphorylation Sites and Associated Proteins." In *Methods in Molecular Biology (Clifton, N.J.)*, Methods in Molecular Biology, eds. Jose R. Botella and Miguel A. Botella. New York, NY: Springer New York, 133–44. http://link.springer.com/10.1007/978-1-4939-3115-6.

Kerry, Rout George et al. 2018. "Microbes and Their Role in Drought Tolerance of Agricultural Food Crops." *Microbial Biotechnology* 2: 253–73.

Kesten, Christopher, Francisco M Gámez-Arjona, et al. 2019. "Pathogen-Induced PH Changes Regulate the Growth-Defense Balance of Plants." *bioRxiv* (February 18): 1–49. https://www.biorxiv.org/content/10.1101/550491v1%0Ahttp://dx.doi.org/10.1101/550491.

Kesten, Christopher, Arndt Wallmann, et al. 2019. "The Companion of Cellulose Synthase 1 Confers Salt Tolerance through a Tau-like Mechanism in Plants." *Nature Communications* 10(1): 857. http://www.nature.com/articles/s41467-019-08780-3.

Kieber, Joseph J., and Joanna Polko. 2019. "The Regulation of Cellulose Biosynthesis in Plants." *The Plant Cell*: tpc.00760.2018. http://www.plantcell.org/content/early/2019/01/15/tpc.18.00760?rss=1.

Kimura, Satoshi et al. 1999. "Immunogold Labeling of Rosette Terminal Cellulose-Synthesizing Complexes in the Vascular Plant Vigna Angularis." *Plant Cell*.

Klemm, Dieter, Brigitte Heublein, Hans Peter Fink, and Andreas Bohn. 2005. "Cellulose: Fascinating Biopolymer and Sustainable Raw Material." *Angewandte Chemie - International Edition*.

Komis, George, Panagiotis Apostolakos, and Basil Galatis. 2002. "Hyperosmotic Stress Induces Formation of Tubulin Macrotubules in Root-Tip Cells of Triticum Turgidum: Their Probable Involvement in Protoplast Volume Control." *Plant and Cell Physiology* 43(8): 911–22.

Kubicki, James D. et al. 2018. "The Shape of Native Plant Cellulose Microfibrils." *Scientific Reports*.

Kurek, Isaac et al. 2002. "Dimerization of Cotton Fiber Cellulose Synthase Catalytic Subunits Occurs via Oxidation of the Zinc-Binding Domains." *Proceedings of the National Academy of Sciences of the United States of America*.

Laemmli, U. K. 1970. "Cleavage of Structural Proteins during the Assembly of the Head of Bacteriophage T4." *Nature*.

Lakhssassi, N. et al. 2012. "The Arabidopsis TETRATRICOPEPTIDE THIOREDOXIN-LIKE Gene Family Is Required for Osmotic Stress Tolerance and Male Sporogenesis." *Plant Physiology* 158(3): 1252–66. http://www.plantphysiol.org/cgi/doi/10.1104/pp.111.188920.

Lamers, Jasper, Tom Van Der Meer, and Christa Testerink. 2020. "How Plants Sense and Respond to Stressful Environments." *Plant Physiology*.

Li, S., L. Lei, C. R. Somerville, and Y. Gu. 2012. "Cellulose Synthase Interactive Protein 1 (CSI1) Links Microtubules and Cellulose Synthase Complexes." *Proceedings of the National Academy of Sciences* 109(1): 185–90. http://www.pnas.org/cgi/doi/10.1073/pnas.1118560109.

Li, Shundai, Lei Lei, Yaroslava G. Yingling, and Ying Gu. 2015. "Microtubules and Cellulose Biosynthesis: The Emergence of New Players." *Current Opinion in Plant Biology* 28: 76–82. http://dx.doi.org/10.1016/j.pbi.2015.09.002.

Lindsey, Benson E. et al. 2017. "Standardized Method for High-Throughput Sterilization of Arabidopsis Seeds." *Journal of Visualized Experiments* 2017(128): 1–7.

Liu, Xin, Jiawei Wang, and Linfeng Sun. 2018. "Structure of the Hyperosmolality-Gated Calcium-Permeable Channel OSCA1.2." *Nature Communications*.

Liu, Zengyu et al. 2016. "Cellulose-Microtubule Uncoupling Proteins Prevent Lateral Displacement of Microtubules during Cellulose Synthesis in Arabidopsis." *Developmental Cell* 38(3): 305–15. http://dx.doi.org/10.1016/j.devcel.2016.06.032.

Ma, Si et al. 2019. "Phloem Unloading Strategies and Mechanisms in Crop Fruits." *Journal of Plant Growth Regulation*.

Ma, Xiyu, Guangyuan Xu, Ping He, and Libo Shan. 2016. "SERKing Coreceptors for Receptors." *Trends in Plant Science*.

McFarlane, Heather E., Anett Döring, and Staffan Persson. 2014. "The Cell Biology of Cellulose Synthesis." *Annual Review of Plant Biology* 65(1): 69–94. http://www.annualreviews.org/doi/10.1146/annurev-arplant-050213-040240.

McNamara, Joshua T., Jacob L.W. Morgan, and Jochen Zimmer. 2015. "A Molecular Description of Cellulose Biosynthesis." *Annual Review of Biochemistry* 84(1): 895–921. http://www.annualreviews.org/doi/10.1146/annurev-biochem-060614-033930.

McNeil, Michael, Alan G. Darvill, Stephen C. Fry, and Peter Albersheim. 1984. "Structure and Function of the Primary Cell Walls of Plants." *Annual Review of Biochemistry*.

Meents, Miranda J., Yoichiro Watanabe, and A. Lacey Samuels. 2018. "The Cell Biology of Secondary Cell Wall Biosynthesis." *Annals of Botany* 121(6): 1107–25.

Mitchison, Tim, and Marc Kirschner. 1984. "Dynamic Instability of Microtubule Growth." *Nature*.

Morgan, Jacob L.W., Joanna Strumillo, and Jochen Zimmer. 2013. "Crystallographic Snapshot of Cellulose Synthesis and Membrane Translocation." *Nature* 493(7431): 181–86. http://dx.doi.org/10.1038/nature11744.

Mueller, Susette C., R. Malcolm Brown, and Tom K. Scott. 1976. "Cellulosic Microfibrils: Nascent Stages of Synthesis in a Higher Plant Cell." *Science*.

Mueller, Susette C., and R. Malcolm Brown. 1980. "Evidence for an Intramembrane Component Associated with a Cellulose Microfibril-Synthesizing Complex in Higher Plants." *Journal of Cell Biology*.

Munns, Rana, and Mark Tester. 2008. "Mechanisms of Salinity Tolerance." *Annual Review of Plant Biology* 59(1): 651–81. http://www.annualreviews.org/doi/10.1146/annurev.arplant.59.032607.092911.

Neuhoff, Volker, Norbert Arold, Dieter Taube, and Wolfgang Ehrhardt. 1988. "Improved Staining of Proteins in Polyacrylamide Gels Including Isoelectric Focusing Gels with Clear Background at Nanogram Sensitivity Using Coomassie Brilliant Blue G-250 and R-250." *Electrophoresis* 9(6): 255–62.

Nguyen, Loc Van, Daniel Bertero, and Long Viet Nguyen. 2020. "Genetic Variation in Root Development

Responses to Salt Stresses of Quinoa." *Journal of Agronomy and Crop Science* (December 2019): 1–10.

Nick, Peter. 2013. "Microtubules, Signalling and Abiotic Stress." *Plant Journal* 75(2): 309–23.

Nishiyama, Yoshiharu. 2009. "Structure and Properties of the Cellulose Microfibril." *Journal of Wood Science*.

Nixon, B. Tracy et al. 2016. "Comparative Structural and Computational Analysis Supports Eighteen Cellulose Synthases in the Plant Cellulose Synthesis Complex." *Scientific Reports*.

Nolan, Trevor M. et al. 2017. "Selective Autophagy of BES1 Mediated by DSK2 Balances Plant Growth and Survival." *Developmental Cell* 41(1): 33-46.e7. http://dx.doi.org/10.1016/j.devcel.2017.03.013.

Nolan, Trevor M. et al. 2020. "Brassinosteroids: Multidimensional Regulators of Plant Growth, Development, and Stress Responses." *The Plant cell* 32(2): 295–318.

Paredez, A. R., S. Persson, D. W. Ehrhardt, and C. R. Somerville. 2008. "Genetic Evidence That Cellulose Synthase Activity Influences Microtubule Cortical Array Organization." *Plant Physiology* 147(4): 1723–34. http://www.plantphysiol.org/cgi/doi/10.1104/pp.108.120196.

Paredez, Alexander R., Christopher R. Somerville, and David W. Ehrhardt. 2006. "Visualization of Cellulose Synthase Demonstrates Functional Association with Microtubules." *Science* 312(5779): 1491–95. http://www.ncbi.nlm.nih.gov/pubmed/16627697.

Pauly, Markus, and Kenneth Keegstra. 2010. "Plant Cell Wall Polymers as Precursors for Biofuels." *Current Opinion in Plant Biology*.

Pear, Julie R. et al. 1996. "Higher Plants Contain Homologs of the Bacterial CelA Genes Encoding the Catalytic Subunit of Cellulose Synthase." *Proceedings of the National Academy of Sciences of the United States of America*.

Persson, S. et al. 2007. "Genetic Evidence for Three Unique Components in Primary Cell-Wall Cellulose Synthase Complexes in Arabidopsis." *Proceedings of the National Academy of Sciences* 104(39): 15566–71. http://www.pnas.org/cgi/doi/10.1073/pnas.0706592104.

Persson, Staffan et al. 2005. "Identification of Genes Required for Cellulose Synthesis by Regression Analysis of Public Microarray Data Sets." *Proceedings of the National Academy of Sciences of the United States of America* 102(24): 8633–38.

Polko, Joanna K. et al. 2018. "SHOU4 Proteins Regulate Trafficking of Cellulose Synthase Complexes to the Plasma Membrane." *Current Biology*: 1–9. https://linkinghub.elsevier.com/retrieve/pii/S0960982218310066.

Powell, Anahid E., and Michael Lenhard. 2012. "Control of Organ Size in Plants." *Current Biology*.

Powell, Wayne. 2006. " Abiotic Stresses: Plant Resistance Through Breeding and Molecular Approaches . Edited by M. Ashraf and P. J. C. Harris. Binghamton, NH, USA: The Haworth Press (2005), Pp. 725, US$89.95. ISBN 1-56022-965-9 ." *Experimental Agriculture*.

Probine, M. C., and R. D. Preston. 1961. "Cell Growth and the Structure and Mechanical Properties of the Wall in Internodal Cells of Nitella Opaca: I. Wall Structure and Growth." *Journal of Experimental Botany*.

Proseus, Timothy E., and John S. Boyer. 2012. "Calcium Deprivation Disrupts Enlargement of Chara Corallina Cells: Further Evidence for the Calcium Pectate Cycle." *Journal of Experimental Botany*.

Qin, Feng, Kazuo Shinozaki, and Kazuko Yamaguchi-Shinozaki. 2011. "Achievements and Challenges in

Understanding Plant Abiotic Stress Responses and Tolerance." *Plant and Cell Physiology*.

Qiu, Quan Sheng et al. 2002. "Regulation of SOS1, a Plasma Membrane Na+/H+ Exchanger in Arabidopsis Thaliana, by SOS2 and SOS3." *Proceedings of the National Academy of Sciences of the United States of America*.

Quan, R. et al. 2007. "SCABP8/CBL10, a Putative Calcium Sensor, Interacts with the Protein Kinase SOS2 to Protect Arabidopsis Shoots from Salt Stress." *the Plant Cell Online* 19(4): 1415–31. http://www.plantcell.org/cgi/doi/10.1105/tpc.106.042291.

Reynolds, Matthew, and Roberto Tuberosa. 2008. "Translational Research Impacting on Crop Productivity in Drought-Prone Environments." *Current Opinion in Plant Biology*.

Rojas, Enrique R., Scott Hotton, and Jacques Dumais. 2011. "Chemically Mediated Mechanical Expansion of the Pollen Tube Cell Wall." *Biophysical Journal*.

Rosado, Abel et al. 2006. "The Arabidopsis Tetratricopeptide Repeat-Containing Protein TTL1 Is Required for Osmotic Stress Responses and Abscisic Acid Sensitivity." *Plant Physiology* 142(3): 1113–26.

Ruan, Yong-Ling. 2014. "Sucrose Metabolism: Gateway to Diverse Carbon Use and Sugar Signaling." *Annual Review of Plant Biology*.

Sampathkumar, Arun et al. 2013. "Patterning and Lifetime of Plasma Membrane-Localized Cellulose Synthase Is Dependent on Actin Organization in Arabidopsis Interphase Cells." *Plant Physiology*.

Sánchez-Rodríguez, Clara et al. 2017. "BRASSINOSTEROID INSENSITIVE2 Negatively Regulates Cellulose Synthesis in *Arabidopsis* by Phosphorylating Cellulose Synthase 1." *Proceedings of the National Academy of Sciences* 114(13): 3533–38. http://www.pnas.org/lookup/doi/10.1073/pnas.1615005114.

Scheible, Wolf Rüdiger et al. 2001. "Modifications of Cellulose Synthase Confer Resistance to Isoxaben and Thiazolidinone Herbicides in Arabidopsis Ixr1 Mutants." *Proceedings of the National Academy of Sciences of the United States of America* 98(18): 10079–84.

Schindelin, Johannes et al. 2012. "Fiji: An Open-Source Platform for Biological-Image Analysis." *Nature Methods* 9(7): 676–82.

Shi, Huazhong et al. 2003. "The Arabidopsis *SOS5* Locus Encodes a Putative Cell Surface Adhesion Protein and Is Required for Normal Cell Expansion." *The Plant Cell* 15(1): 19–32. http://www.plantcell.org/lookup/doi/10.1105/tpc.007872.

Shoji, Tsubasa et al. 2006. "Salt Stress Affects Cortical Microtubule Organization and Helical Growth in Arabidopsis." *Plant and Cell Physiology* 47(8): 1158–68.

Somerville, Chris. 2006. "Cellulose Synthesis in Higher Plants." *Annual Review of Cell and Developmental Biology* 22(1): 53–78. http://www.annualreviews.org/doi/10.1146/annurev.cellbio.22.022206.160206.

Somerville, Chris et al. 2010. "Feedstocks for Lignocellulosic Biofuels." *Science*.

Sorek, Nadav et al. 2015. "Identification of MEDIATOR16 as the Arabidopsis COBRA Suppressor MONGOOSE1." *Proceedings of the National Academy of Sciences of the United States of America* 112(52): 16048–53.

Stein, Ofer, and David Granot. 2019. "An Overview of Sucrose Synthases in Plants." *Frontiers in Plant Science* 10(February): 1–14.

Steinwand, Blaire J. et al. 2014. "Alterations in Auxin Homeostasis Suppress Defects in Cell Wall Function." *PLoS ONE*.

Tenhaken, Raimund. 2015. "Cell Wall Remodeling under Abiotic Stress." *Frontiers in Plant Science* 5(JAN): 1–9.

Tester, Mark and Langridge, P. 2010. "Breeding Technologies to Increase Crop Production in a Changing World." *Science* 818(5967): 818–22. http://www.sciencemag.org/cgi/content/abstract/327/5967/818.

Tester, Richard F., John Karkalas, and Xin Qi. 2004. "Starch - Composition, Fine Structure and Architecture." *Journal of Cereal Science*.

Vain, Thomas et al. 2014. "The Cellulase KORRIGAN Is Part of the Cellulose Synthase Complex." *Plant Physiology* 165(4): 1521–32.

Wang, Che, Jiejie Li, and Ming Yuan. 2007. "Salt Tolerance Requires Cortical Microtubule Reorganization in Arabidopsis." *Plant and Cell Physiology* 48(11): 1534–47.

Wang, Songhu, Jasmina Kurepa, Takashi Hashimoto, and Jan A. Smalle. 2011. "Salt Stress-Induced Disassembly of Arabidopsis Cortical Microtubule Arrays Involves 26S Proteasome-Dependent Degradation of SPIRAL1." *Plant Cell*.

Wang, Wangxia, Basia Vinocur, and Arie Altman. 2003. "Plant Responses to Drought, Salinity and Extreme Temperatures: Towards Genetic Engineering for Stress Tolerance." *Planta* 218(1): 1–14.

Wang, Xia et al. 2007. "Arabidopsis Microtubule-Associated Protein18 Functions in Directional Cell Growth by Destabilizing Cortical Microtubules." *Plant Cell* 19(3): 877–89.

Wang, Yi Hong, and Yi Hong Wang. 2008. "How Effective Is T-DNA Insertional Mutagenesis in Arabidopsis?" *Journal of Biochemical Technology* 1(1): 11–20.

Wang, Zhi Ping et al. 2015. "Egg Cell-Specific Promoter-Controlled CRISPR/Cas9 Efficiently Generates Homozygous Mutants for Multiple Target Genes in Arabidopsis in a Single Generation." *Genome Biology* 16(1): 1–12. http://dx.doi.org/10.1186/s13059-015-0715-0.

Wasteneys, Geoffrey O. 2004. "Progress in Understanding the Role of Microtubules in Plant Cells." *Current Opinion in Plant Biology* 7(6): 651–60.

Wolf, Sebastian et al. 2012. "Plant Cell Wall Homeostasis Is Mediated by Brassinosteroid Feedback Signaling." *Current Biology* 22(18): 1732–37.

Wolf, Sebastian et al. 2017. "Plant Cell Wall Signalling and Receptor-like Kinases." *Biochemical Journal* 474(4): 471–92. http://biochemj.org/lookup/doi/10.1042/BCJ20160238.

Xiao, Chaowen et al. 2016. "Xyloglucan Deficiency Disrupts Microtubule Stability and Cellulose Biosynthesis in Arabidopsis, Altering Cell Growth and Morphogenesis." *Plant Physiology* 170(1): 234–49. http://www.plantphysiol.org/lookup/doi/10.1104/pp.15.01395.

Xie, Liqiong, Cangjing Yang, and Xuelu Wang. 2011. "Brassinosteroids Can Regulate Cellulose Biosynthesis by Controlling the Expression of CESA Genes in Arabidopsis." *Journal of Experimental Botany* 62(13): 4495–4506.

Xing, Hui Li et al. 2014. "A CRISPR/Cas9 Toolkit for Multiplex Genome Editing in Plants." *BMC Plant Biology* 14(1): 1–12.

Xu, Shou Ling, Abidur Rahman, Tobias I. Baskin, and Joseph J. Kieber. 2008. "Two Leucine-Rich Repeat Receptor Kinases Mediate Signaling, Linking Cell Wall Biosynthesis and ACC Synthase in Arabidopsis." *Plant Cell* 20(11): 3065–79. http://www.plantcell.org/cgi/doi/10.1105/tpc.108.063354.

Xue, Hui et al. 2017. "Arabidopsis Thaliana FLA4 Functions as a Glycan-Stabilized Soluble Factor via Its Carboxy-Proximal Fasciclin 1 Domain." *Plant Journal*.

Yang, Jing et al. 2005. "Molecular Basis for TPR Domain-Mediated Regulation of Protein Phosphatase 5." *EMBO Journal*.

Yang, Tao et al. 2015. "Receptor Protein Kinase FERONIA Controls Leaf Starch Accumulation by Interacting with Glyceraldehyde-3-Phosphate Dehydrogenase." *Biochemical and Biophysical Research Communications* 465(1): 77–82. http://dx.doi.org/10.1016/j.bbrc.2015.07.132.

Yang, Yinong, Rugang Li, and Min Qi. 2000. "In Vivo Analysis of Plant Promoters and Transcription Factors by Agroinfiltration of Tobacco Leaves." *Plant Journal* 22(6): 543–51.

Yeats, Trevor et al. 2016. "Rapid Determination of Cellulose, Neutral Sugars, and Uronic Acids from Plant Cell Walls by One-Step Two-Step Hydrolysis and HPAEC-PAD." *Bio-Protocol* 6(20): 1–14.

Yeats, Trevor H., Hagit Sorek, David E. Wemmer, and Chris R. Somerville. 2016. " Cellulose Deficiency Is Enhanced on Hyper Accumulation of Sucrose by a H + -Coupled Sucrose Symporter ." *Plant Physiology* 171(1): 110–24.

Yuan, Fang et al. 2014. "OSCA1 Mediates Osmotic-Stress-Evoked Ca2+ Increases Vital for Osmosensing in Arabidopsis." *Nature*.

Zhang, Shuang Shuang et al. 2016. "Cellulose Synthesis Genes CESA6 and CSI1 Are Important for Salt Stress Tolerance in Arabidopsis." *Journal of integrative plant biology* 58(7): 623–26.

Zhang, Yang. 2008. "I-TASSER Server for Protein 3D Structure Prediction." *BMC Bioinformatics* 9: 1–8.

Zhu, Jian Kang. 2016. "Abiotic Stress Signaling and Responses in Plants." *Cell* 167(2): 313–24. http://dx.doi.org/10.1016/j.cell.2016.08.029.

Zhu, Jianhua et al. 2010. "A Cellulose Synthase-like Protein Is Required for Osmotic Stress Tolerance in Arabidopsis." *Plant Journal* 63(1): 128–40. http://doi.wiley.com/10.1111/j.1365-313X.2010.04227.x.

ZU Zafar, H Manzoor, H Rasul, S Noreen, Q Ali, M Iqbal, M Javed, HS Gul, Z Ahmad, F Shahzad, CC Ogbaga, H-u-R Athar, M Ashraf. 2017. "Strategies to Improve Crop Salt and Drought Tolerance: Success and Limitations." *Quality and Quantum Improvement in Field Crops*: 265–98.